I.O.S.

# WAVES RECORDED OFF THE EDDYSTONE LIGHTHOUSE SEPTEMBER 1978 — AUGUST 1981

BY
B.C.H. FORTNUM

REPORT NO. 132
1982

NATURAL ENVIRONMENT RESEARCH COUNCIL

INSTITUTE OF OCEANOGRAPHIC SCIENCES

INSTITUTE OF OCEANOGRAPHIC SCIENCES

Wormley, Godalming,
Surrey, GU8 5UB.
(0428 - 79 - 4141)

(Director: Dr. A.S. Laughton FRS)

Bidston Observatory,
Birkenhead,
Merseyside, L43 7RA.
(051 - 653 - 8633)

(Assistant Director: Dr. D.E. Cartwright)

Crossway,
Taunton,
Somerset, TA1 2DW.
(0823 - 86211)

(Assistant Director: M.J. Tucker)

---

*When citing this document in a bibliography the reference should be given as follows:-*

FORTNUM, B.C.H. 1982 Waves recorded off the Eddystone Lighthouse. Data for September 1978 to August 1981 at position 50°10'N, 004°15'W. Summary analysis and interpretation report.
*Institute of Oceanographic Sciences, Report*, No. 132, [113pp.]

INSTITUTE OF OCEANOGRAPHIC SCIENCES

TAUNTON

# Waves recorded off the Eddystone Lighthouse

Data for September 1978 to August 1981
at position 50°10'N, 004°15'W

Summary analysis and interpretation report

by

B.C.H. Fortnum

I.O.S. Report No. 132

1982

*The preparation of this report and the collection of the data contained in it have been financed by the Departments of Energy and of Industry*

CONTENTS

LIST OF FIGURES

3.5.2.1 Occurrences (parts per thousand) of Hs and Tbar combined - spring
3.5.2.2 Occurrences (parts per thousand) of Hs and Tbar combined - summer
3.5.2.3 Occurrences (parts per thousand) of Hs and Tbar combined - autumn
3.5.2.4 Occurrences (parts per thousand) of Hs and Tbar combined - winter
3.5.2.5 Occurrences (parts per thousand) of Hs and Tbar combined - annual

3.5.3.1 Occurrences (parts per thousand) of Hs and Te combined - spring
3.5.3.2 Occurrences (parts per thousand) of Hs and Te combined - summer
3.5.3.3 Occurrences (parts per thousand) of Hs and Te combined - autumn
3.5.3.4 Occurrences (parts per thousand) of Hs and Te combined - winter
3.5.3.5 Occurrences (parts per thousand) of Hs and Te combined - annual

3.6.1.1 Mean durations and numbers of calms v. Hs - spring
3.6.1.2 Mean durations and numbers of calms v. Hs - summer
3.6.1.3 Mean durations and numbers of calms v. Hs - autumn
3.6.1.4 Mean durations and numbers of calms v. Hs - winter
3.6.1.5 Mean durations and numbers of calms v. Hs - annual

3.6.2.1 Mean durations and numbers of storms v. Hs - spring
3.6.2.2 Mean durations and numbers of storms v. Hs - summer
3.6.2.3 Mean durations and numbers of storms v. Hs - autumn
3.6.2.4 Mean durations and numbers of storms v. Hs - winter
3.6.2.5 Mean durations and numbers of storms v. Hs - annual

3.7.1 Distribution of wave energy with Hs and Te - spring
3.7.2 Distribution of wave energy with Hs and Te - summer
3.7.3 Distribution of wave energy with Hs and Te - autumn
3.7.4 Distribution of wave energy with Hs and Te - winter
3.7.5 Distribution of wave energy with Hs and Te - annual

3.8.1 Percentage occurrence of Qp - spring
3.8.2 Percentage occurrence of Qp - summer
3.8.3 Percentage occurrence of Qp - autumn
3.8.4 Percentage occurrence of Qp - winter
3.8.5 Percentage occurrence of Qp - annual

4.1.1 Time series Hs - Inshore Buoy
4.1.2 Time series Hs - Deepwater Buoy

4.2 Wind rose for times of wave data comparison

4.3.1 Comparison of Hs derived from two buoy positions
4.3.2 comparison of Tz derived from two buoy positions

4.4 Comparison of average spectra for the two buoy positions

4.5 Deepwater v. Inshore spectral comparison by frequencies

# 1. INTRODUCTION

## 1.1 Site description

The site at which the wave measurements were taken is shown on the map in figure 1.1. The buoy is moored in water of depth approximately 40 metres, at position 50°10'N, 004°15'W. It is about ½ kilometre south of the Eddystone Rocks on which the lighthouse is situated; the Rocks themselves are 15 kilometres south of Rame Head which is to the west of Plymouth Sound. In order to assess whether data from this site are representative of a wider area, a short term comparison was made with measurements taken from a more exposed site. The results of this work are reported in Appendix IV.

## 1.2 Description of measuring and recording systems

The wave measurements were made by a Waverider buoy which measures the vertical acceleration of the water surface; this acceleration is integrated twice on the buoy to give the elevation of the water surface above the mean water level, which is then transmitted by a radio link to the receiving equipment located at Wembury, near Plymouth. The buoy was moored to the sea-bed using a mooring similar to that described in HUMPHERY(1975,1982(in press)), except that it was modified to suit local conditions. The chain linking the anchor and sub-surface float was uprated to 9mm, and its length adjusted so that the float was approximately 12m below the surface. The total length of mooring components above the float was 20m to allow the Waverider to follow the surface waves. Waverider maintenance visits were normally possible at any time of year; visits were normally made at 6-monthly intervals however. Heavy zinc sacrificial anodes were used to protect metal parts where appropriate. At Wembury the information about the water surface elevation is sampled twice each second and recorded digitally on magnetic cartridge by a Microdata data logger. Each data record contains 2048 values of elevation (covering approximately 17 minutes), and the time between starts of successive records is 3 hours. (In addition, data are recorded in analogue form by a chart recorder and as an fm signal on magnetic cassette, purely for back-up purposes. The fm records may be used to replace missing or invalid Microdata records, but before an fm record can be used in the Microdata validation and analysis system, it must be subjected to a digitisation process; this produces a digital record identical in format to that of the Microdata records.) Cartridge translation is carried out at the Taunton laboratory using a replay unit interfaced to a DEC PDP-11 computer.

## 1.3 Calibration and maintenance

Each buoy is calibrated both before and after its deployment; users of the primary data may obtain details of these calibrations from IOS. Over a number of years of operating systems of Waverider buoys and receiving equipment, IOS has found that the sensitivity of the buoy is stable to within about ±2%, and to within about ±1% for the receiving/demodulation system. Thus the overall sensitivity of the system is stable to within about ±3%. A brief account of the calibration methods may be found in Appendix I.

Routine servicing of the equipment (including changing charts, magnetic tapes and cassettes) was carried out on site by a local agent. Major servicing was carried out by IOS personnel whenever a significant fault was reported.

1.4 Wave data coverage and return (figures 1.4(a) - 1.4(j))
The period covered by the data is 1 September 1978 to 31 August 1981. For this period 2401 of the 8768 possible Microdata records (i.e. 27.4%) were either missing or classified invalid. However 869 of these missing/invalid records have been replaced using data from the fm back-up system, and so the number of records used in the preparation of this report is 7236 (an overall data return of 82.5%). No attempt has been made to correct any bias which may have resulted from missing/invalid records, because of the uncertain reliability of available techniques. (Simple gap-filling by linear interpolation, up to a maximum of 7 consecutive records, has been carried out for the purpose of persistence calculations only: see section 3.6.) The approximate times when missing/invalid records occurred may be derived from the plots in figure 1.4 which show Hs as a time series. On these plots each vertical line represents a valid record, and the height of the line is proportional to the value of Hs for that record: therefore these plots also indicate the variation of Hs with time.

2. WIND DATA - COMPARISON WITH THE LONG-TERM AVERAGE
The meteorological station nearest to the wave measurement site is Plymouth (Mountbatten) (50°21'N, 004°07'W) where wind data have been analysed for a 15-year period from September 1966 to August 1981. Winds approaching from directions which have very limited fetches associated with them have not been considered, so that only winds in the sector from 075° to 255° have been considered in this report (including a proportion of calms and variables). The data used are hourly wind speeds.

2.1 Monthly variation of wind speeds (figure 2.1)
For each month, the monthly means of wind speed are plotted for each year. Three months (November, December and March) have monthly means which are significantly greater than their fifteen-year monthly means; and January 1981 has a monthly mean wind speed less than 50% of its 'long-term' mean.

2.2 Yearly variation of wind speeds (figure 2.2)
The year-to-year variability of wind conditions is illustrated in this figure. It shows, for each year, the maximum value of wind speed, and also the means of the next N highest wind speeds, where N = 5, 10, 20, 50, 100 (thus the highest 186 wind speeds are represented). The figure shows that the highest wind speeds in 1978/9 and 1979/80 were amongst the top wind speeds recorded in the fifteen-year period. Whilst 1980/1 shows a deficiency of very high wind speeds when compared with the other two years, its mean wind speed is the second highest for the whole fifteen-year period.

## 3. WAVE DATA - DESCRIPTION AND DISCUSSION OF THE PRESENTATIONS

Where figures show seasonal data, the seasons are defined as follows:

spring - March, April, May
summer - June, July, August
autumn - September, October, November
winter - December, January, February

The maximum value of Hs in these three years of data is 6.68 metres; the associated value of Tz is 7.98 seconds, and of Hmax(3hr) is about 12.8 metres.

### 3.1 Statistics of variations of wave heights

#### 3.1.1 Monthly variation of Hs (figure 3.1.1)

For each month, the mean of the significant wave height is calculated and plotted separately for each year. The highest values of monthly mean Hs are for March and December; January has rather low values of monthly mean Hs.

#### 3.1.2 Yearly variation of Hs (figure 3.1.2)

The year-to-year variability of wave conditions is illustrated in this figure. It shows, for each year, the maximum value of Hs, and also the means of the next N highest values of Hs, where N = 5, 10, 20, 50, 100 (thus the highest 186 values of Hs are represented). The plot shows that the mean wave conditions were quite consistent over the three years, although the very highest values of Hs for 1979/80 were about 25% higher than for the other two years.

### 3.2 Statistics of wave heights

#### 3.2.1 Occurrence of Hs (figures 3.2.1.1-3.2.1.5)

The percentage occurrence of Hs is shown on histograms. The most frequently occurring values of Hs may be seen, from figure 3.2.1.5, to lie between 0.5 and 1.0 metres, accounting for 36.1% of the total.

#### 3.2.2 Exceedance of Hs and Hmax(3hr) (figures 3.2.2.1-3.2.2.5)

These graphs may be used to estimate the fraction of the time during which Hs was greater than, or less than, a given height. For instance, from figure 3.2.2.4 it may be seen that during winter the significant wave height exceeded 3 metres for approximately 6 per cent of the time.

### 3.3 Design wave heights (figures 3.3.1(A),(B)-3.3.4(A),(B))

The methods used to calculate the design wave height (the most probable height of the highest wave with a return period of 50 years) are described in Appendix III.

The top classes of Hs (those with high probabilities of non-exceedance) are much more likely than the lower classes to come from the same population as Hs(50 years); however, since the top 5 classes, for example, contain only ½% of all the Hs observations, the statistical reliability of these classes, and therefore of the distribution estimated from them, is relatively low. As more of the lower classes are included in the estimate of the distribution so this estimate

becomes more reliable statistically, but the distribution is less likely to contain Hs(50 years). There is little relevant theory to indicate the number of upper classes which should be used to provide the best estimate of the distribution containing Hs(50 years). A rather arbitrary choice has been made to use the top 9 classes (containing 7½% of the Hs values) in the estimation of the various distributions, and the values of Hs(50 years) derived from these distributions are tabulated below; for comparison, values of Hs(50 years) based on the full data set are also tabulated. For this site, using the full and the partial data sets leads to quite large differences in Hs(50 years), larger than the differences found for other nearshore sites. The inclusion of this table of design wave heights is intended more to illustrate that the value of the design wave height depends on the fraction (arbitrarily chosen) of the Eddystone data set used, than to provide definitive values of design wave heights.

| TOP 7½% OF DATA (538 OBSERVATIONS) | | | | |
|---|---|---|---|---|
| Distribution of Hs | Parameter | Hs(50) | Approx Tz | Design Wave Height |
| Weibull | Lower limit,A=0.0m | 9.75m | 10.5sec | 18.24m |
| Fisher-Tippett I | | 9.67m | 10.5sec | 18.09m |
| Fisher-Tippett III | Upper limit,A=10m | 8.20m | 10.0sec | 15.40m |
| Individual Wave Model Steepness=1:18 1/Mean period=.218Hz | | | | 18.20m |

| ALL DATA (7236 OBSERVATIONS) | | | | |
|---|---|---|---|---|
| Distribution of Hs | Parameter | Hs(50) | Approx Tz | Design Wave Height |
| Weibull | Lower limit,A=0.33m | 9.43m | 10.5sec | 17.64m |
| Fisher-Tippett I | | 9.43m | 10.5sec | 17.64m |
| Fisher-Tippett III | Upper limit,A=6000m | 9.49m | 10.5sec | 17.76m |
| Individual Wave Model Steepness=1:18 1/Mean period=.218Hz | | | | 19.40m |

The values of design wave height derived from the individual wave model are systematically higher than those based on the Fisher-Tippett III distribution alone, for reasons stated in Appendix III.

3.4 Statistics of wave periods

The percentage occurrences of each of three wave period parameters (Tz, Tbar or Te) are shown on a histogram.

3.4.1 Occurrence of Tz (figures 3.4.1.1-3.4.1.5)

The most frequently occurring values of Tz in the data set lie between 4.0 and 4.5 seconds (18.7% of the total), and all values of Tz lie between 2.0 and 11.5 seconds (figure 3.4.1.5).

3.4.2 Occurrence of Tbar (figures 3.4.2.1-3.4.2.5)
For Tbar, the modal class is 4.0 to 5.0 seconds (31.1% of the total), and the range is from 2.0 to 13.5 seconds (figure 3.4.2.5).

3.4.3 Occurrence of Te (figures 3.4.3.1-3.4.3.5)
For Te, the modal class is 5.5 to 6.5 seconds (26.7%), and the range is from 2.5 to 15.0 seconds (figure 3.4.3.5).

3.5 Statistics of wave height and period combined
These figures (sometimes called "scatter" plots) show the numbers of wave records having particular combinations of values of Hs and period parameters (Tz, Tbar or Te). The numbers of wave records are presented as parts per thousand (the total number of valid observations being shown on each figure), except for those which would be less than one part per thousand; these are shown instead as single occurrences and are distinguished by being underlined.

3.5.1 Occurrences of Hs and Tz combined (figures 3.5.1.1-3.5.1.5)
On these figures points of equal occurrences are joined by contour lines to give an indication of the bivariate probability distribution of Hs and Tz, and to illustrate the correlation between them. A wave "steepness" (as defined in Appendix III) can be calculated for each (Hs,Tz) pair. On figure 3.5.1.5 a steepness line of 1:12 is drawn; only two (Hs,Tz) pairs calculated for the Eddystone data have greater "steepnesses" (1:11.6 and 1:11.8). (Wave "steepnesses" as shown in this figure are significantly less than the maximum of 1:7 for an individual wave, since Hs and Tz are parameters averaged over a number of waves most of which have steepnesses less than this maximum.)

3.5.2 Occurrences of Hs and Tbar combined (figures 3.5.2.1-3.5.2.5)
These figures show data boundaries similar to those of wave "steepness" in figures 3.5.1.1 to 3.5.1.5, although the physical significance of these boundaries is not so obvious.

3.5.3 Occurrences of Hs and Te combined (figures 3.5.3.1-3.5.3.5)
On these figures lines of constant wave power per unit length of wave crest are shown (in kW/m), using the formula applicable to deep water (see Appendix II). (It should be noted that using the deep water formula instead of the depth-dependent formula results in an underestimate of the wave power; the magnitude of this underestimate depends on the depth of the water and on the form of the spectrum, but it is typically about 5% at this site.)

3.6 Statistics of persistence of wave conditions
These figures show the means and standard deviations of the durations of storms and calms against each threshold value of Hs, and also the percentage of the total duration occupied by each event. Gaps in the data series of 7 or less records are filled (for the purpose of persistence calculations <u>only</u> ) by linear interpolation; larger gaps are not filled, effectively reducing the series to a number of smaller sub-series, each with a correspondingly smaller total duration. (For storms, the curves showing percentage of time occupied by the events are, for all practical

purposes, the same as those showing percentage exceedance of Hs as described in section 3.2.2.)

3.6.1 Persistence of calms of Hs (figures 3.6.1.1-3.6.1.5)
Information about, for example, calms of Hs less than 0.9 metres at the Eddystone site during winter can be derived from figure 3.6.1.4. The mean duration of such calms was approximately 23 hours (with a standard deviation of 23 hours); they occupied about 24% of the total duration of 4845 hours, i.e. about 1160 hours; and therefore there were 50 or 51 such calm events during this period.

3.6.2 Persistence of storms of Hs (figures 3.6.2.1-3.6.2.5)
Similar information can be derived for storms. For Hs of 1.9 metres during summer, figure 3.6.2.2 shows that the mean duration of such storms was approximately 10 hours (with a standard deviation of 8 hours); the total time occupied was 3% of 5607 hours, i.e. about 168 hours; and therefore the number of such storm events in this period was 16 or 17.

3.7 Distribution of wave energy with Hs and Te (figures 3.7.1-3.7.5)
For each wave record the wave energy per metre of wave crest is calculated from Hs and Te, using the formula applicable to deep water (see note in section 3.5.3). For each class of (Hs,Te) the energy from all records with Hs and Te values falling within that class is summed. The total energy within each class is then expressed in parts per thousand of the overall total energy and presented in these figures (a zero indicates less than one part per thousand, which on figure 3.7.5, for instance, means less than 156 kWh/m for the three-year period). In figure 3.7.5 it can be seen that a large proportion of the wave energy measured at the site during this three-year period is associated with values of Hs and Te in the lower halves of their ranges.

3.8 Occurrence of Qp (figures 3.8.1-3.8.5)
For each record Qp is calculated (see Appendix II) which is proportional to the degree of peakedness of the spectrum associated with the record. The most frequently occurring values of Qp in the data set lie between 1.5 and 2.0 (38.3% of the total), and all values of Qp lie between 0.5 and 9.0 (figure 3.8.5).

4. ACKNOWLEDGEMENTS
Contributions have been made towards the collection, analysis and presentation of the Eddystone wave data by several members of the Applied Wave Research Group and of the Instrument Engineering Group, both based at the Taunton laboratory of the Institute of Oceanographic Sciences. Assistance from Trinity House lighthouse keepers who informed IOS when the buoy did not appear to be operating satisfactorily, and from the Meteorological Office who supplied the wind data, is gratefully acknowledged.

## 5. REFERENCES

HUMPHERY J D 1975. Waverider moorings and their modification at IOS. 42-46 in Technology of Buoy Systems. London: Society for Underwater Technology.

HUMPHERY J D (in press). Operational experiences with Waverider buoys and their moorings. Institute of Oceanographic Sciences Report.

APPENDIX I

Method of system calibration

I.1 Method of calibration of Waverider buoys using the facilities of the National Maritime Institute, Hythe

The Waverider is clamped between two rigid parallel bars, which are supported at their mid-points on bearings mounted at the apexes of two supporting A-frames. The Waverider is driven through a vertical circle, 3 metres in diameter, by a variable speed motor through belt-drives. The buoy is maintained in the vertical position throughout by chain-drives. Rig-speed is electronically controlled, and is monitored by a tachometer giving angular velocity in revolutions per minute. However all IOS calibrations are made using a stop-watch to time several revolutions; an average rotation period is then calculated. Height-modulated radio emissions are received from the buoy on a standard Warep receiver. The receiver converts the signals into a pen-deflection on a chart recorder, and into an analogue voltage output, which is recorded on a precision chart recorder. The precision chart recorder is calibrated with a laboratory standard D.C. source, and the Warep receiver is calibrated with a precision frequency source. Hence the sensitivity of the Warep used for buoy calibration can be determined in Hz/v, and the buoy/Warep combination in V/m. Hence the buoy sensitivity in Hz/m can be derived. For a more detailed description of the Waverider calibration method, see HUMPHERY(in press).

II.2 References

HUMPHERY J D (in press). The calibration of Waverider systems by IOS Taunton. Institute of Oceanographic Sciences, Report No 133.

APPENDIX II

Method of spectral analysis and derivations of wave parameters

The digital time-series of water surface elevations (recorded for approximately 17 minutes with a sampling interval of 0.5 seconds) allows an estimate to be made of the spectrum of the sea for the three-hour period over which the time-series is considered to be representative. An outline of the method of spectral analysis used is given below.

II.1 The Fast Fourier Transform

Using the Fourier theorem, the elevation of the sea surface above its mean at time t is given by

$$h(t) = \sum_{i=1}^{\infty} \left\{ a_i \cos \frac{2\pi i t}{T} + b_i \sin \frac{2\pi i t}{T} \right\}$$

where

$$a_i = \frac{2}{T} \int_0^T h(t) \cos \frac{2\pi i t}{T} \, dt$$

$$b_i = \frac{2}{T} \int_0^T h(t) \sin \frac{2\pi i t}{T} \, dt$$

T is the record length.

The Fast Fourier Transform, based on the above relationships, is used to compute the pairs of coefficients, $a_i$ and $b_i$, at the fundamental frequency

$$f_0 = \frac{1}{T}$$

and at integral multiples of this frequency up to the Nyquist frequency

$$f_{max} = \frac{1}{2\Delta T}$$

where $\Delta T$ is the sampling interval.

The sample estimate of the spectrum at the ith frequency, $\Phi_i$, is then computed as

$$\Phi_i = \frac{1}{2f_0} (a_i^2 + b_i^2) .$$

II.2 Tapering of the data

Variance of the wave record which is not located at one of the harmonic frequencies appears in the spectral estimates not only of the harmonics adjacent to the true frequency but in a band of harmonics. This 'leakage' leads to biassed estimates in that on balance a small proportion of the variance which should appear in the neighbourhood of the spectral peak 'leaks' towards higher and lower frequencies. The effect can be reduced by tapering the ends of the time-series data smoothly to zero before performing the Fast Fourier Transform; a 'cosine taper'

applied to 12½% of the record at each end has been used on the data described in this report. (This leads to a small increase in the sampling errors of the spectral estimate.)

II.3 Smoothing the spectral estimates

The spectral estimates, $\Phi_i$, have a standard error of 100%. This large standard error may be reduced by taking the average of consecutive spectral estimates, and assigning to it the mid-frequency of the band of estimates used. Some of the data used in this report are derived from smoothed spectral estimates, $S_j$, which have been averaged in blocks of ten.

$$S_j = \frac{1}{10} \sum_{i=10j-9}^{10j} \Phi_i$$

and $$f_j = (10j - 4.5) f_0.$$

II.4 Application to the wave data

The wave data described in this report are derived from time-series containing 2048 values of sea surface elevation taken at 0.5 second intervals.

Therefore $$f_0 = \frac{1}{2048} \text{ Hz} = .0009766 \text{ Hz}$$

and $$f_{max} = 1 \text{ Hz}.$$

Smoothing the spectral estimates in blocks of ten results in 102 smoothed estimates at the following frequencies

$$f_1 = .00537 \text{ Hz}$$

$$f_{max} = .992 \text{ Hz}$$

$$\Delta f = .009766 \text{ Hz}.$$

The normalised standard error of the smoothed spectral estimates is 32%, although the tapering process increases this error by a small amount.

II.5 Definition of spectral moments

The nth moment of a continuous spectrum is

$$m_n = \int_0^\infty f^n E(f)\, df$$

where $E(f)$ is the spectral density at frequency $f$.

For the discrete spectra produced from the digital time-series, the following equation has been used in the calculation of the spectral moments.

$$m_n = \frac{1}{T} \sum_{i=i_L}^{i_U} f_i{}^n \Phi_i$$

where $i_L = 42$; $(f_{42} = .0410\text{Hz})$,
$i_U = 651$; $(f_{651} = .6357\text{Hz})$.

II.6 Derivation of wave parameters

The wave parameters presented in this report are derived from the spectral moments using the following identities.

$$Hs = 4\sqrt{m_0}$$

$$Tz = \sqrt{\frac{m_0}{m_2}}$$

$$\overline{T}\ (Tbar) = \frac{m_0}{m_1}$$

$$Te = \frac{m_{-1}}{m_0}\ .$$

The spectral peakedness parameter Qp (GODA(1970)) is computed from

$$Qp = \frac{2\sum_{j=j_L}^{j_U}(f_j S_j^2)}{Tm_0^2}$$

where $j_L = 5$; ($f_5 = .0444$Hz)
$j_U = 65$; ($f_{65} = .6304$Hz).
(It should be noted that the smoothed spectral estimates are used in the calculation of the peakedness parameter.)

Wave power may be calculated from the spectra using the expression

$$P = \int E(f)\, V_g(f,d)\, df$$

where $V_g$ is the group velocity at frequency f and in water of depth d. An approximation to this expression has been used in this report, based on the assumption that the wave measurements were made in deep water: in this case

$$V_g(f,d) = V_g(f) = \frac{g}{4\pi f}$$

which leads to

$$P' = 0.49\, Hs^2\, Te$$

where $P'$ is in kilowatts per metre of wave crest
Hs is in metres
Te is in seconds.

II.7 Reference

GODA Y 1970. Numerical experiments on wave statistics with spectral simulation. Report of the Port and Harbour Research Institute 9, No 3, 3-57.

APPENDIX III

Details of methods used for calculating design wave heights

III.1 By finding the long-term distribution of Hs

III.1.1 Hs is used as a measure of the "sea-state" (i.e. the intensity of wave activity), and it is sampled every 3 hours. It is assumed that a set of Hs data for one year, or an integral number of years, is representative of the wave climate.
For each value of Hs, the probability that this value will not be exceeded is calculated; this probability is then plotted against Hs. The axes are scaled according to a long-term distribution, so that data with a perfect fit would appear as a straight line on the diagram. This procedure is carried out using long-term distributions defined in the following ways

Weibull

$$\text{Prob}(Hs \leqslant h) = \begin{cases} 1 - \exp\left[-\left(\frac{h-A}{B}\right)^C\right], & \text{for } h > A \\ 0, & \text{for } h \leqslant A \end{cases}$$

where B and C are positive, and A represents a lower bound on h.

Fisher-Tippett I (first asymptote)

$$\text{Prob}(Hs \leqslant h) = \exp\left[-\exp(-ah+b)\right].$$

Fisher-Tippett III (third asymptote)

$$\text{Prob}(Hs \leqslant h) = \begin{cases} \exp\left[-\left(\frac{A-h}{B}\right)^C\right], & \text{for } h \leqslant A \\ 1, & \text{for } h > A \end{cases}$$

where B and C are positive, and A represents an upper bound on h. (See FISHER AND TIPPETT(1928) and GUMBEL (1958) for the derivations of these distributions.)

For each long-term distribution the best-fit straight line is drawn; this line is then extrapolated to the desired probability (see section III.1.2) and the corresponding value of Hs is read off as the "design sea-state".

III.1.2 To calculate the "sea-state" which will be exceeded only once in N years, a storm duration of D hours needs to be assumed. The probability that a randomly chosen time will be within this storm is then

$$\frac{D}{24 \times 365.25 \times N}$$

IOS uses D = 3 hours (this choice is discussed in section III.1.5) which gives

$$\text{Probability} = \frac{3.422 \times 10^{-4}}{N}$$

$$= 6.845 \times 10^{-6} \quad \text{for} \quad N = 50 \text{ years.}$$

III.1.3 The value of Tz for the "design sea-state" is required before the highest wave in the storm can be calculated. This is derived from the bivariate distribution of Hs and Tz (figure 3.5.1.5). A line is drawn across this at the "design sea-state" value of Hs and the most likely value of Tz (the modal value) is then estimated using extrapolations of the probability contours.

III.1.4 The most probable value of the highest zero-up-cross wave in the storm is then derived by assuming that the heights of such waves follow a Rayleigh distribution whose probability density function is

$$\text{prob}(h) = \frac{2h}{(Hrms)^2} \exp\left[-\left(\frac{h}{Hrms}\right)^2\right]$$

where $Hrms \approx \frac{Hs}{\sqrt{2}}$ .

Exact theory is not available for zero-up-cross wave heights, but this distribution has been found to be an adequate fit to measured data. If there are n waves in the recording interval (3hr), then the probability that the highest wave, H, in three hours is less than h is

$$\text{Prob}(H \leq h) = \left\{1 - \exp\left[-\left(\frac{h}{Hrms}\right)^2\right]\right\}^n$$

with a corresponding probability density function

$$\frac{2n}{(Hrms)^2} h \exp\left[-\left(\frac{h}{Hrms}\right)^2\right] \left\{1 - \exp\left[-\left(\frac{h}{Hrms}\right)^2\right]\right\}^{n-1} .$$

The most probable value (the mode) of this probability density function is usually used and is given by

$$Hmax(3hr) = Hrms\sqrt{\Psi}$$

where $\Psi$ is a function of Tz which may be found using either figure 7 or equation 6.1-2 in TANN(1976).

III.1.5 In choosing the value of storm duration D, it should be noted that the effect of increasing D is to decrease the value of Hs for a given return period N. However, it also increases the ratio of Hmax(3hr) to Hs. It is found that in practice these effects roughly cancel and typically the value of Hmax(3hr) changes by only 3 per cent for a change of D from 3 to 15 hours. The choice of D is therefore not critical.

Many details of the above procedures may be found in TANN(1976).

III.2 By a wave-by-wave method

III.2.1 BATTJES(1970) shows that the probability that a randomly chosen wave will have a height $H$ greater than $h$ is

$$\text{Prob}(H>h) = \frac{\int_0^\infty \int_0^\infty R(h,Hs)\, Tz^{-1}\, p(Tz,Hs)\, dHs\, dTz}{\int_0^\infty \int_0^\infty Tz^{-1}\, p(Tz,Hs)\, dHs\, dTz} \quad \ldots\ldots\ldots\ldots\ldots\ldots (1)$$

where $R(h,Hs)$ is the Rayleigh cumulative probability function and $p(Tz,Hs)$ is the joint probability density function of Hs and Tz.

III.2.2 TANN makes the following suggestion in an unpublished manuscript. In order that values of Hs higher than those actually measured may be represented in the calculation of this probability, the values of Hs are assumed to have a long-term cumulative probability function $F(Hs)$, and a probability density function $f(Hs) = F'(Hs)$.

For each value of Hs throughout the long-term distribution, an average value of $Tz^{-1}$ is used (denoted by $\overline{Tz^{-1}(Hs)}$). It is defined as

$$\overline{Tz^{-1}(Hs)} = \int_0^\infty Tz^{-1}\, \frac{p(Tz,Hs)}{P(Hs)}\, dTz$$

where $P(Hs) = f(Hs)$.

Therefore

$$\int_0^\infty Tz^{-1}\, p(Tz,Hs)\, dTz = \overline{Tz^{-1}(Hs)}$$

which, when substituted into equation (1), allows the probability of exceedance to be written

$$\text{Prob}\,(H>h) = \frac{\int_0^\infty R(h,Hs)\, \overline{Tz^{-1}(Hs)}\, f(Hs)\, dHs}{\int_0^\infty \overline{Tz^{-1}(Hs)}\, f(Hs)\, dHs} .$$

The value of $\overline{Tz^{-1}(Hs)}$ used with each value of Hs is chosen to satisfy the condition of constant wave "steepness", where the relationship between "steepness"(1:s), water depth(d), Hs and Tz is

$$Tz = \sqrt{\frac{2\pi s Hs}{g}\, \coth\left(\frac{2\pi d}{sHs}\right)} .$$

The value for the steepness used in this report is given in section 3.3.4.

The long-term distribution used in the computation for this report is the Fisher-Tippett III extreme-value distribution, whose probability density function is

$$f(Hs) = \frac{C}{A-Hs}\left(\frac{A-Hs}{B}\right)^C \exp\left[-\left(\frac{A-Hs}{B}\right)^C\right] .$$

The constants A,B,C are determined graphically as described in section III.1.1, and their values as used in this report are given in section 3.3.3.

III.2.3 Thus the probability of a wave exceeding each particular wave height may be found, and this probability may be converted into a return period of N years using the formula

$$N = \frac{1}{365.25 \times 24 \times 3600 \times Tave^{-1} \times Prob}$$

where $Tave^{-1} = \frac{1}{\text{average period}}$ .

The value of the average wave period is contained in section 3.3.4. Since $Tave^{-1}$ is a non-analytic function of Prob, the simplest way of solving the problem is to calculate Prob for various values of h, calculate N for each of these values of Prob, and then interpolate to find the height h corresponding to the required value of N (in this case 50 years).

Whereas the method described in section III.1 assumes that the highest wave in a 50-year period will come from the most stormy 3-hour period in 50 years, the individual wave method takes into account the probability that storms other than the highest may provide the wave with a 50-year return period. Consequently the height of a 50-year wave as estimated by this method is likely to be greater than that estimated from the method of using a long-term distribution of Hs.

III.3 References

BATTJES J A 1970. Long-term wave height distribution at seven stations around the British Isles. National Institute of Oceanography, Internal Report No A44.

FISHER R A AND TIPPETT L H C 1928. Limiting forms of frequency distribution of the largest or smallest member of a sample. Proceedings of the Cambridge Philosophical Society 24, 180-190.

GUMBEL E J 1958. Statistics of Extremes. New York: Columbia University Press. 371 pp.

TANN H M 1976. The estimation of wave parameters for the design of offshore structures. Institute of Oceanographic Sciences, Report No 23.

APPENDIX IV

## A comparison between the Eddystone buoy and a short term deployment in more exposed water

### IV.1 Procedure

An additional waverider buoy recording simultaneously with the long term buoy was deployed in deeper, more exposed water. By comparing the data collected by the two buoys it was hoped to discover whether the wave climate recorded at the inshore site (referred to in the main text of this report) is of more general application to the sea area to the south of the Eddystone or is specific to only a localised area near the reef.

### V.2 Site description.

The site at which the buoy operated was some 3 km south of the inshore buoy (figure 1) at position 50°08´N 4°10.5´W. The mean water depth of 73m was typical of the general area and contrasts with the mean depth of 40m at the inner buoy position.

### IV.3 Measuring and recording. Buoy calibration and maintenance.

Full details of the measuring and recording systems and their calibration and maintenance can be found in the main text paragraphs 1.2 and 1.3, and appendix I.

### IV.4 Wave data coverage (figures 4.1.1 and 4.1.2).

The comparisons were carried out using data collected from the buoys between December 1981 and February 1982. All the data were subjected to the initial analysis described in appendix II. However the number of records which could be compared was determined by the limited data return from the deep water site. A buoy was deployed on 1 December 1981 and was subsequently lost, presumed sunk,on the 16 December. A second buoy deployed at the same site on 22 January 1982 suffered a similar fate on 12 February. This gave a total of 249 acceptable record pairs for comparison, equivalent to 31 days.

### IV.5 Wind data (figure 4.2).

Wind data were obtained from the meteorological station at Plymouth (Mountbatten) ( 50°21´N 004°07´W ) for the period of the experiment. Those data collected at times when wave records were compared are presented in the form of a wind rose. The coastline lies to the north of the buoys stretching from headlands approximately 075° (Prawle Point) to 255° (the Lizard ) , with a completely open water sector, leading to the Atlantic, between 200° (I.d'Ouessant) and 255°.

IV.6 Comparison of Hs and Tz (figures 4.3.1 and 4.3.2).
The comparison of these data when separated into two sets covering each of the two deep water buoy deployments showed no significant differences, therefore all further analysis was carried out on the combined sets.
Both Hs and Tz from the two sites were highly correlated. Standard least squares regression techniques were used to fit a linear model to the data. These predictive models were used so that the best estimates of the deep water conditions could be found given the results contained in the main body of this report. From this work

$$Hsd = 0.14 + 0.88\ Hsi$$
$$Tzd = 0.67 + 0.84\ Tzi$$

where the suffices d (deep water) and i(long term -inshore) are used for the buoy positions.
These results show that waveheights at the deepwater site were from +2% ( Hsi = 1m ) to -9% ( Hsi = 5m ) relative to the inshore conditions. Wave periods at the deepwater site were from +6% (Tzi = 3s) to -10% (Tzi = 12s) compared with the inshore site. Further work was carried out in an attempt to identify the mechanisms causing these differences ( section IV.8 ).
Attention should be drawn to the atypical wind conditions, as compared to the long term, experienced during these deployments. The major events ( Hs > 2m ) occured with NW or SE winds, indeed the bulk, some 46 % , of the winds for the whole period were offshore and only 16 % from the prevailing SW sector.

IV.7 Comparison of spectra (figure 4.4).
The two spectra shown are each derived by taking the average energy content of each frequency band for all the valid records used in the comparison.The marked energy decrease at the lower end of the spectrum recorded for the outer site shows why the Hs and Tz values are expected to be lower than the inner buoy (evident from the models for Hs > 1m; Tz > 4s). As all the buoys were carefully calibrated prior to deployment and the inner buoy was recalibrated after recovery with particular attention being paid to the low frequency end of its response, it is believed that the differences in the spectra cannot be attributed to instrument malfunction. This belief is further reinforced by the similarity found when the inshore buoy is compared to the two outer buoy data sets seperately.

IV.8 Mechanisms for wave climate differences (figure 4.5).
Three potential sources of wave modification were considered for the area around the Eddystone rocks, these were refraction, reflection and tidal currents.
1) Wave refraction investigations were carried out using IOS computer programs based on the theory developed by the Hydraulics Research Station (1974). The deepwater parameters were used as boundary conditions and the inshore buoy position as the target zone.

Hs values were found to be greater at the inshore site when waves approaching from the open water sector were associated with deepwater periods greater than 8 seconds. The increase reached a maximum of 10% for Tzd = 10s and approach angle 210°. These changes were associated with an increase of energy at the lower frequency end of the spectrum so that individual smoothed estimates could increase by up to 50%.
The wind sea was usually fetch-limited, and came from the open water sector for only 16% of the time. However inspection of individual spectra showed that there were always small and sometimes significant amounts of energy in the swell band (~ 0.1Hz). This indicates that there was always a band of frequencies which would have been subjected to refraction.
The individual spectra were examined in more detail to see if the averaging performed to obtain figure 4.4 hid useful information. The pairs of individual spectral estimates were compared for each of the smoothed estimates. A linear model passing through the origin was fitted to the data minimising the perpendicular sum of squares. The slopes obtained gave a mean ratio for each estimate and its associated confidence limits. Except for the first two these are plotted as figure 4.5.The effects of refraction are clearly visible at low frequencies.
2) Further inspection of figure 4.5 shows regular oscillations in the plot extending throughout the frequency range. This type of pattern is similar to that produced by standing wave effects. However calculations of wave reflection were inconclusive due to the difficulties in precisely identifying both the depth and distance of a reflector near the inshore site. Therefore it was not possible to confirm that the patterns were due to reflection.
3) Finally it was observed that the maximum ratios of Hs values were mostly associated with spring tides. However there were insufficient data available to confirm this as a contributory factor to the modification of the wave regime at the Eddystone.

In summary, the differences between the two buoy sites can be explained almost completely by refraction effects. There is evidence to suggest that wave reflection and tidal current effects may have a limited effect depending upon the prevailing open water conditions.

References

ABERNETHY,C.L. and GILBERT,G.1974.Refraction of a wave spectrum. Hydraulics Research Station HRS INT 117

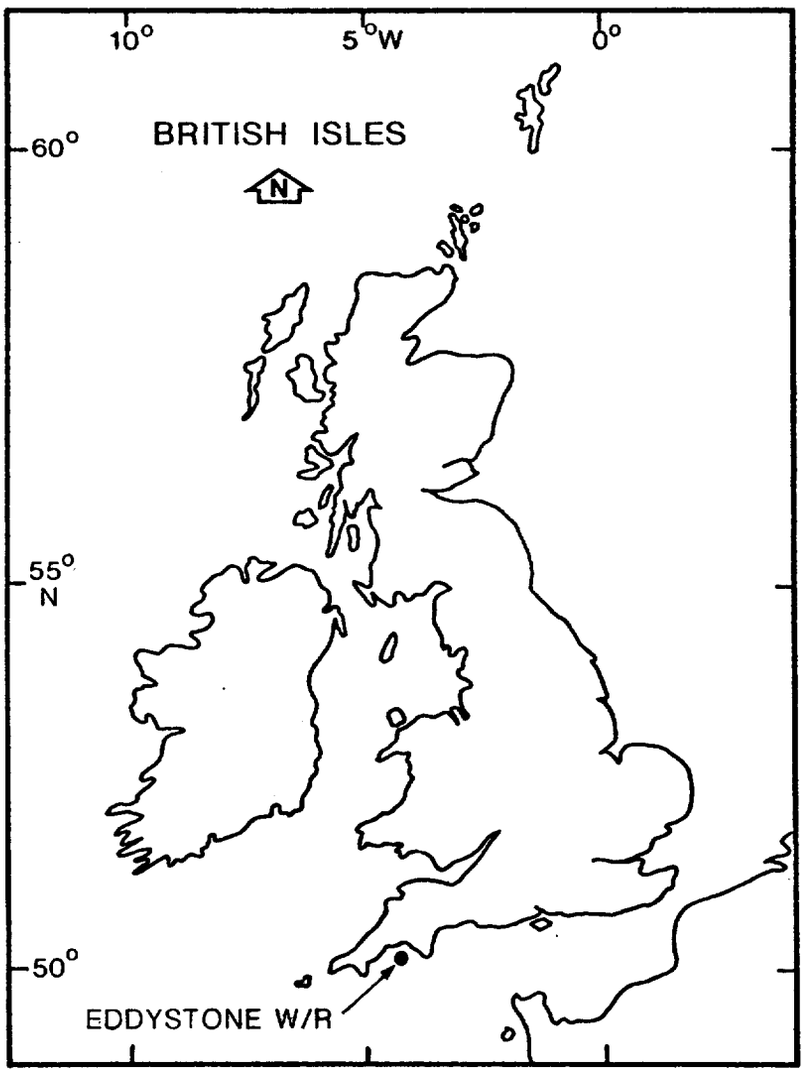


LOCATION MAP OF EDDYSTONE WAVERIDER BUOY

FIG 1.1

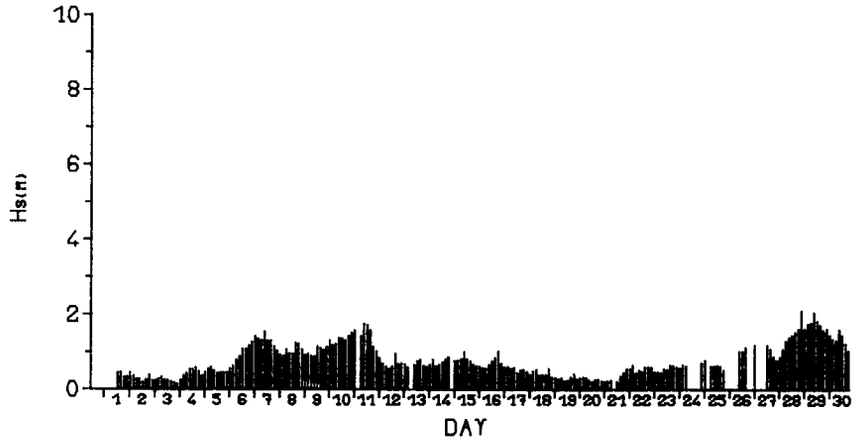


SEP 1978

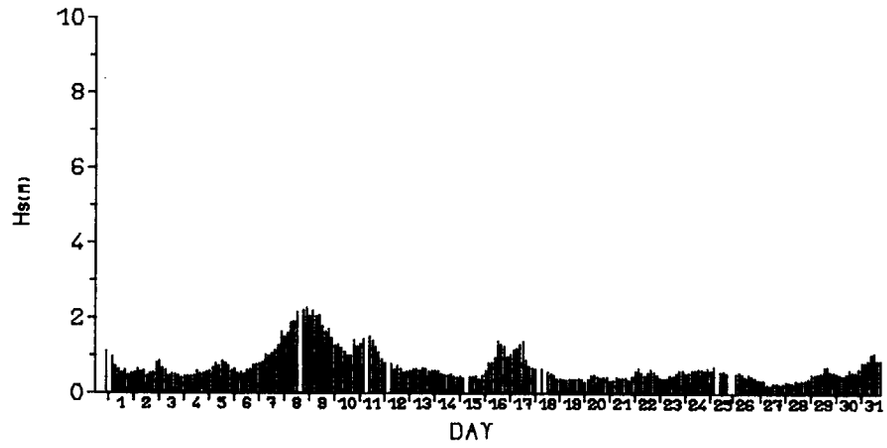


OCT 1978

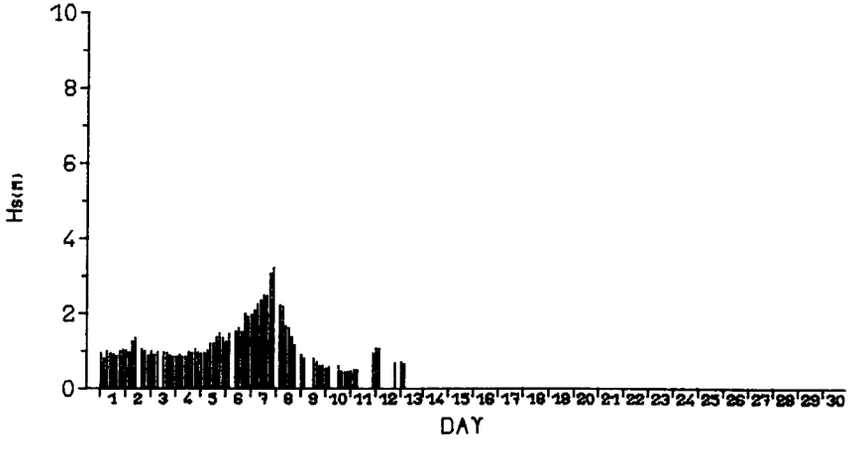


NOV 1978

# TIME SERIES OF Hs

# EDDYSTONE SEPT 1978 - AUG 1981

FIG 1.4(A)

ED7881

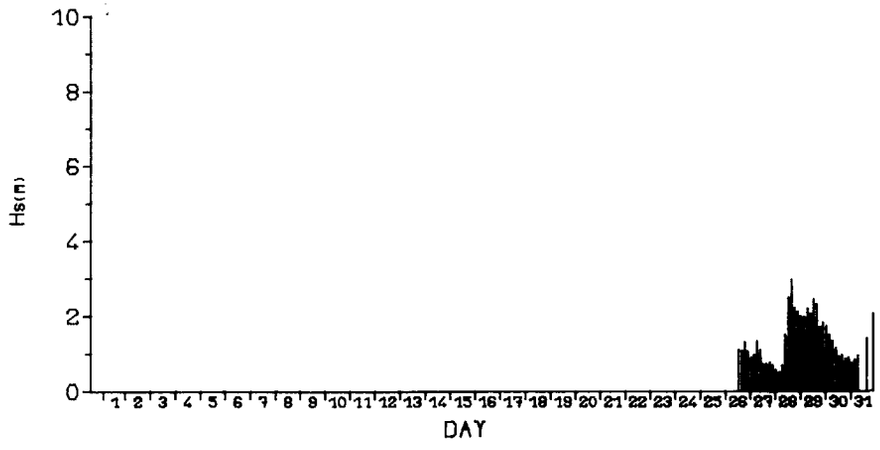


JAN 1979

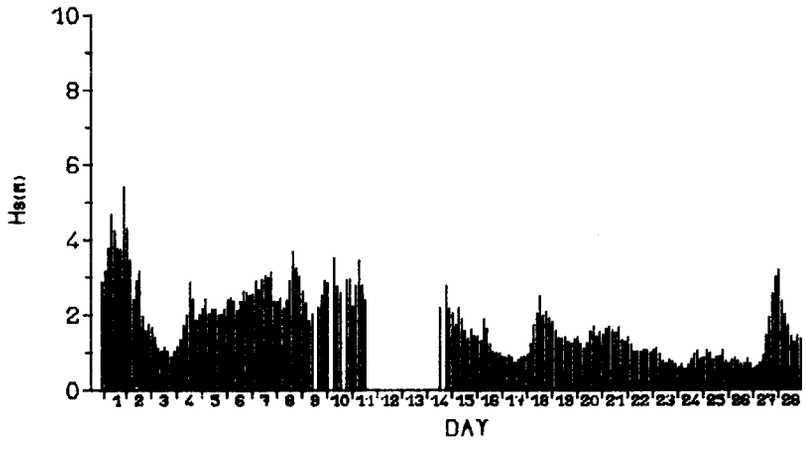


FER 1979

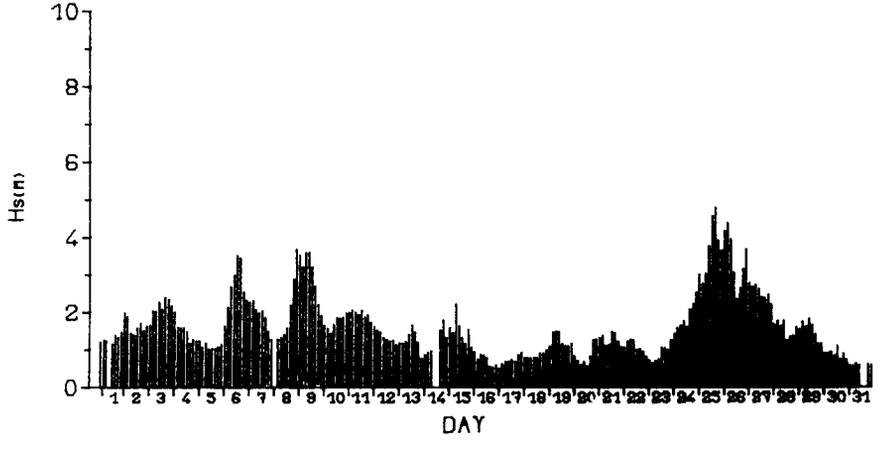


MAR 1979

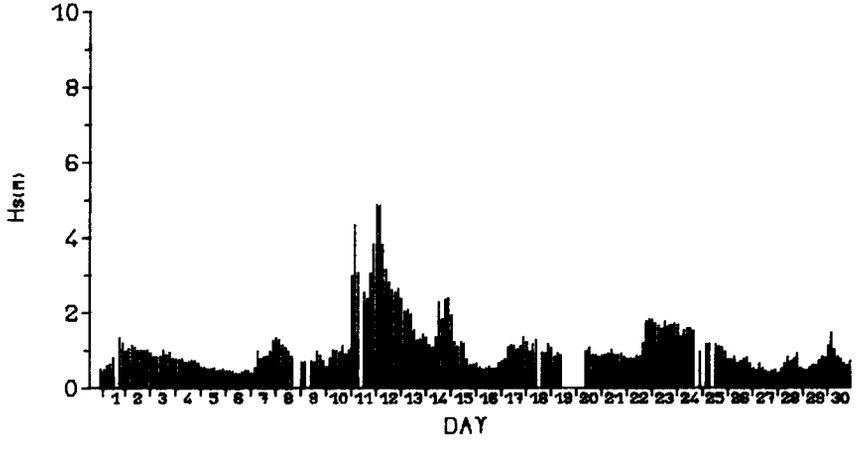


APR 1979

# TIME SERIES OF Hs

# EDDYSTONE SEPT 1978 - AUG 1981

FIG 1.4(B)

ED7881

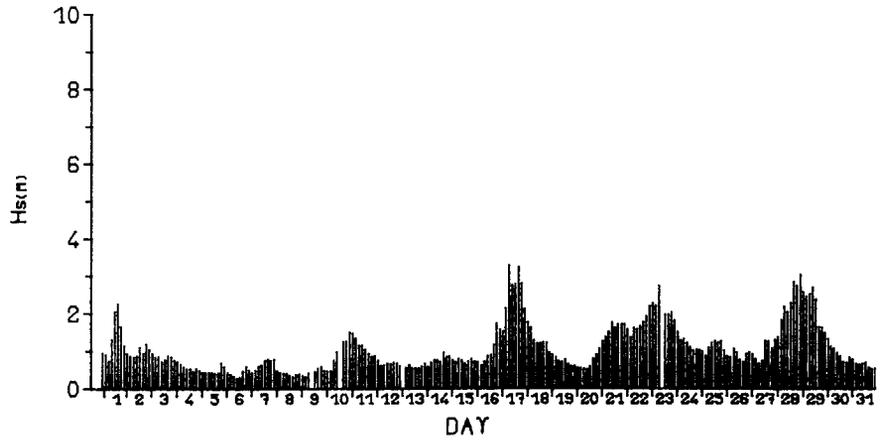


MAY 1979

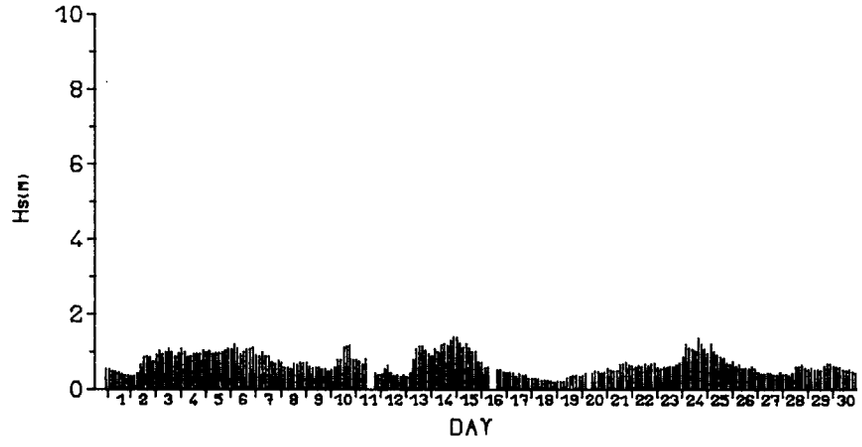


JUN 1979

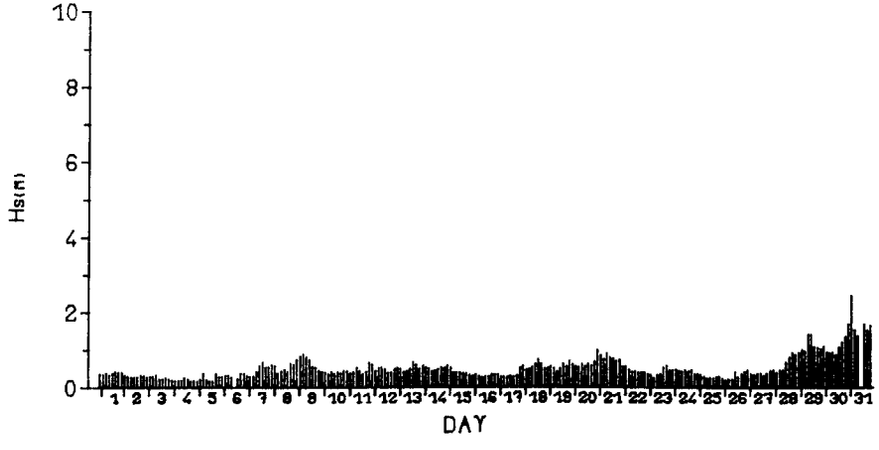


JUL 1979

# TIME SERIES OF Hs

# EDDYSTONE SEPT 1978 - AUG 1981

FIG 1.4(C)

ED7881

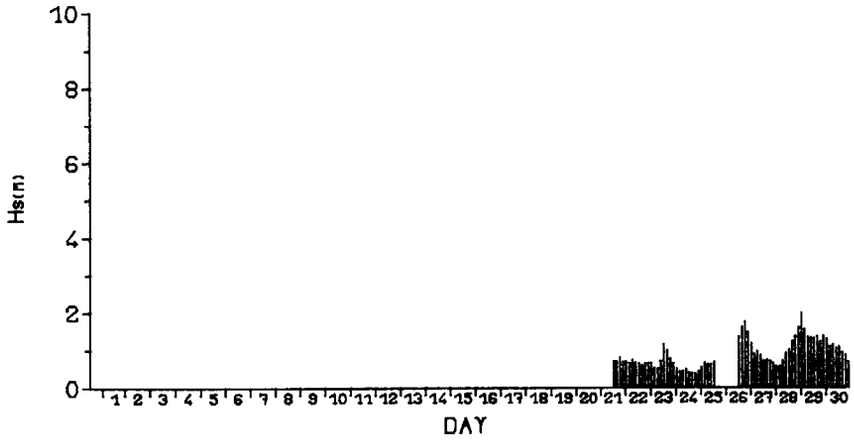


SEP 1979

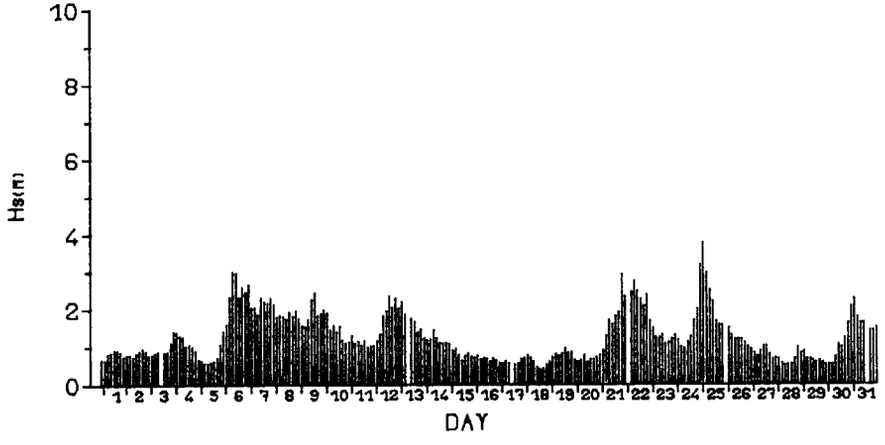


OCT 1979

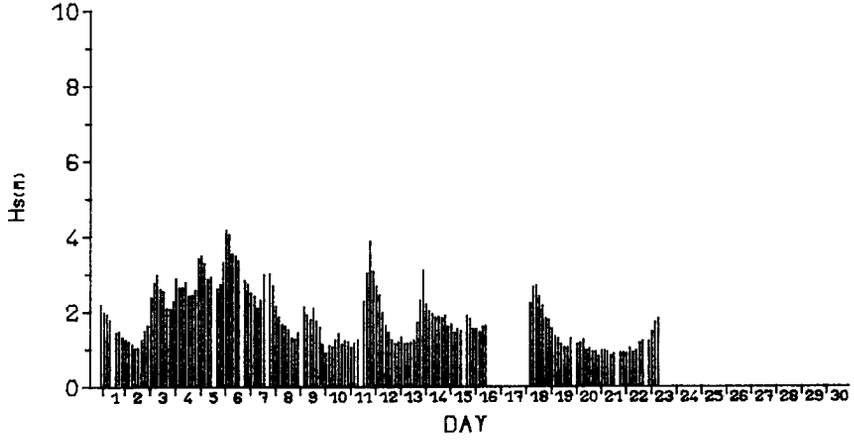


NOV 1979

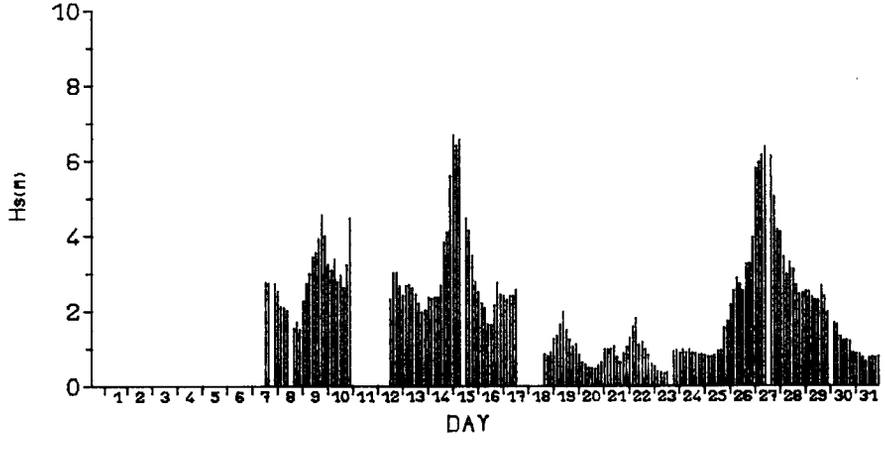


DEC 1979

# TIME SERIES OF Hs

# EDDYSTONE SEPT 1978 - AUG 1981

FIG 1.4(D)

ED7881

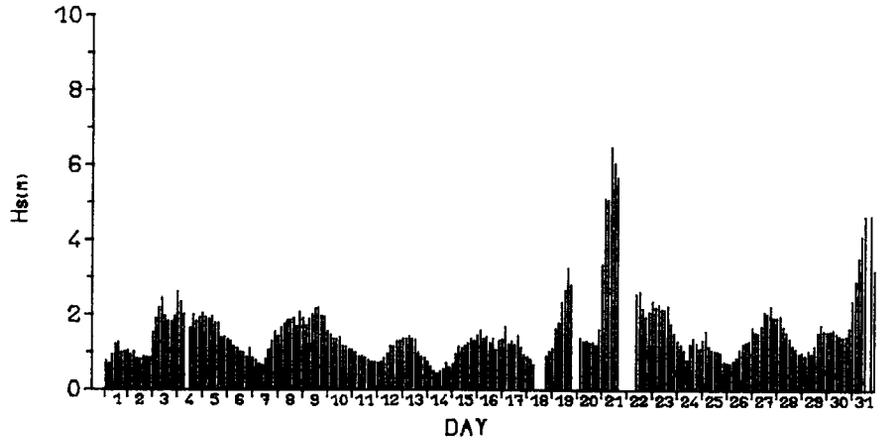


JAN 1980

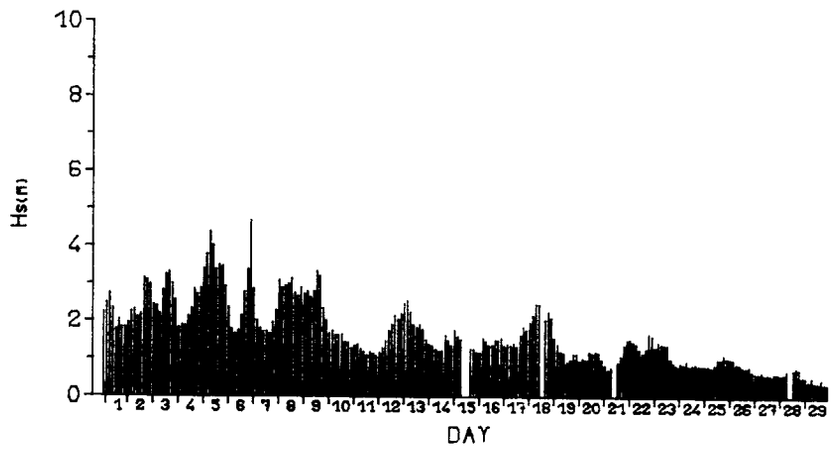


FEB 1980

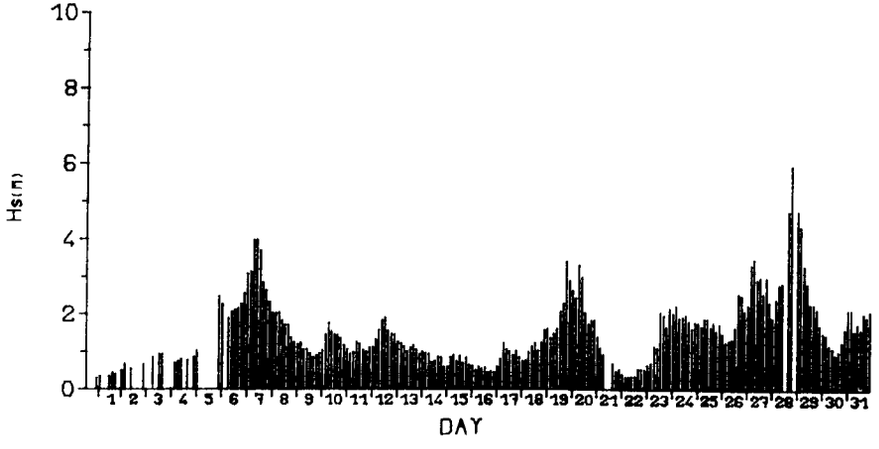


MAR 1980

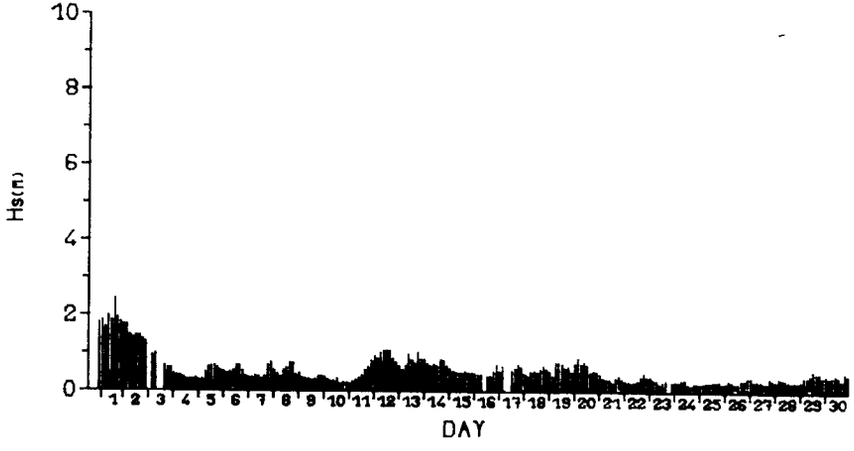


APR 1980

# TIME SERIES OF Hs

# EDDYSTONE SEPT 1978 - AUG 1981

FIG 1.4(E)

ED7881

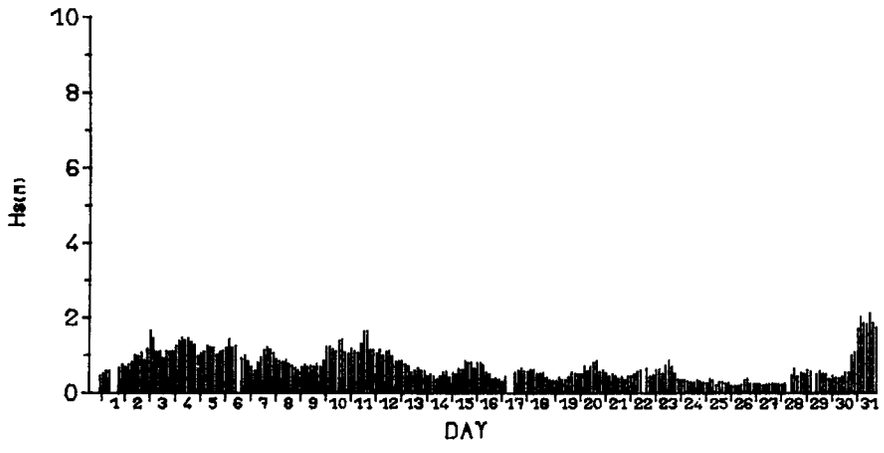


MAY 1980

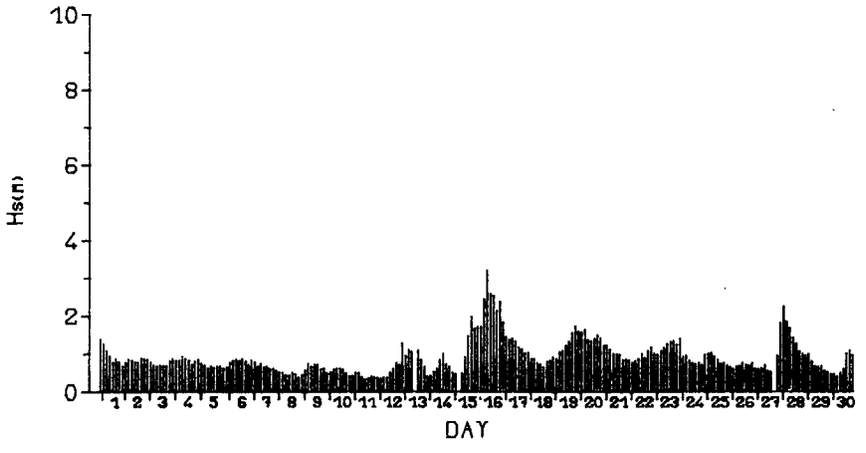


JUN 1980

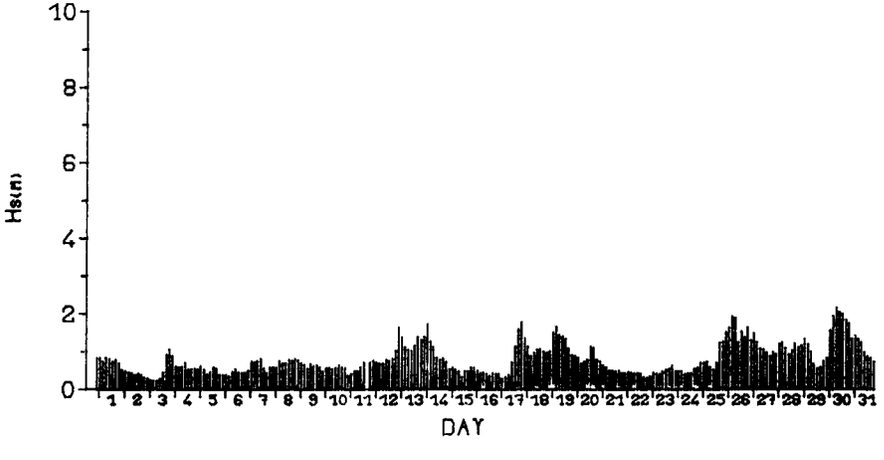


JUL 1980

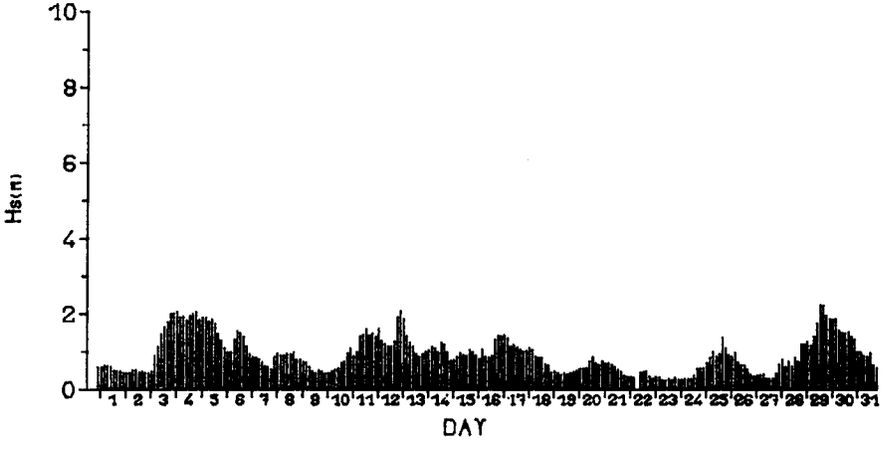


AUG 1980

# TIME SERIES OF Hs

# EDDYSTONE SEPT 1978 - AUG 1981

FIG 1.4(F)

ED7881

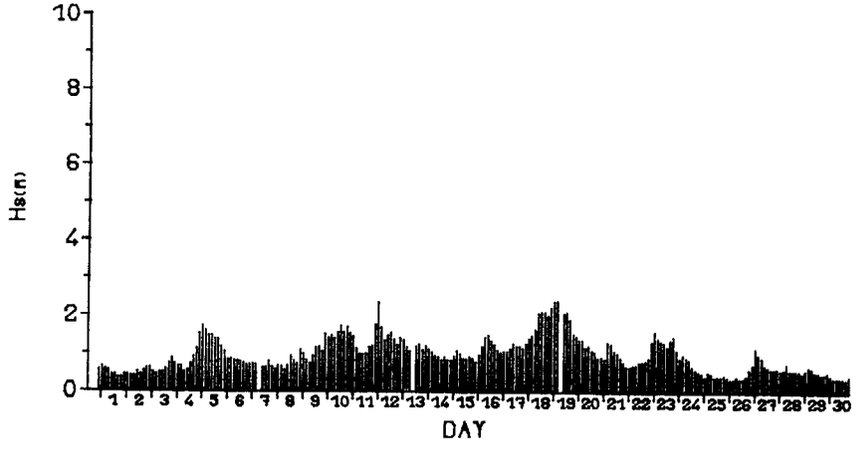


SEP 1980

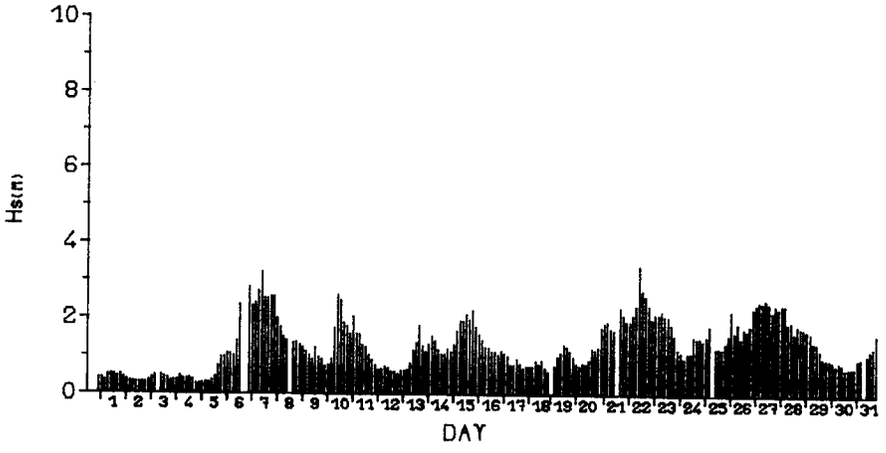


OCT 1980

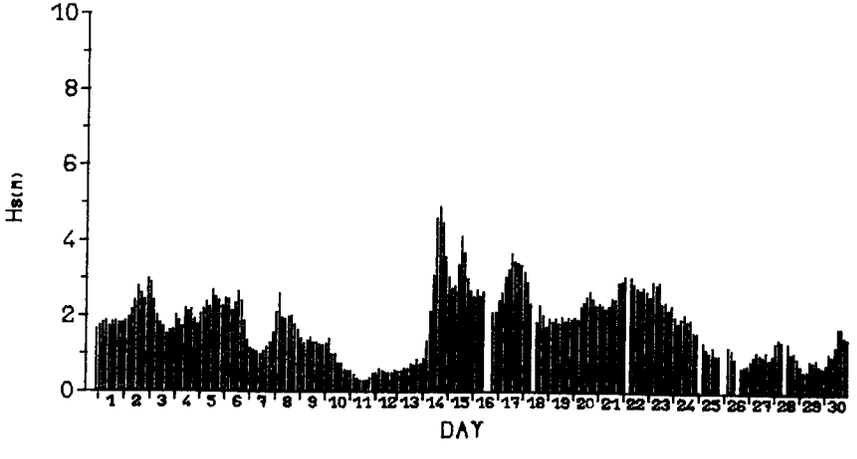


NOV 1980

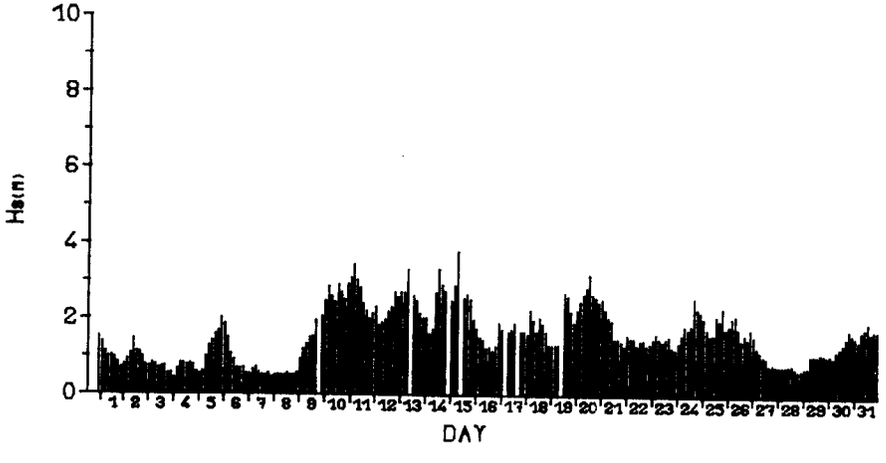


DEC 1980

# TIME SERIES OF Hs

# EDDYSTONE SEPT 1978 - AUG 1981

FIG 1.4(G)

ED7881

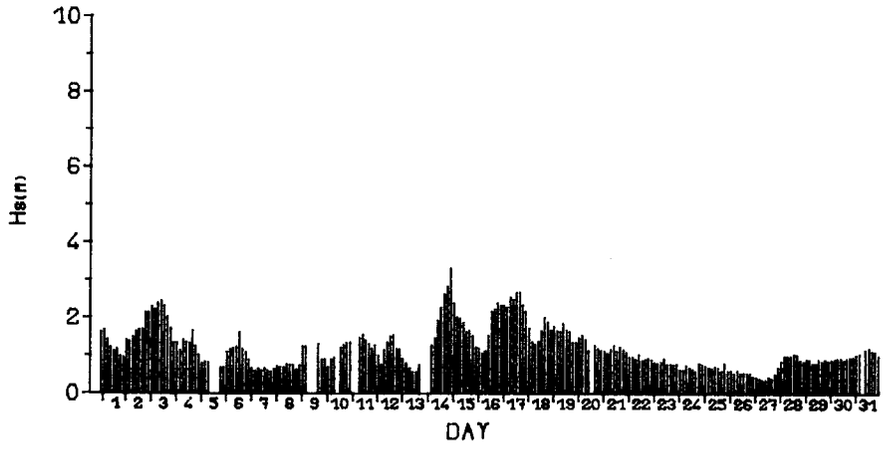


JAN 1981

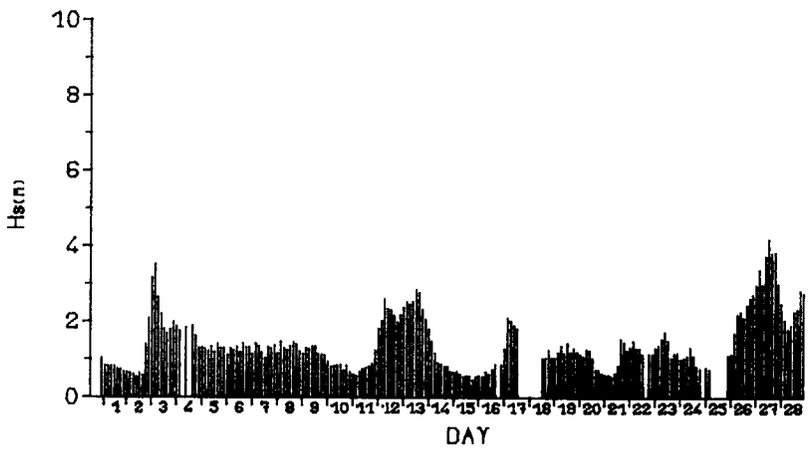


FEB 1981

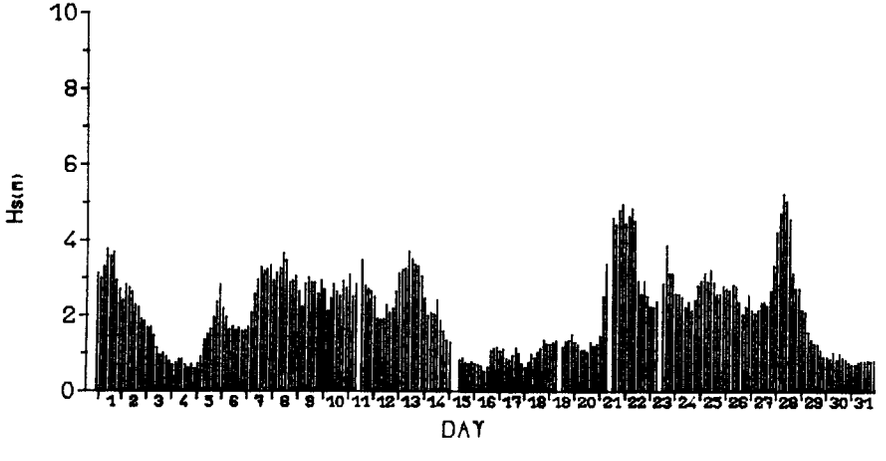


MAR 1981

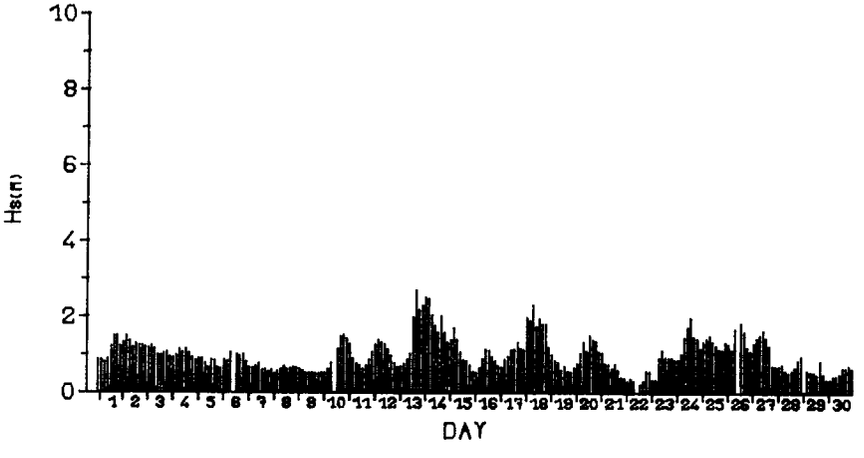


APR 1981

# TIME SERIES OF Hs

# EDDYSTONE SEPT 1978 - AUG 1981

FIG 1.4(H)

ED7881

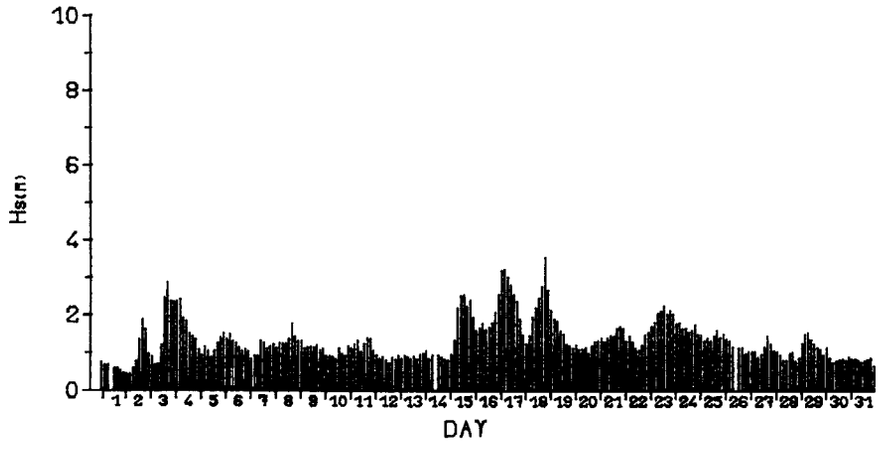


MAY 1981

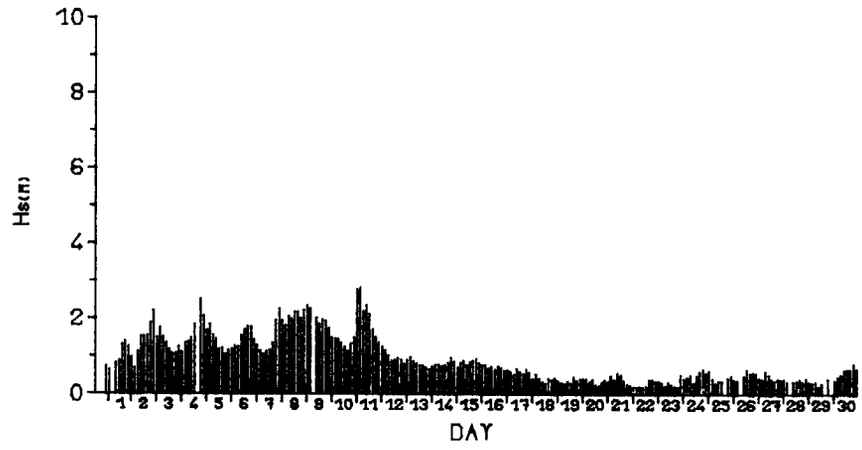


JUN 1981

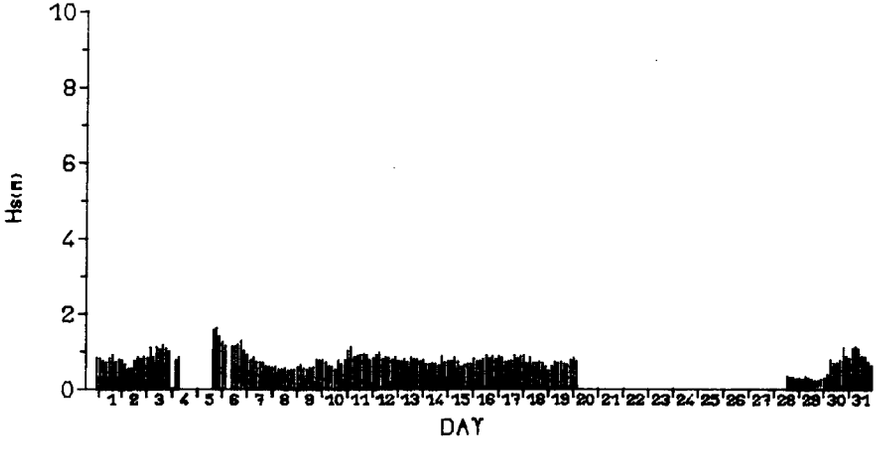


JUL 1981

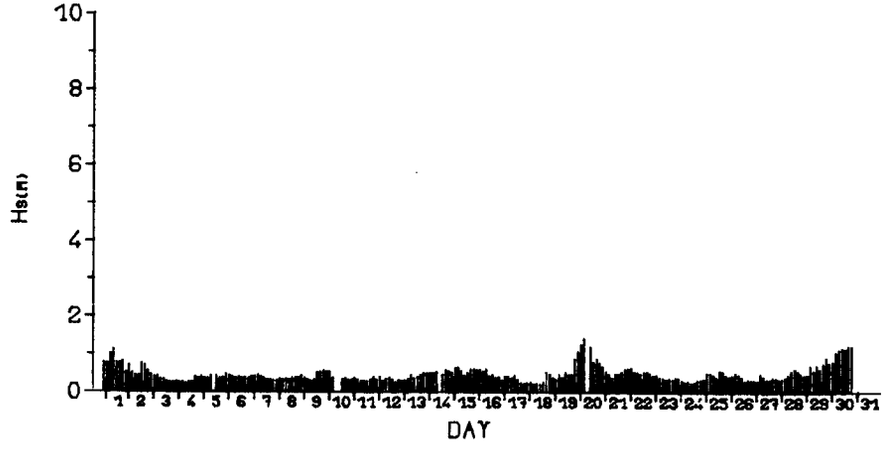


AUG 1981

# TIME SERIES OF Hs

# EDDYSTONE SEPT 1978 - AUG 1981

FIG 1.4(I)

ED7881

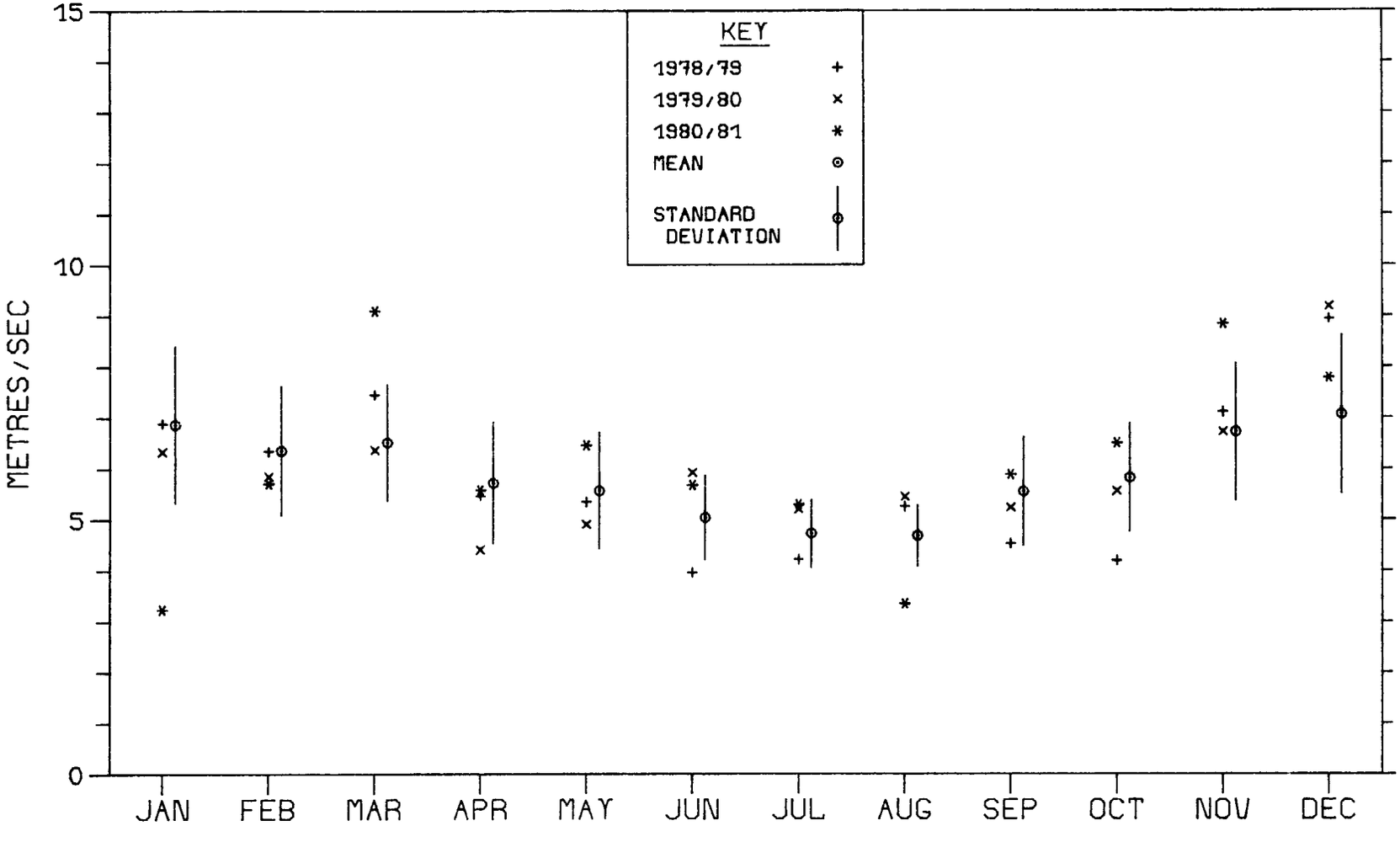


MEAN AND STANDARD DEVIATION OF THE MONTHLY MEAN OF WIND SPEED

PLYMOUTH SEP 1966 - AUG 1981

FIG 2.1

CA7881

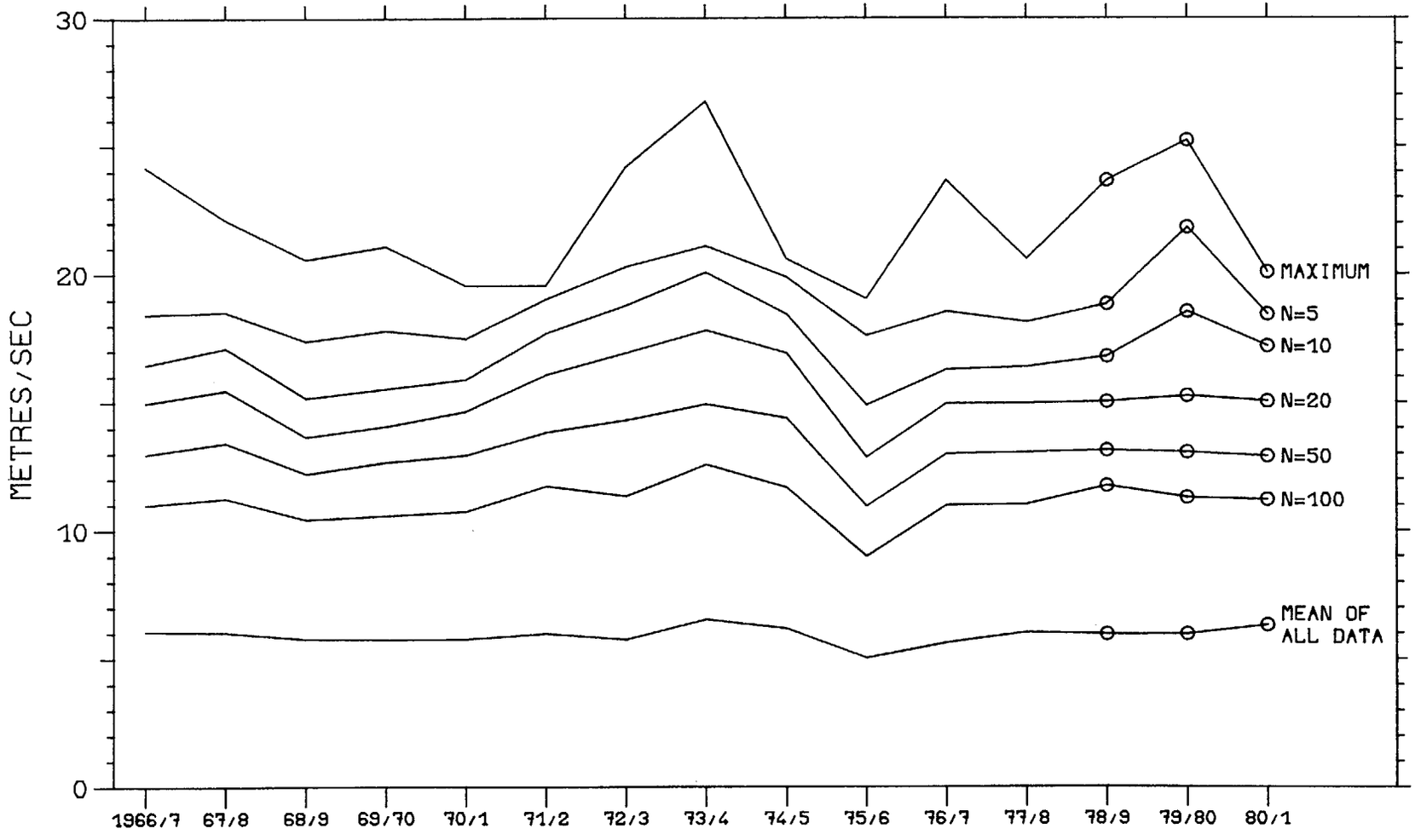


MEAN OF N LARGEST VALUES OF WIND SPEED

EDDYSTONE SEP 1966 - AUG 1981

FIG 2.2

CA7881

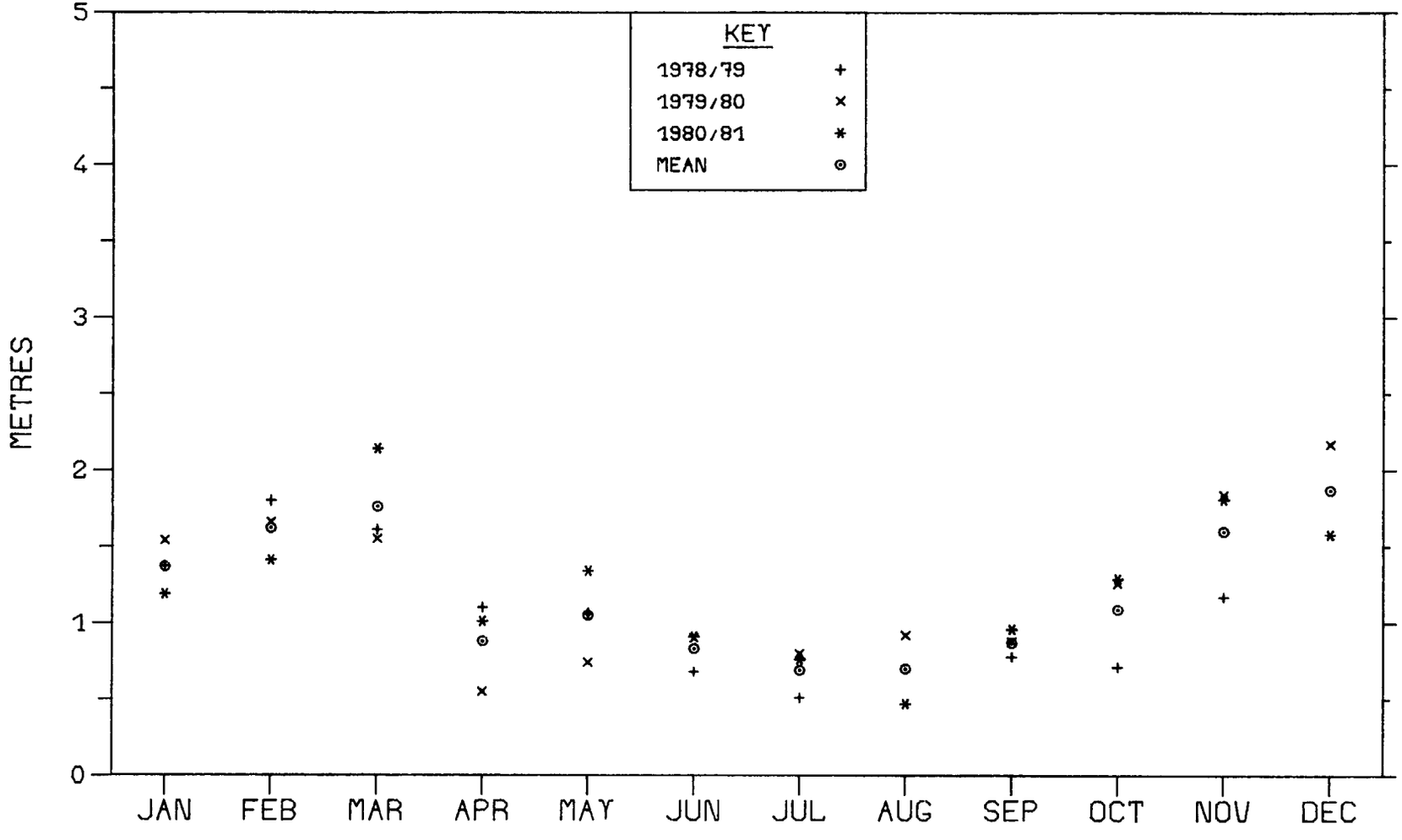


MONTHLY MEANS OF Hs FOR EACH YEAR

EDDYSTONE SEPT 1978 - AUG 1981

FIG 3.1.1

CA7881

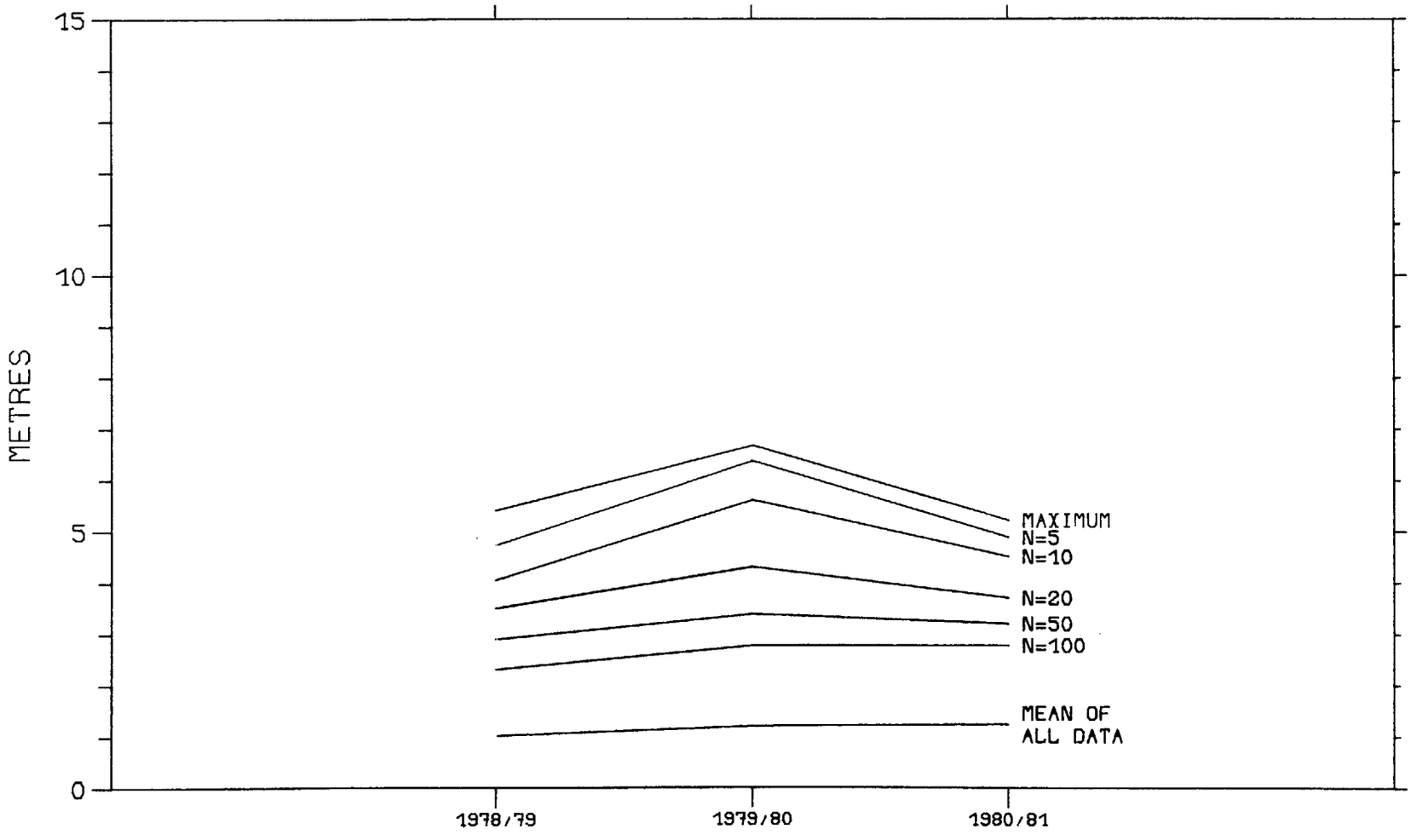


MEAN OF N LARGEST VALUES OF Hs

EDDYSTONE SEPT 1978 - AUG 1981

FIG 3.1.2

CA7881

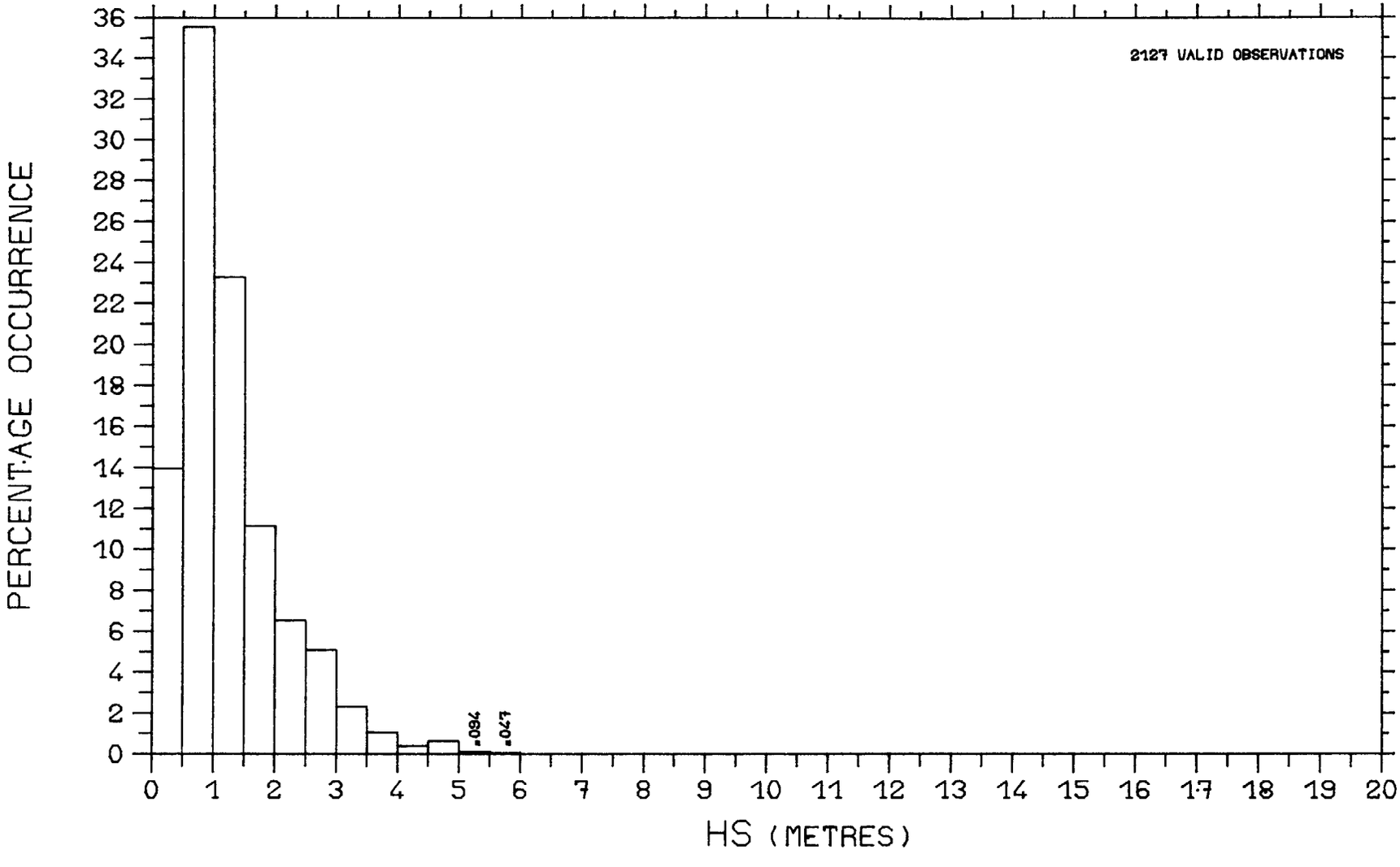


PERCENTAGE OCCURRENCE HISTOGRAM

EDDYSTONE SEPT 1978 - AUG 1981 SPRINGS

3.2.1.1

CA7881

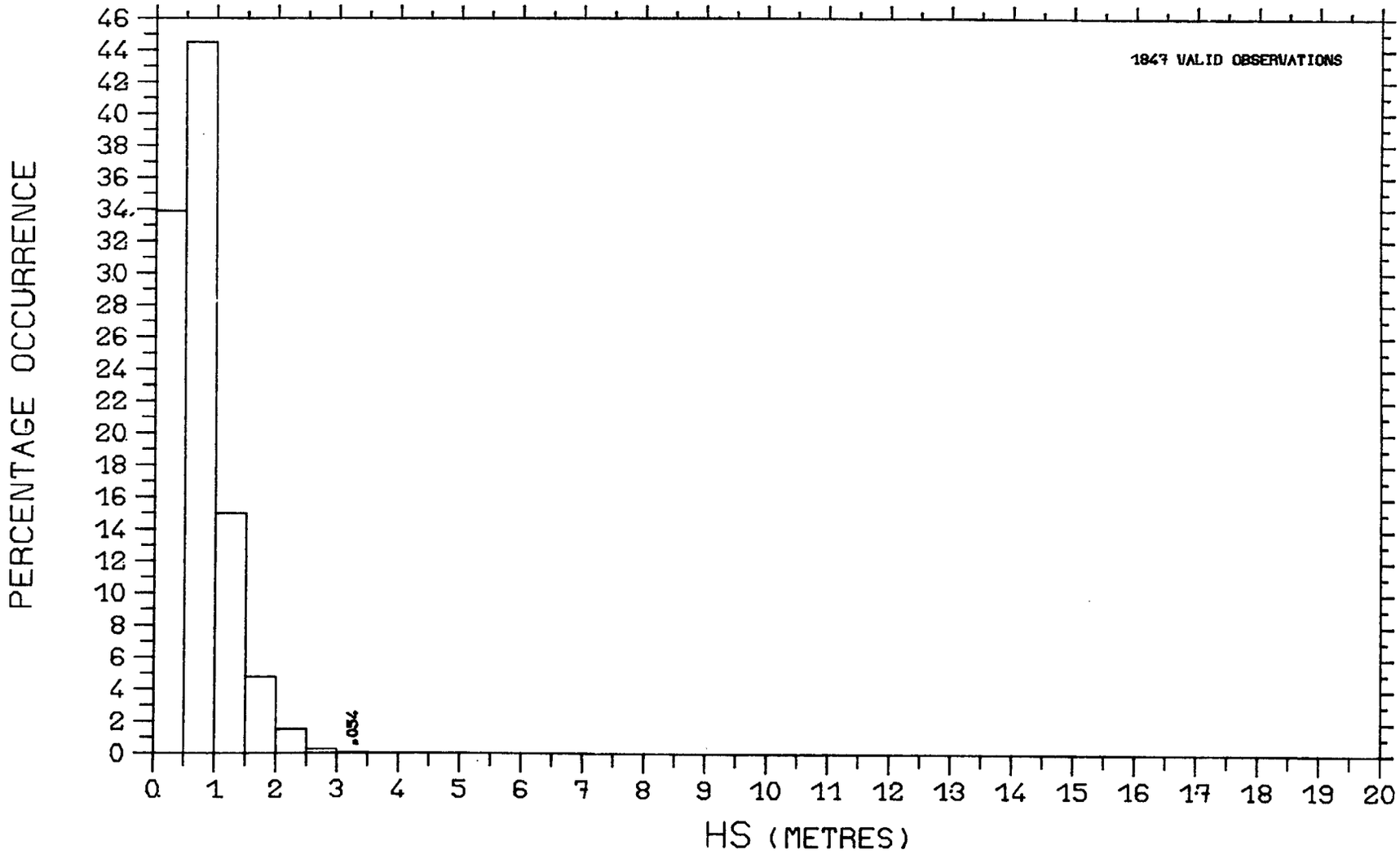


PERCENTAGE. OCCURRENCE. HISTOGRAM

EDDYSTONE. SEPT 1978 - AUG 1981. SUMMERS

3.2.1.2

CA7881

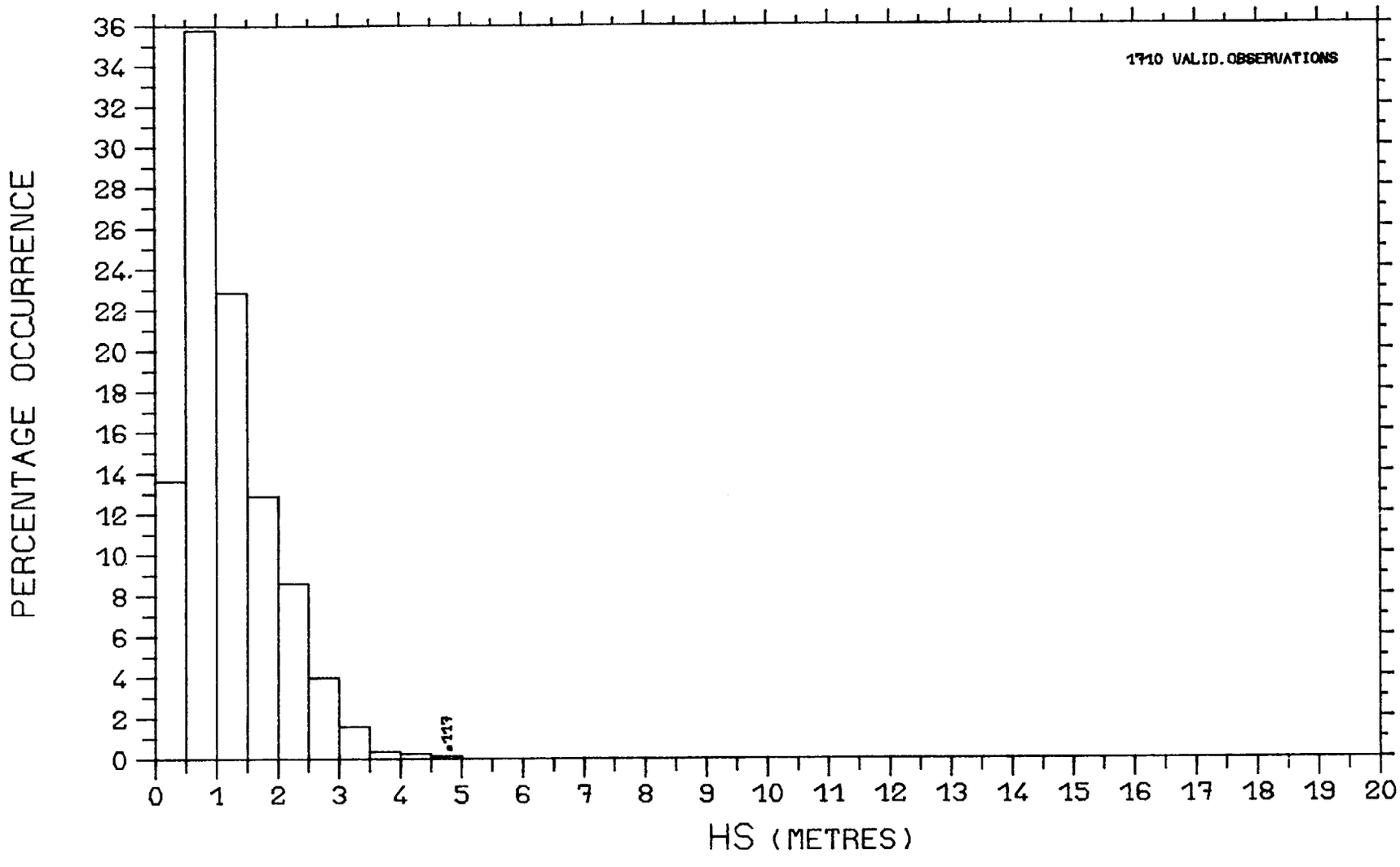


PERCENTAGE. OCCURRENCE. HISTOGRAM

EDDYSTONE. SEPT 1978 - AUG 1981. AUTUMNS

3.2.1.3

CA7881

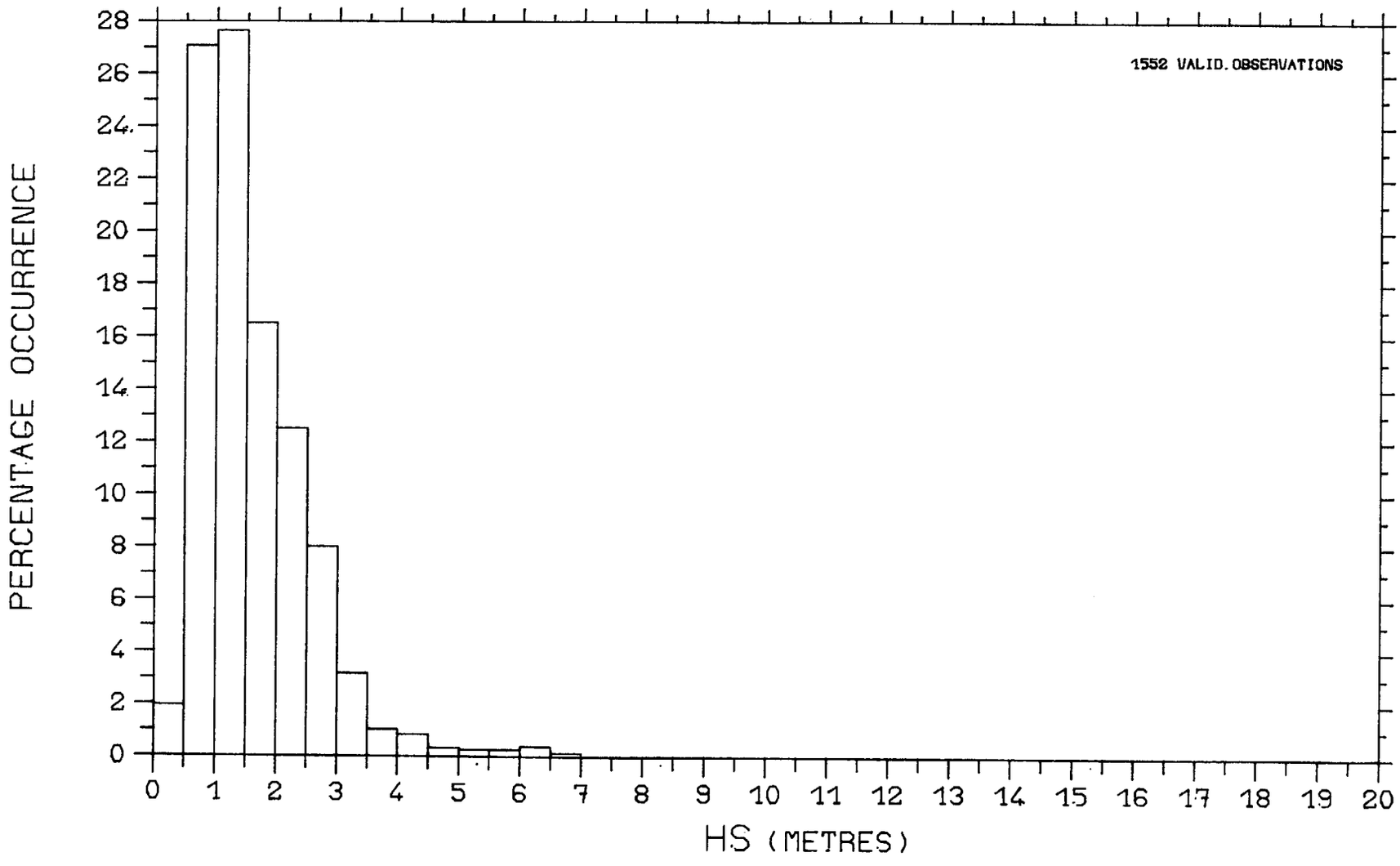


PERCENTAGE. OCCURRENCE. HISTOGRAM

EDDYSTONE SEPT 1978 - AUG 1981. WINTERS

3.2.1.4

CA7881

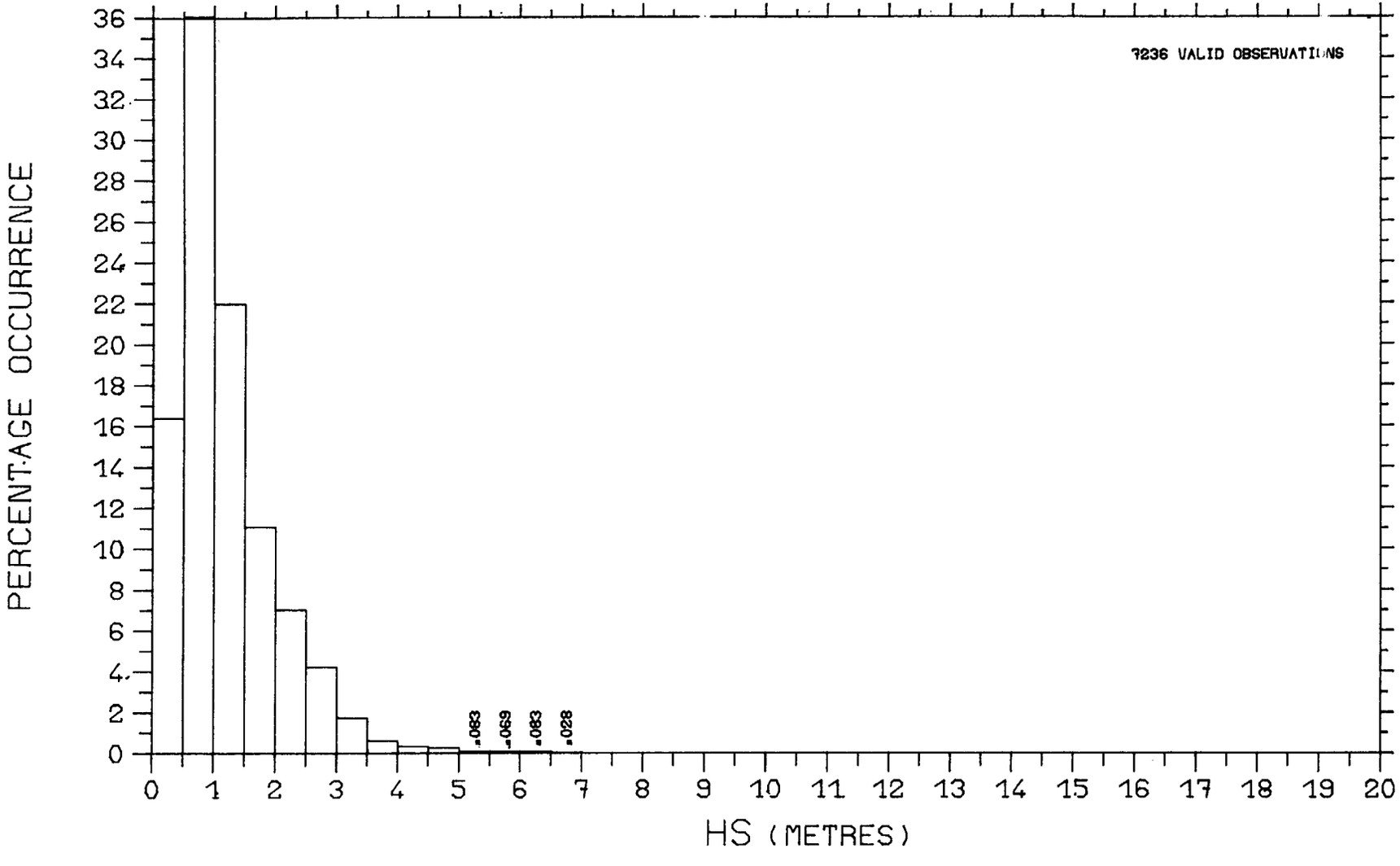


PERCENTAGE OCCURRENCE HISTOGRAM

EDDYSTONE SEPT 1978 - AUG 1981

3.2.1.5

CA7881

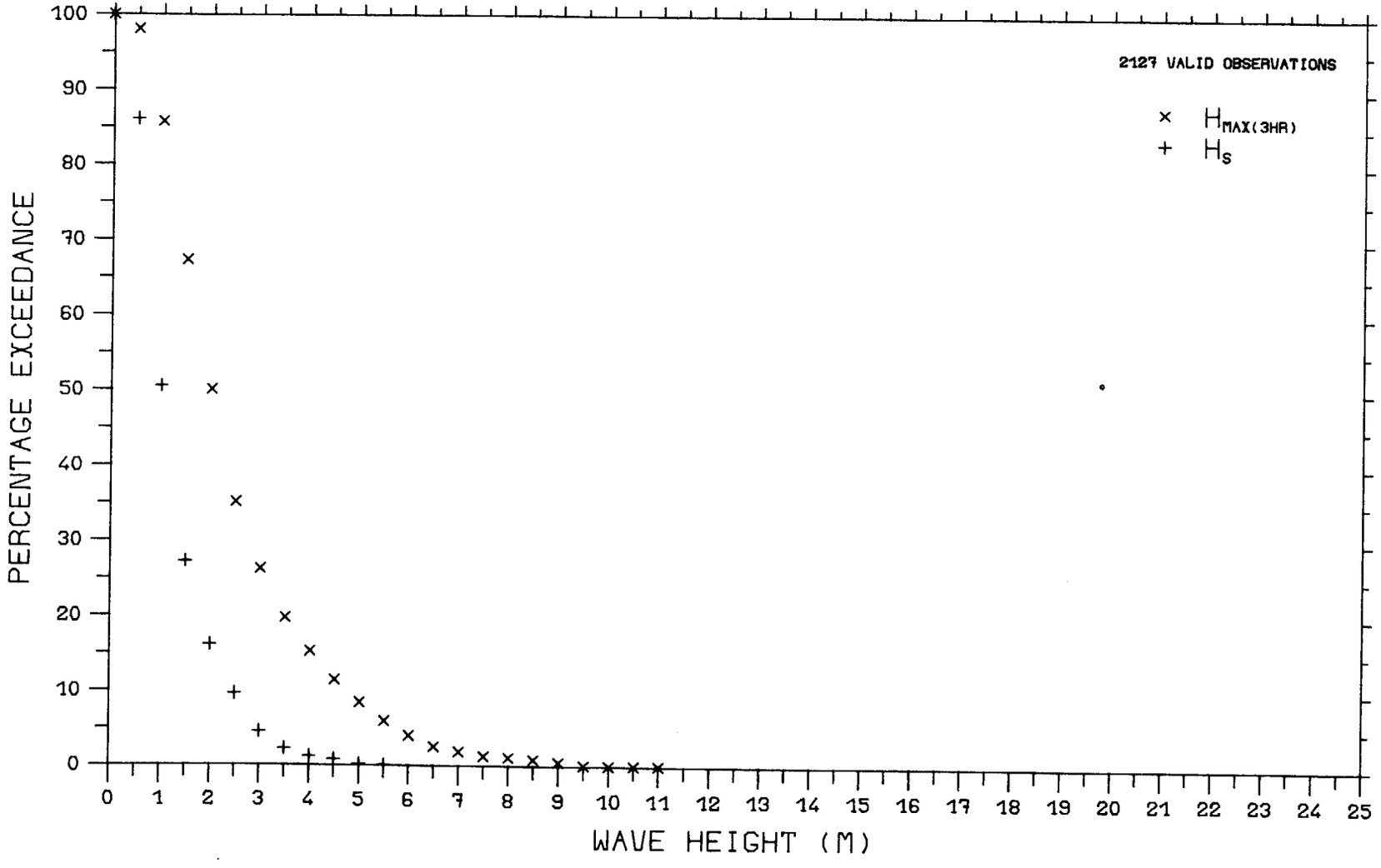


PERCENTAGE EXCEEDANCE OF $H_S$ AND $H_{MAX(3HR)}$

EDDYSTONE SEPT 1978 - AUG 1981 SPRINGS

FIG 3.2.2.1

CA7881

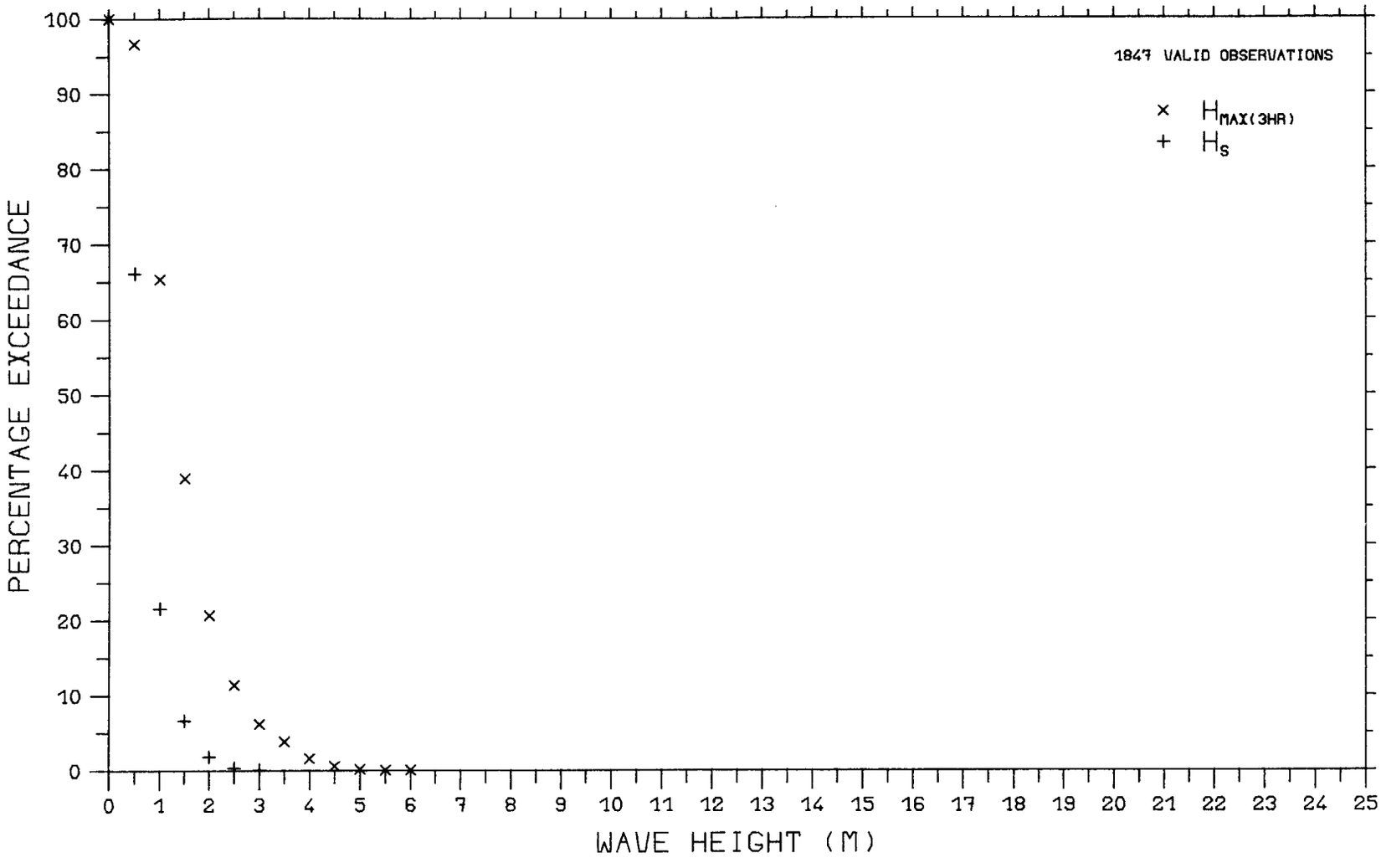


PERCENTAGE EXCEEDANCE OF $H_S$ AND $H_{MAX(3HR)}$

EDDYSTONE SEPT 1978 - AUG 1981 SUMMERS

FIG 3.2.2.2

CA7881

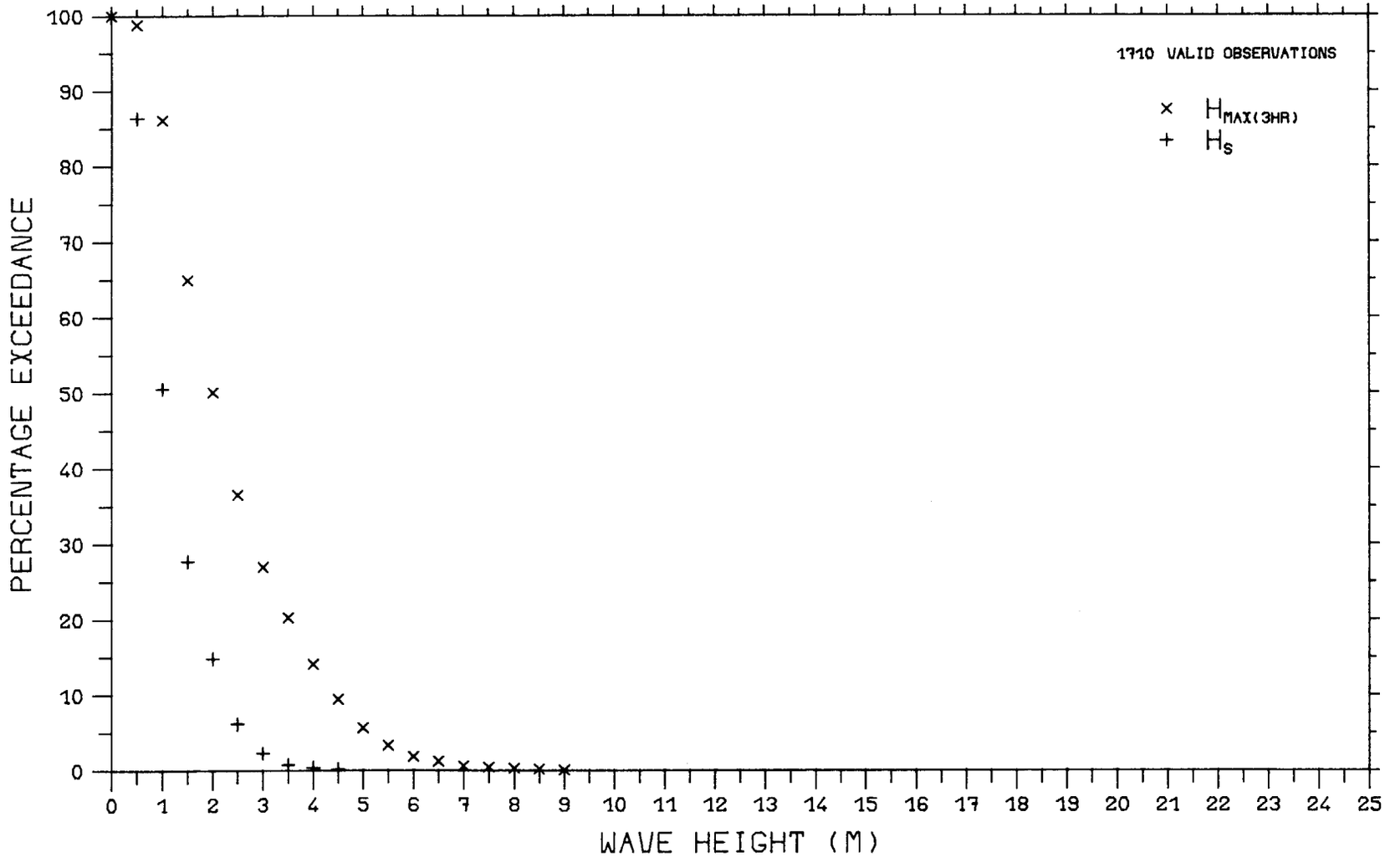


PERCENTAGE EXCEEDANCE OF $H_S$ AND $H_{MAX(3HR)}$

EDDYSTONE SEPT 1978 - AUG 1981 AUTUMNS

FIG 3.2.2.3

CA7881

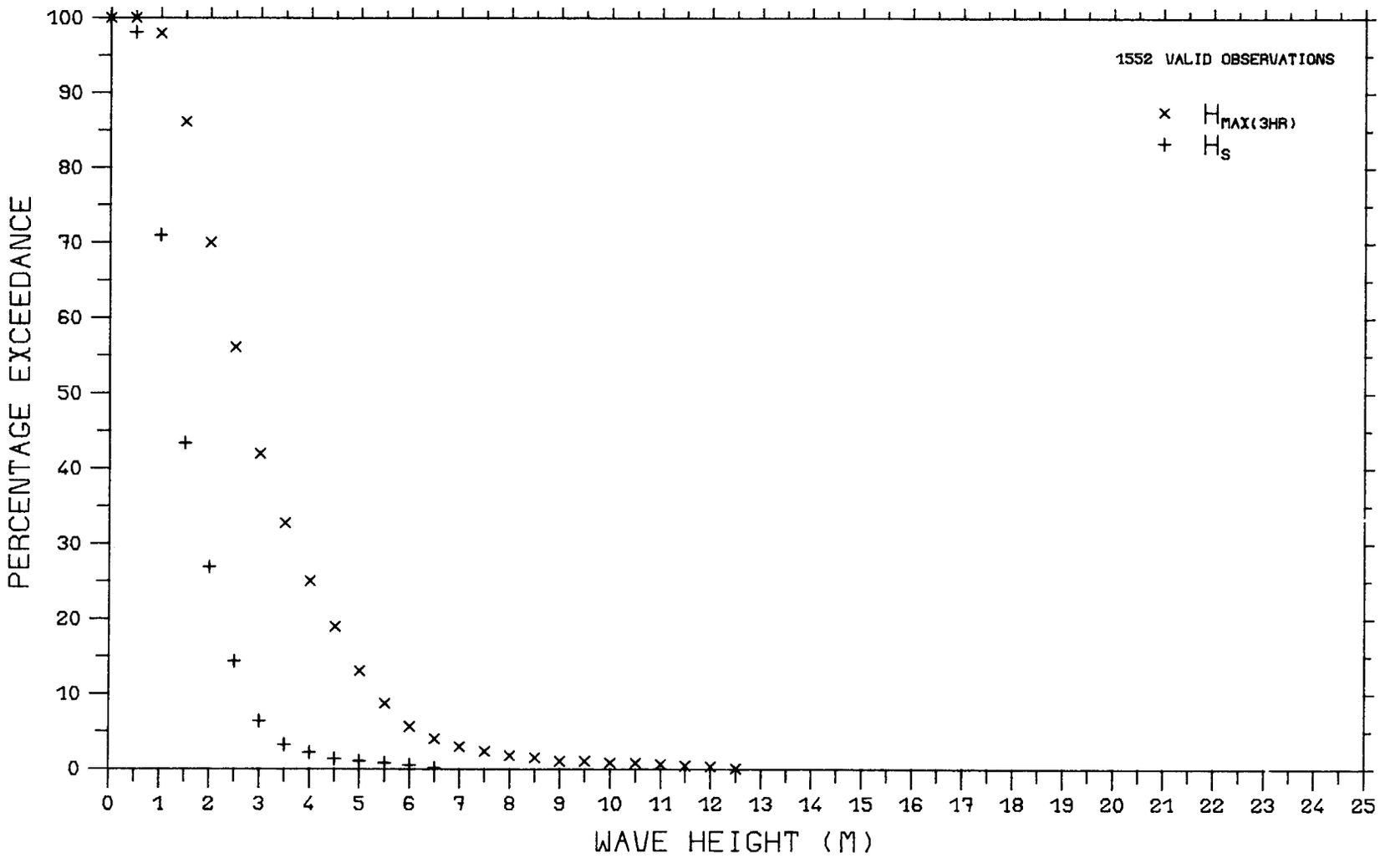


PERCENTAGE EXCEEDANCE OF $H_S$ AND $H_{MAX(3HR)}$

EDDYSTONE SEPT 1978 - AUG 1981 WINTERS

FIG 3.2.2.4

CA7881

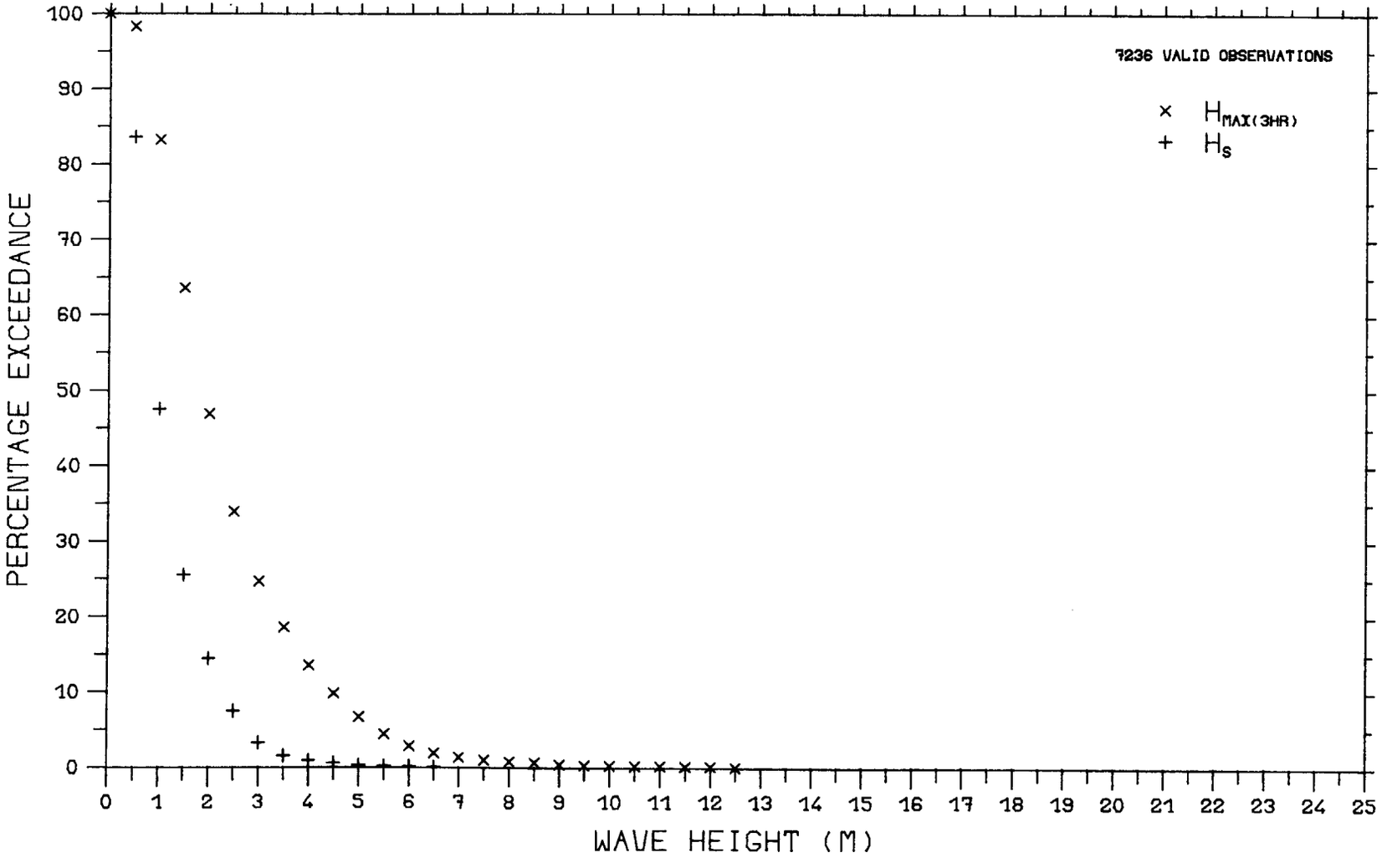


PERCENTAGE EXCEEDANCE OF $H_S$ AND $H_{MAX(3HR)}$

EDDYSTONE SEPT 1978 - AUG 1981

FIG 3.2.2.5

CA7881

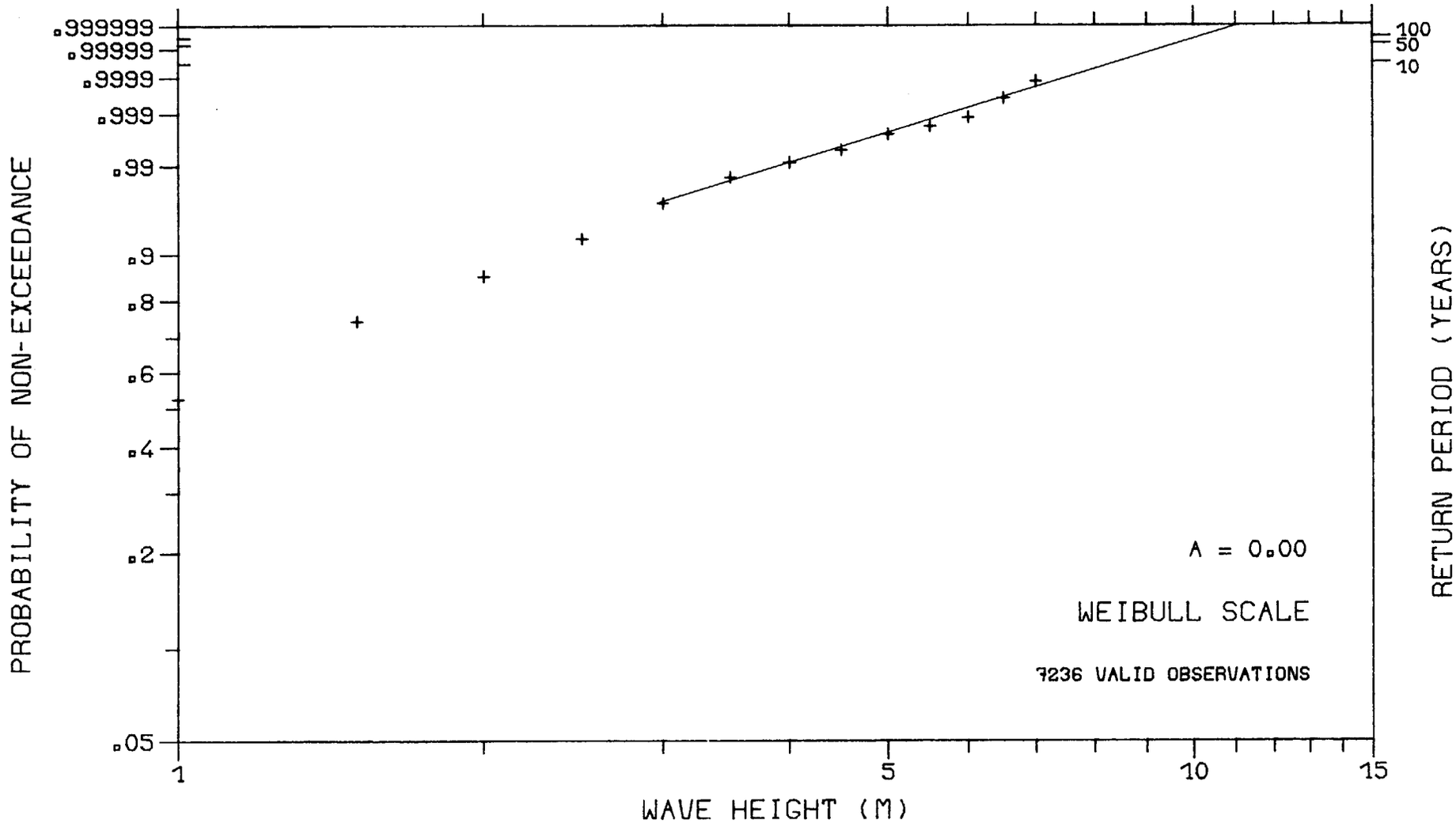


CUMULATIVE DISTRIBUTION OF WAVE HEIGHT, HS

EDDYSTONE SEP 1978 - AUG 1981

FIG 3.3.1(A)

CA7881

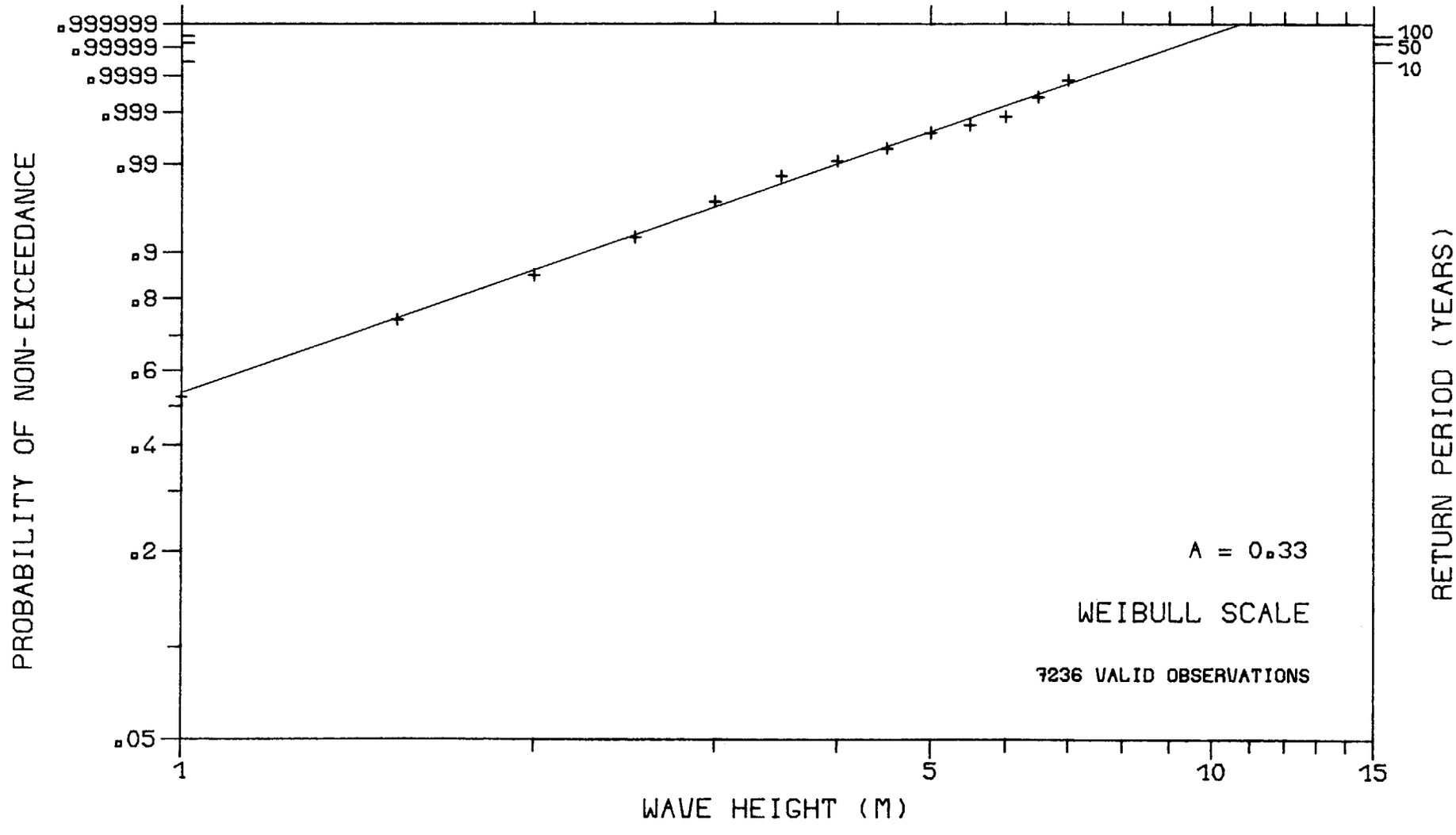


CUMULATIVE DISTRIBUTION OF WAVE HEIGHT, HS

EDDYSTONE SEP 1978 - AUG 1981

FIG 3.3.1(B)

CA7881

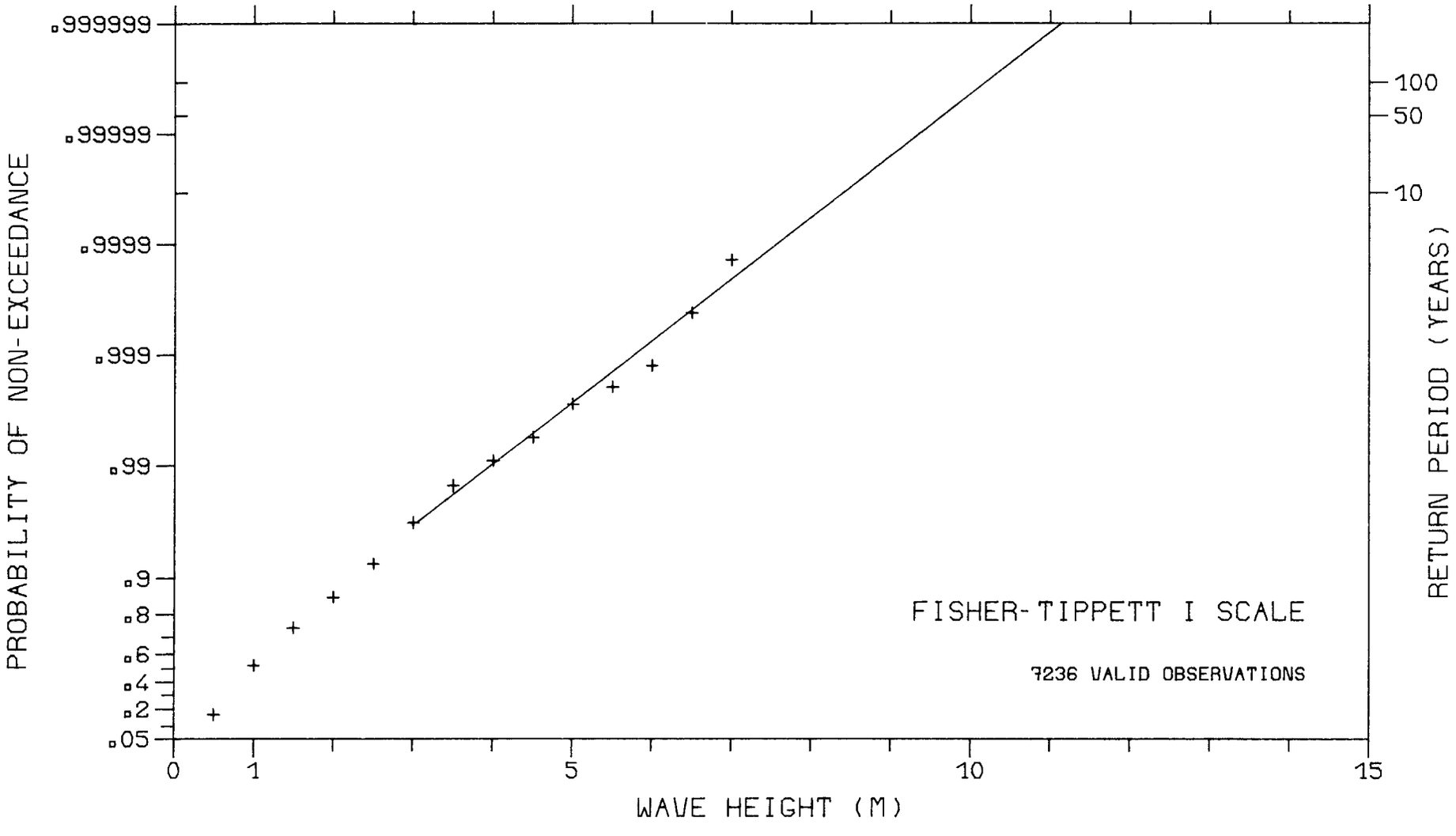


CUMULATIVE DISTRIBUTION OF WAVE HEIGHT; HS

EDDYSTONE SEP 1978 - AUG 1981

FIG 3.3.2(A)

CA7881

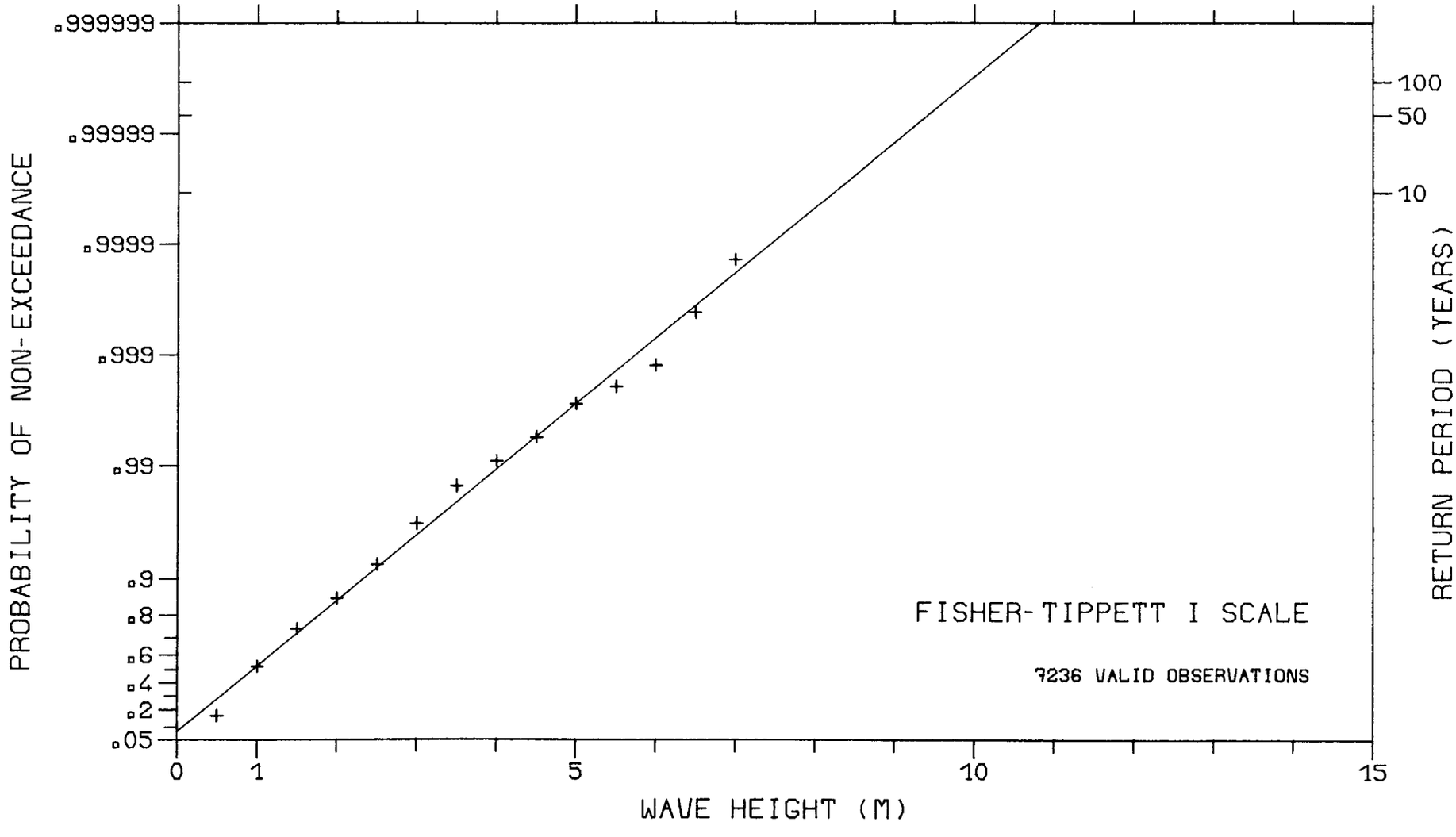


CUMULATIVE DISTRIBUTION OF WAVE HEIGHT; HS

EDDYSTONE SEP 1978 - AUG 1981

FIG 3.3.2(B)

CA7881

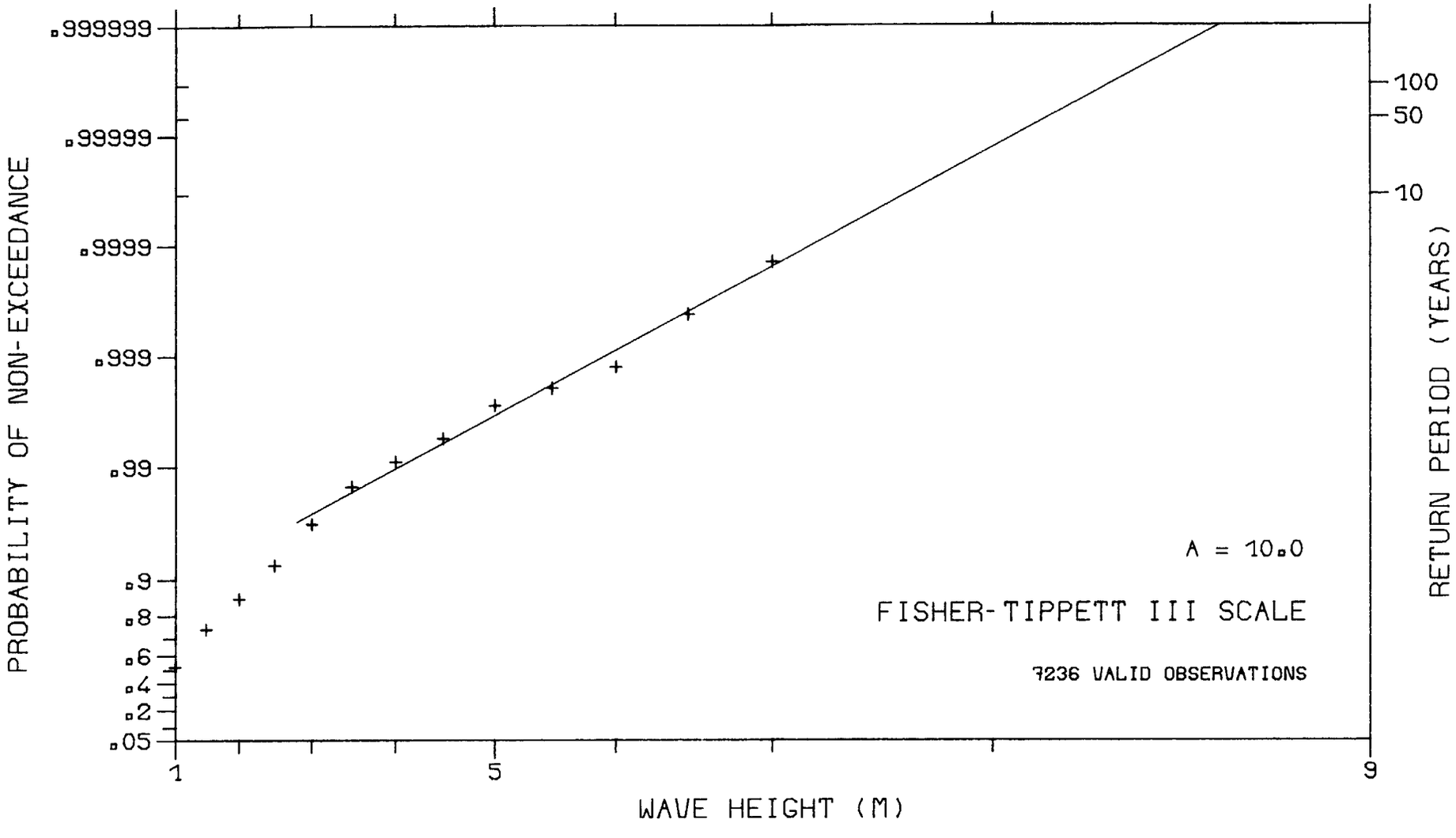


CUMULATIVE DISTRIBUTION OF WAVE HEIGHT; HS

EDDYSTONE SEP 1978 - AUG 1981

FIG 3.3.3(A)

CA7881

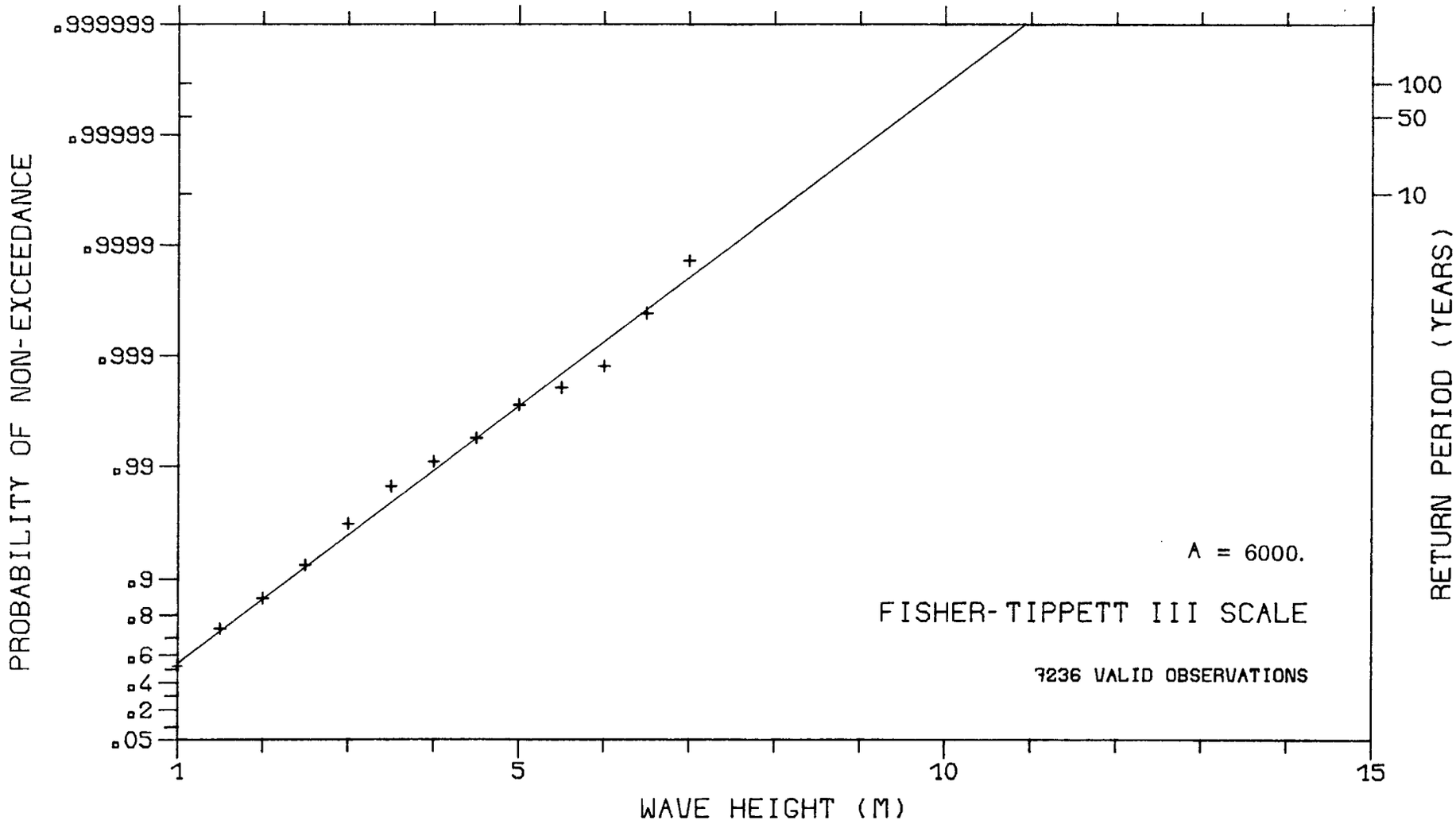


CUMULATIVE DISTRIBUTION OF WAVE HEIGHT; HS

EDDYSTONE SEP 1978 - AUG 1981

FIG 3.3.3(B)

CA7881

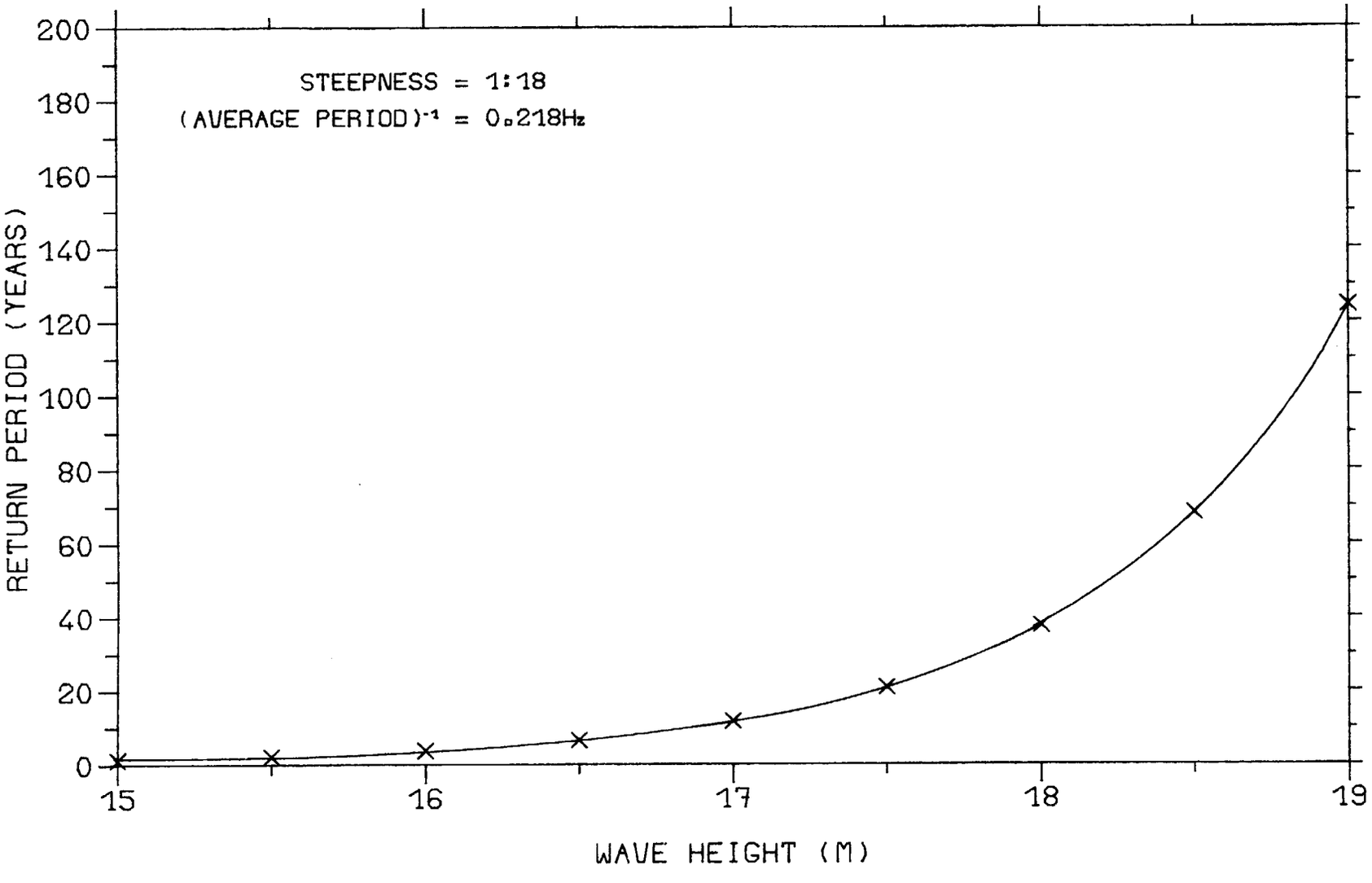


RETURN PERIOD v. WAVE HEIGHT - INDIVIDUAL WAVE MODEL

EDDYSTONE SEPT 1978 - AUG 1981

FIG 3.3.4(A)

CA7881

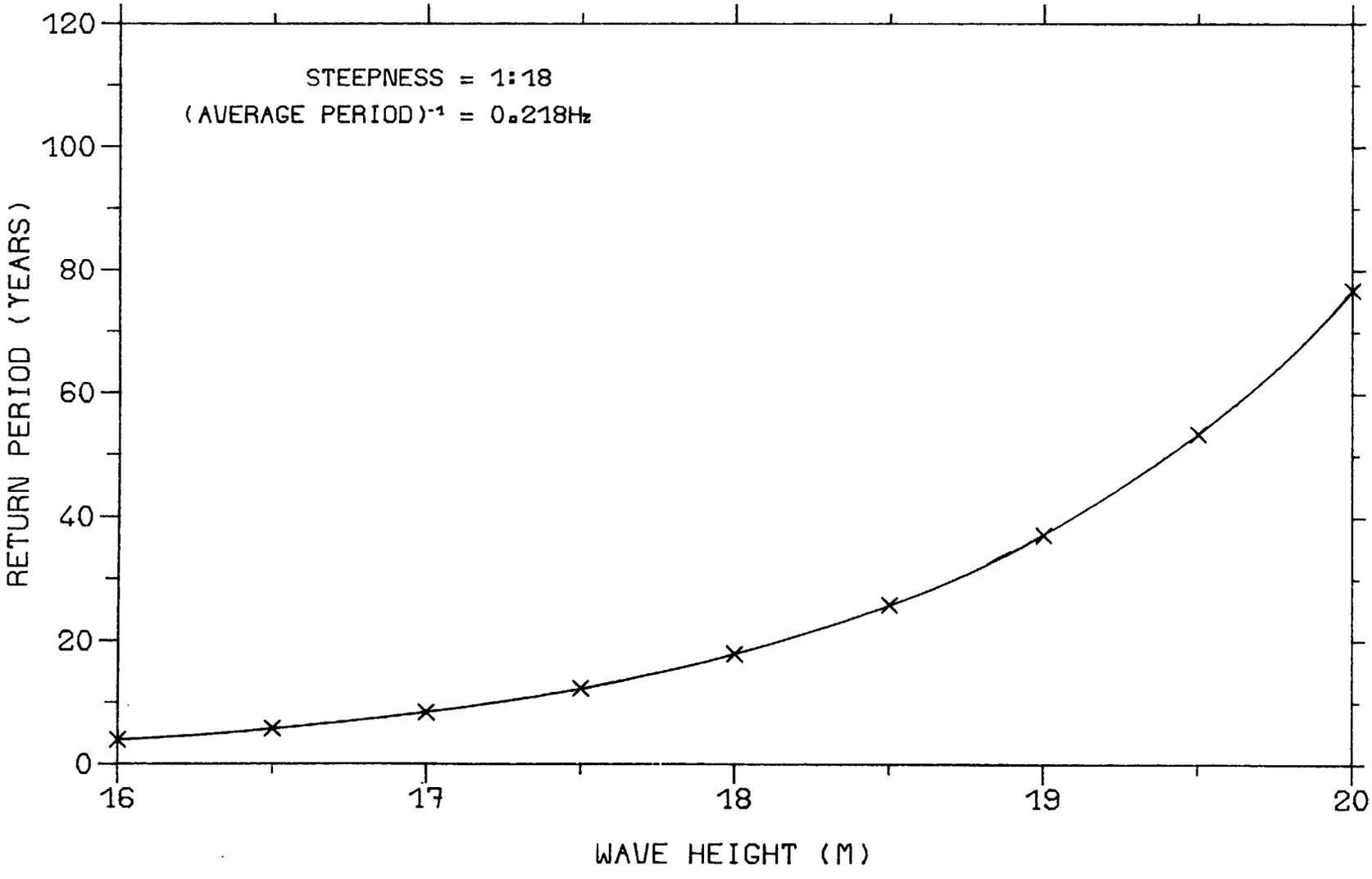


RETURN PERIOD v. WAVE HEIGHT - INDIVIDUAL WAVE MODEL

EDDYSTONE SEPT 1978 - AUG 1981

FIG 3.3.4(B)

CA7881

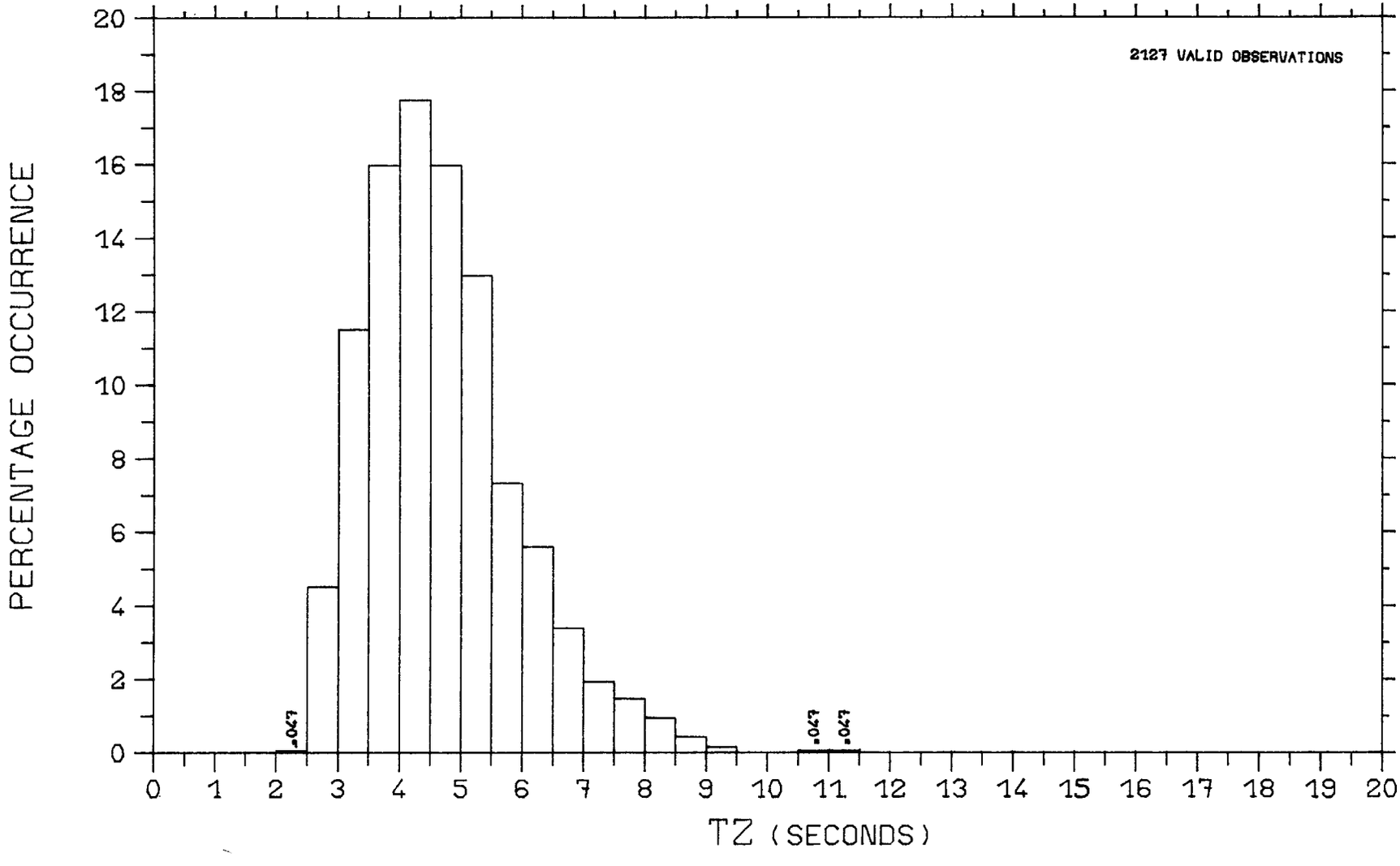


PERCENTAGE OCCURRENCE. HISTOGRAM

EDDYSTONE SEPT 1978 - AUG 1981 SPRINGS

3.4.1.1

CA7881

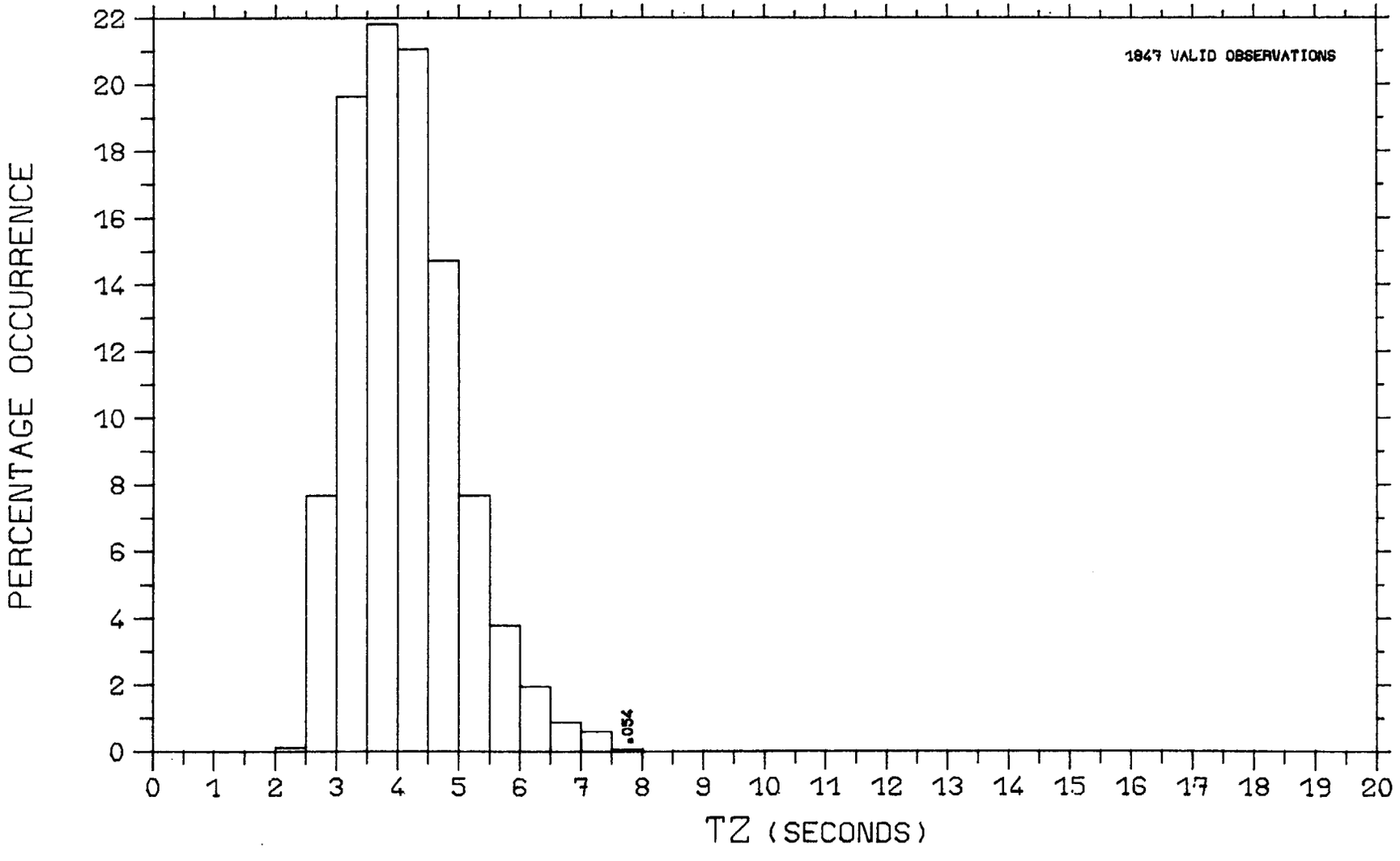


PERCENTAGE OCCURRENCE HISTOGRAM

EDDYSTONE SEPT 1978 - AUG 1981 SUMMERS

3.4.1.2

CA7881

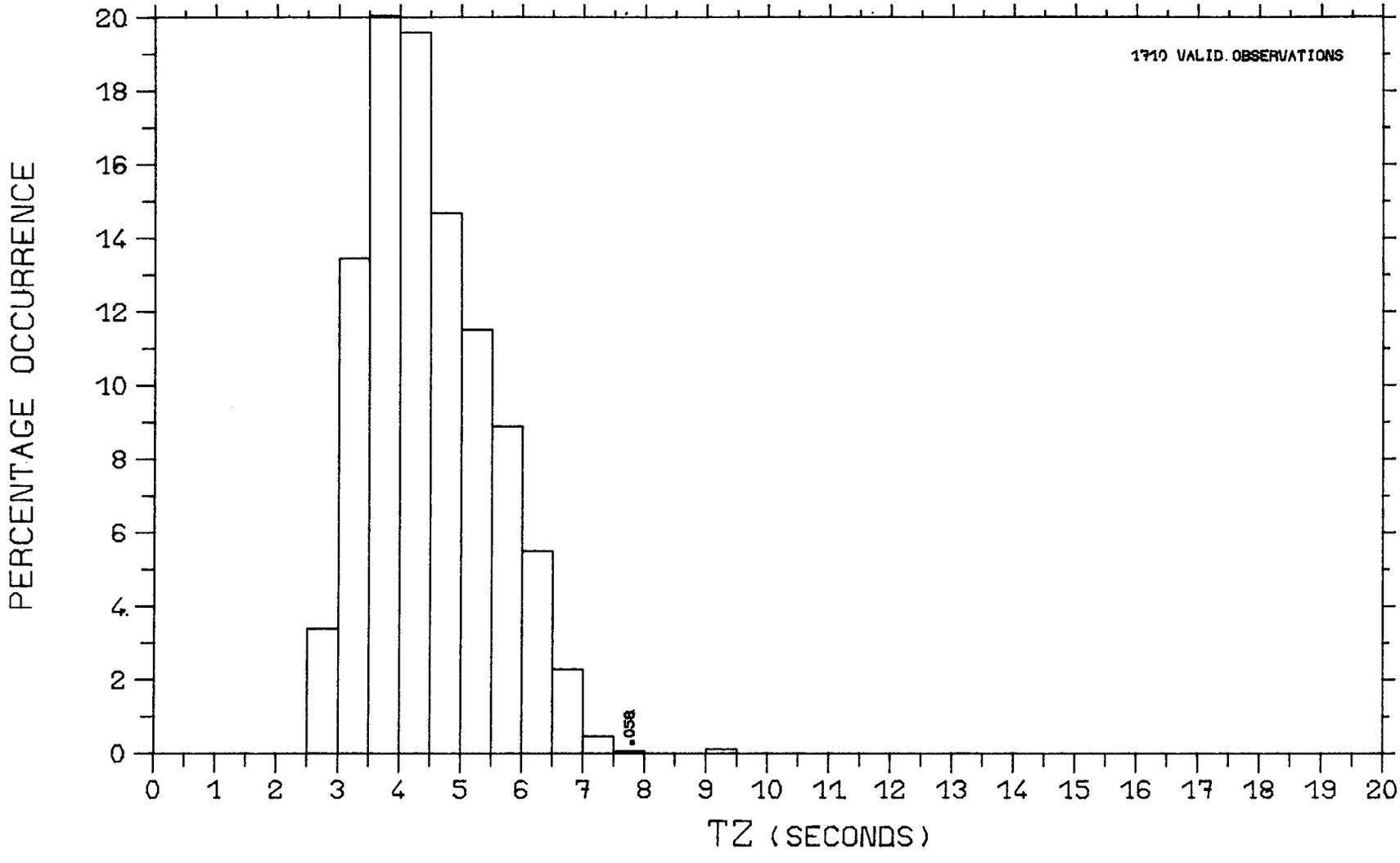


PERCENTAGE OCCURRENCE HISTOGRAM

EDDYSTONE SEPT 1978 - AUG 1981 AUTUMNS

3.4n.1.3

CA7881

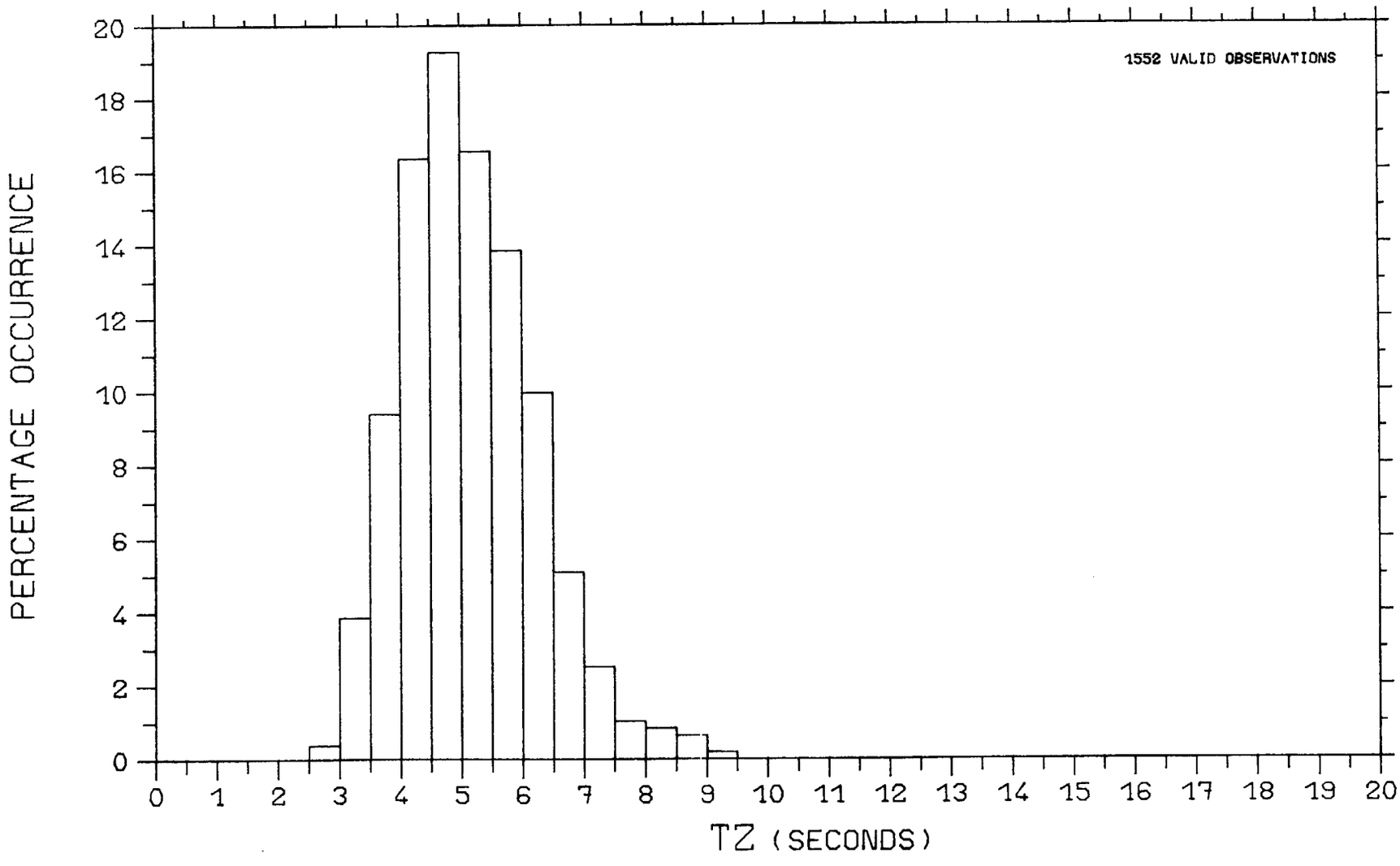


PERCENTAGE OCCURRENCE HISTOGRAM

EDDYSTONE SEPT 1978 - AUG 1981 WINTERS

3.4.1.4

CA7881

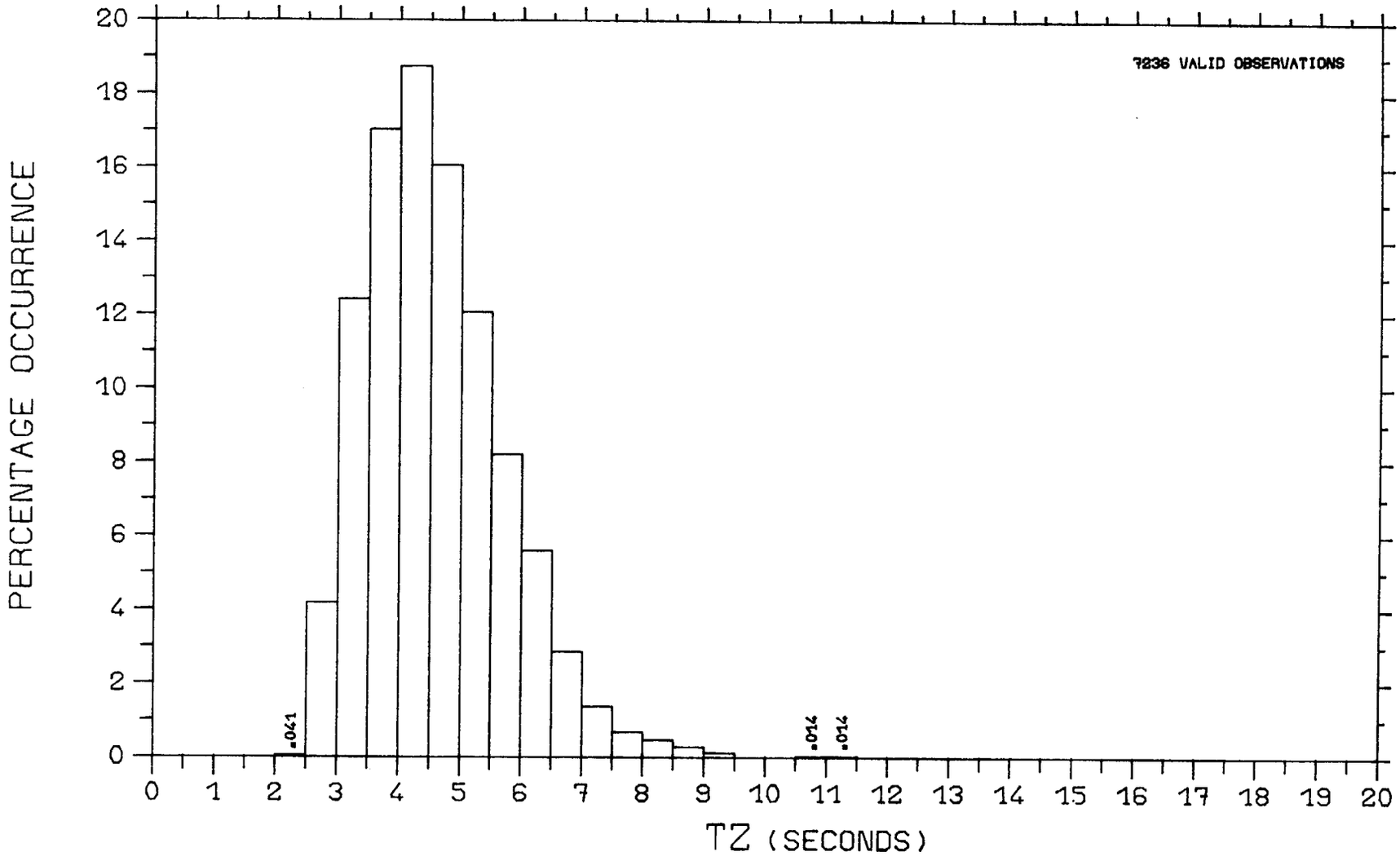


PERCENTAGE OCCURRENCE HISTOGRAM

EDDYSTONE SEPT 1978 - AUG 1981

3.4.1.5

CA7881

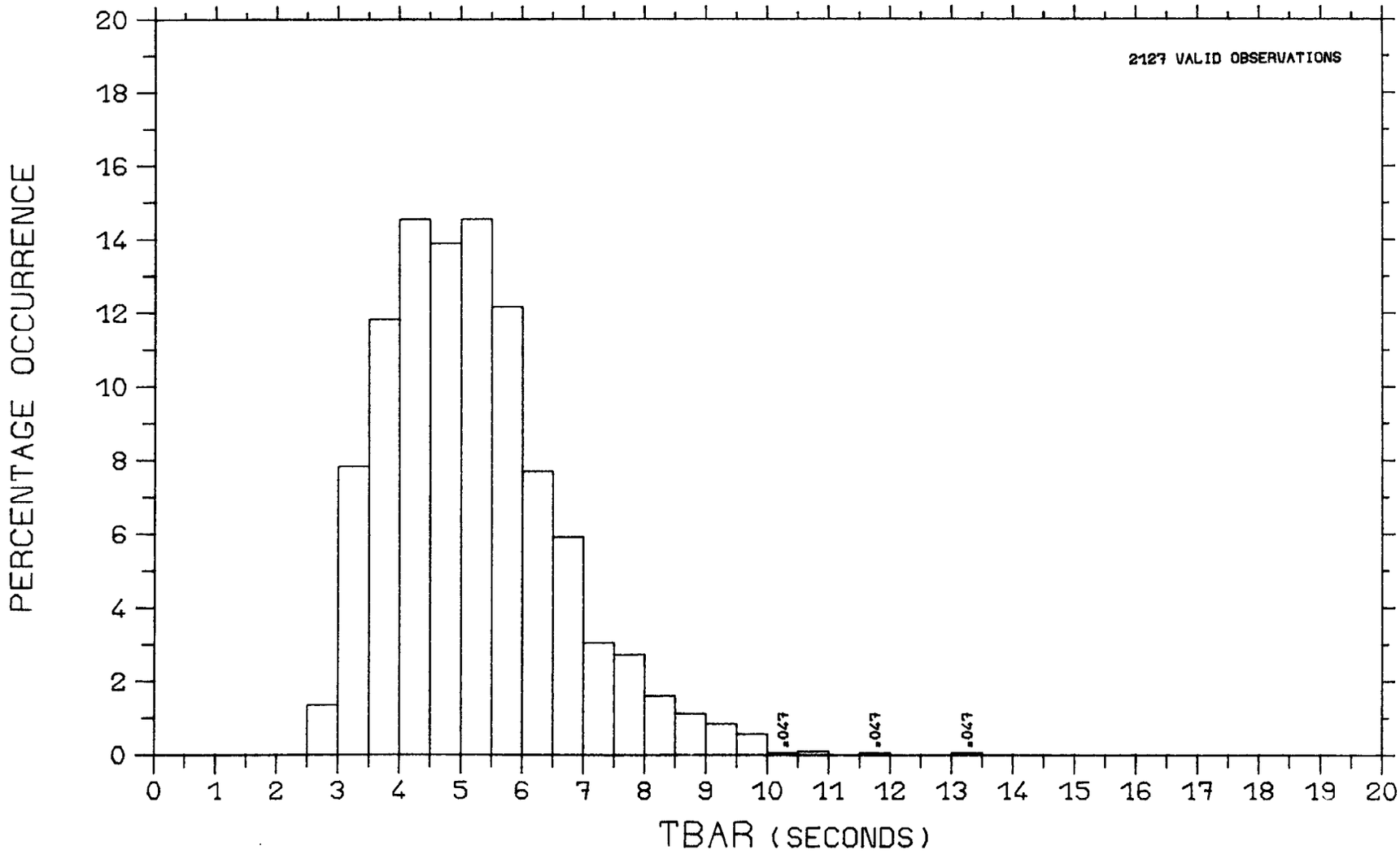


PERCENTAGE OCCURRENCE HISTOGRAM

EDDYSTONE SEPT 1978 - AUG 1981 SPRINGS

3.4.2.1

CA7881

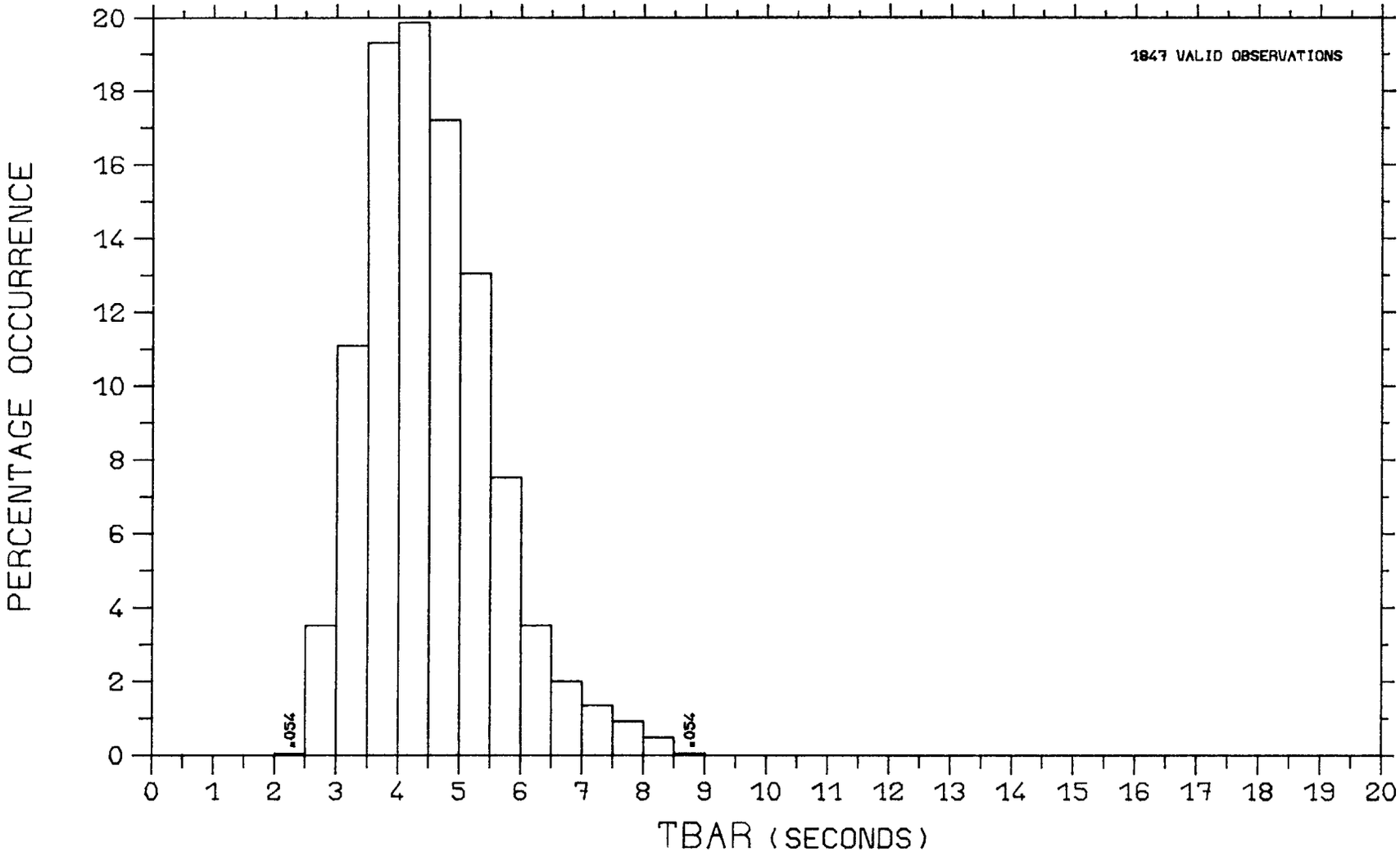


PERCENTAGE OCCURRENCE HISTOGRAM

EDDYSTONE SEPT 1978 - AUG 1981 SUMMERS

3.4.2.2

CA7881

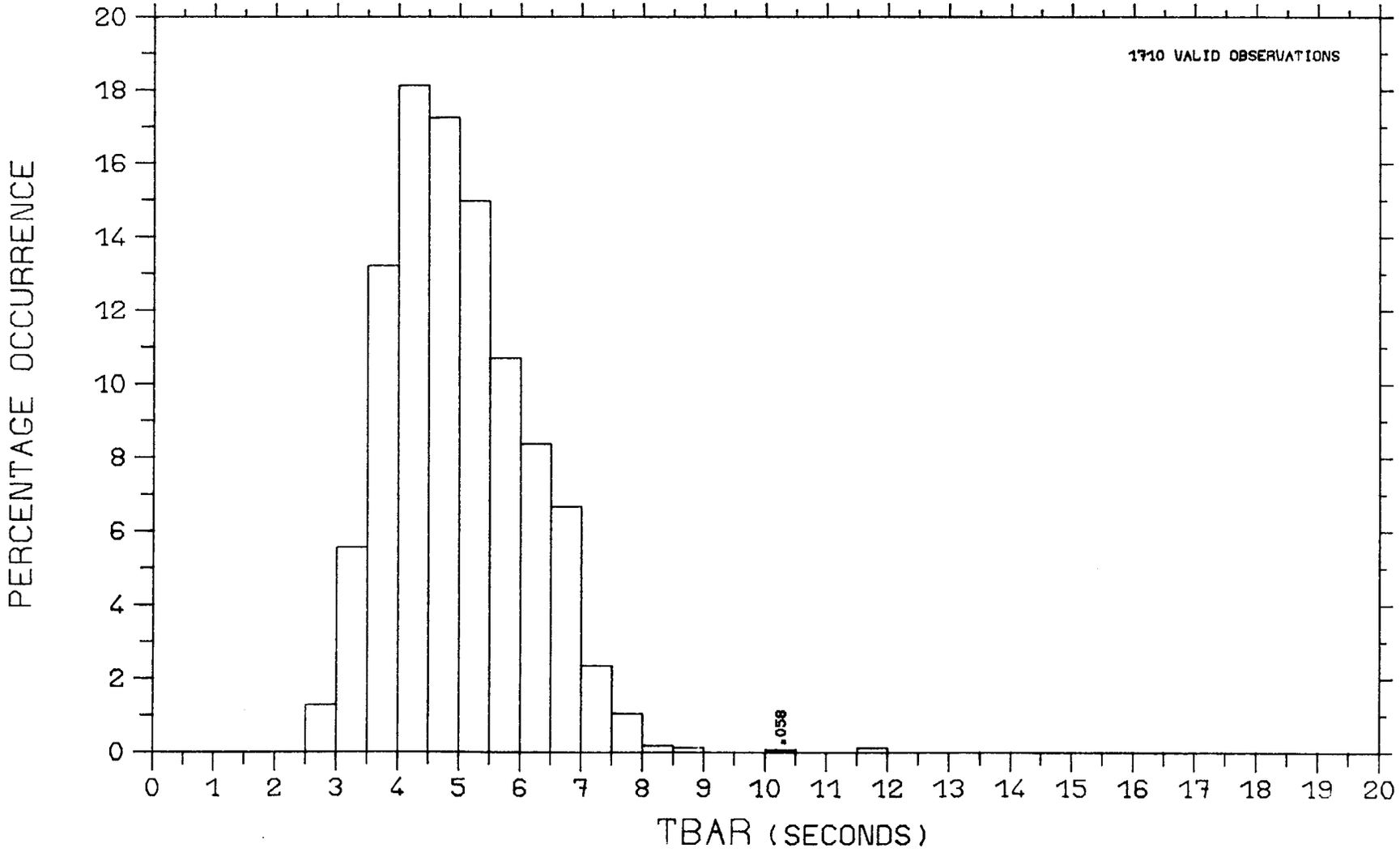


PERCENTAGE OCCURRENCE HISTOGRAM

EDDYSTONE SEPT 1978 - AUG 1981 AUTUMNS

3.4.2.3

CA7881

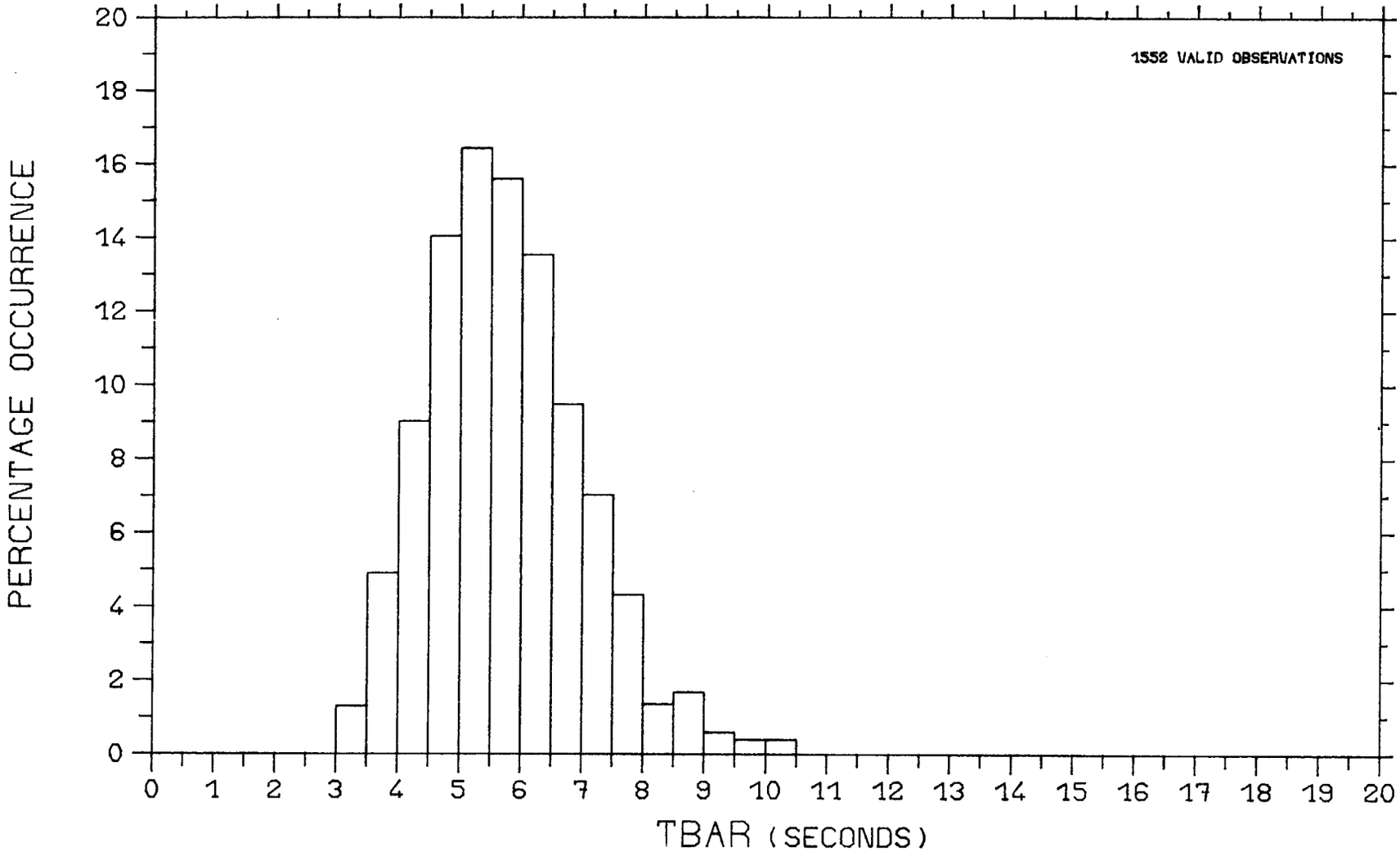


PERCENTAGE OCCURRENCE HISTOGRAM

EDDYSTONE SEPT 1978 - AUG 1981 WINTERS

3.4.2.4

CA7881

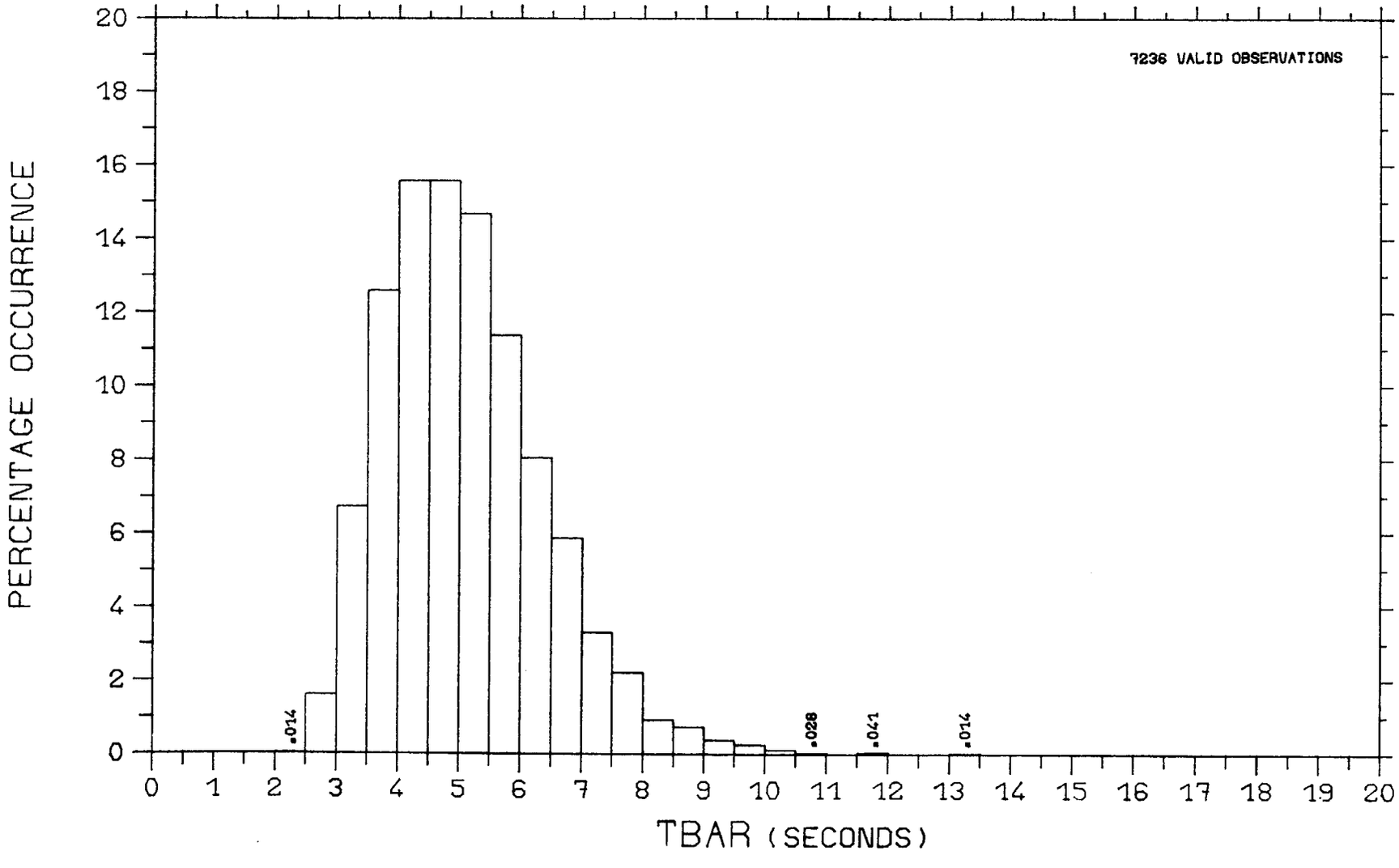


PERCENTAGE OCCURRENCE HISTOGRAM

EDDYSTONE SEPT 1978 - AUG 1981

3.4.2.5

CA7881

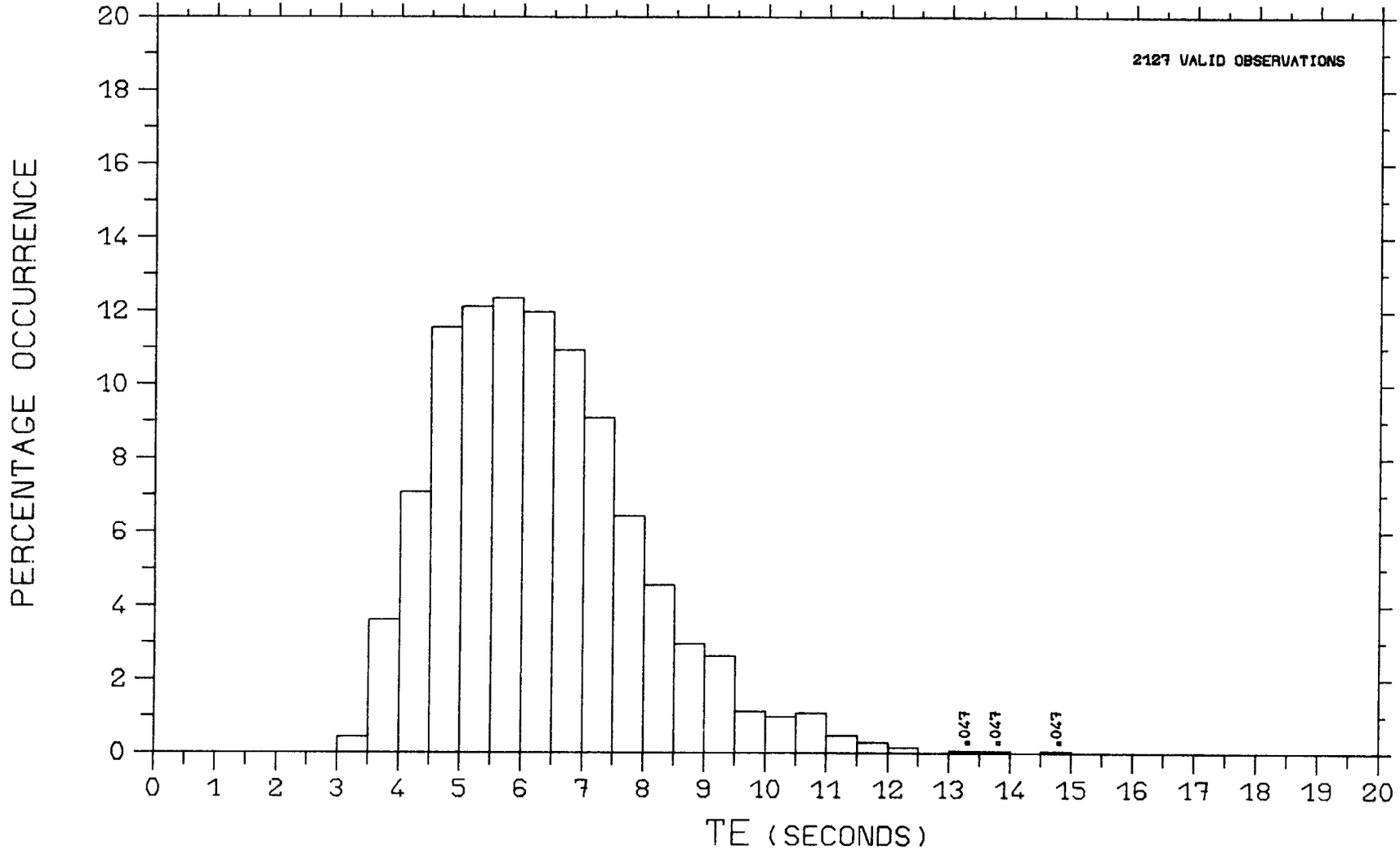


PERCENTAGE OCCURRENCE HISTOGRAM

EDDYSTONE SEPT 1978 - AUG 1981 SPRINGS

3.4.3.1

CA7881

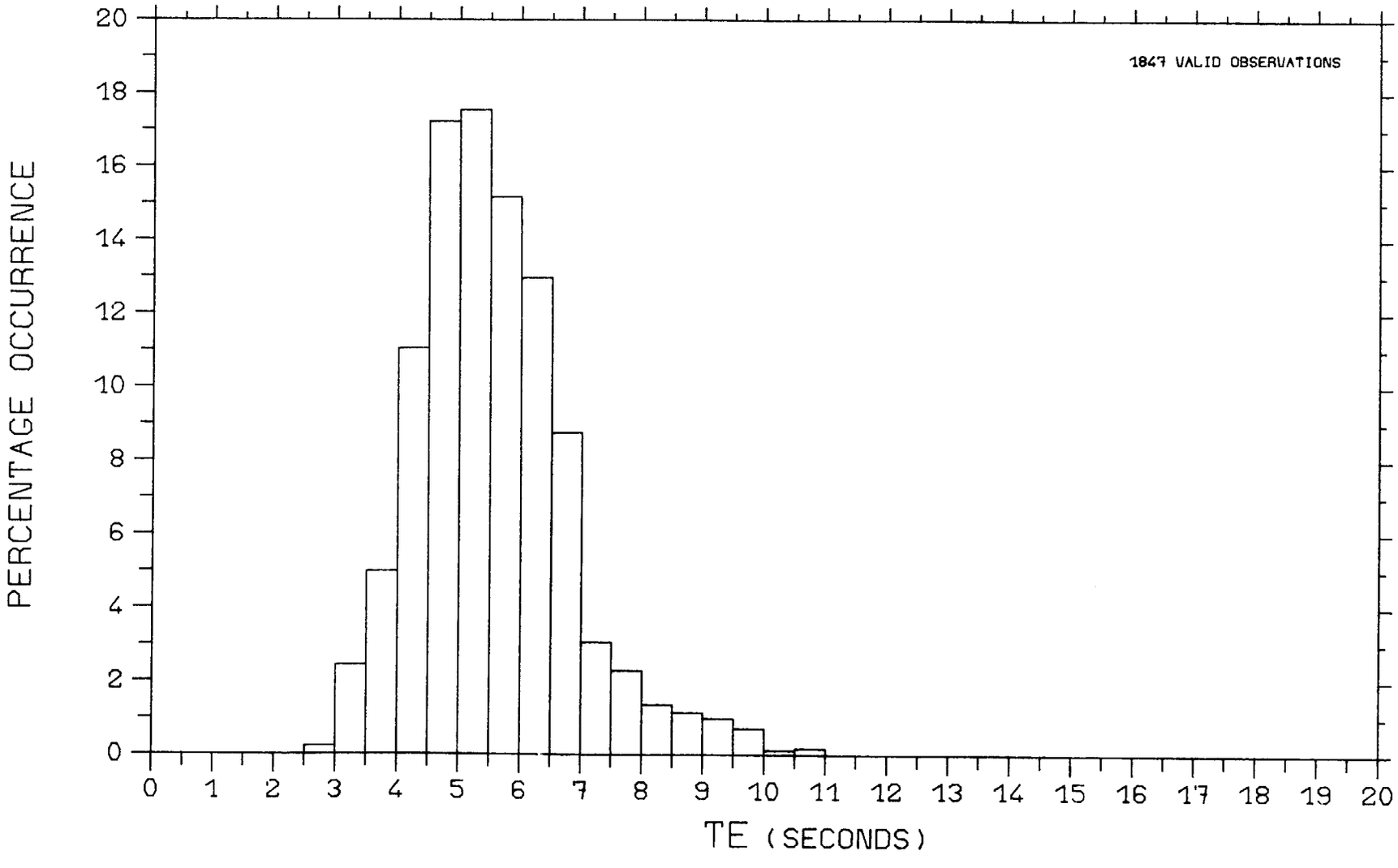


PERCENTAGE OCCURRENCE HISTOGRAM

EDDYSTONE SEPT 1978 - AUG 1981 SUMMERS

3.4.3.2

CA7881

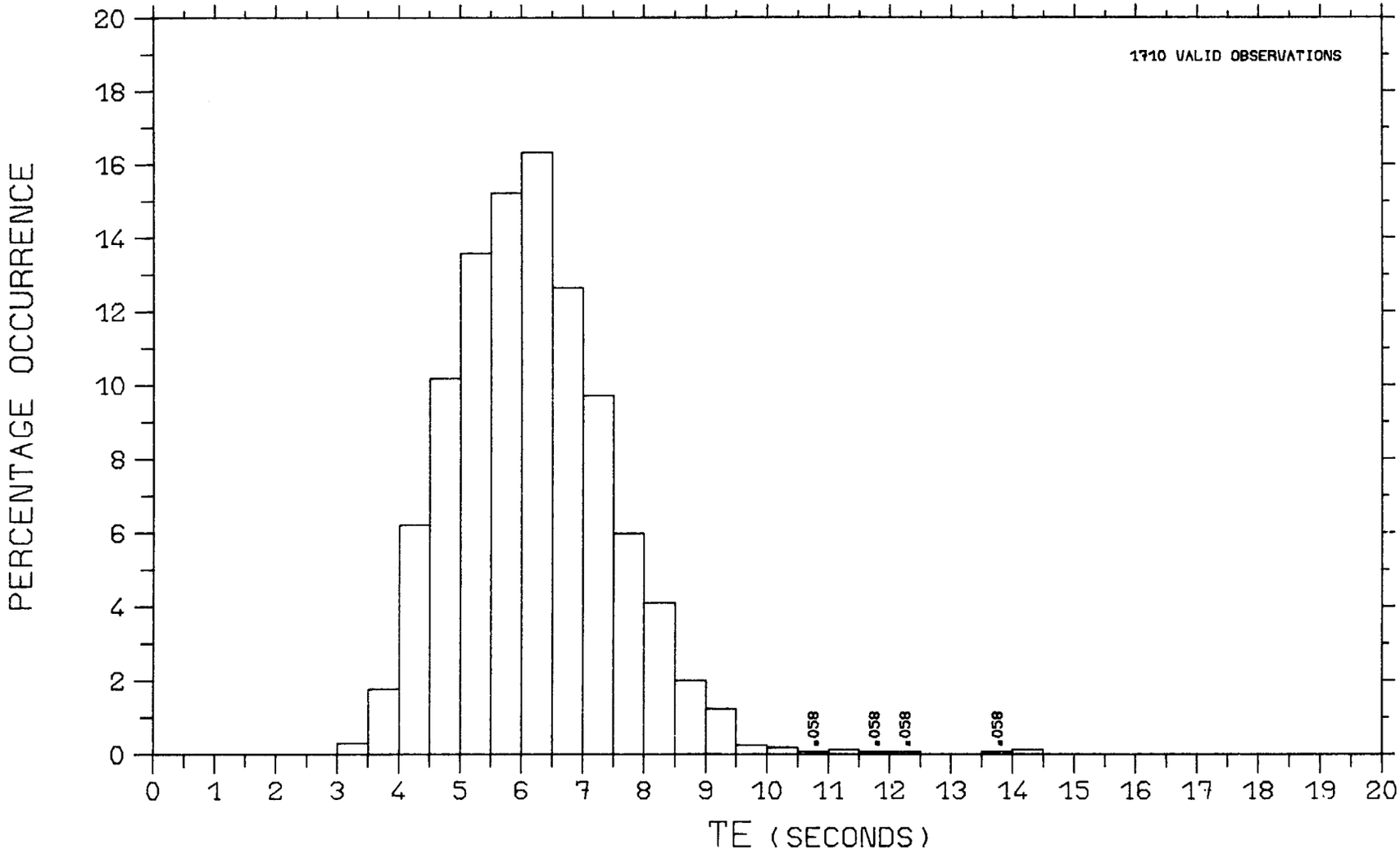


PERCENTAGE OCCURRENCE HISTOGRAM

EDDYSTONE SEPT 1978 - AUG 1981 AUTUMNS

3.4.3.3

CA7881

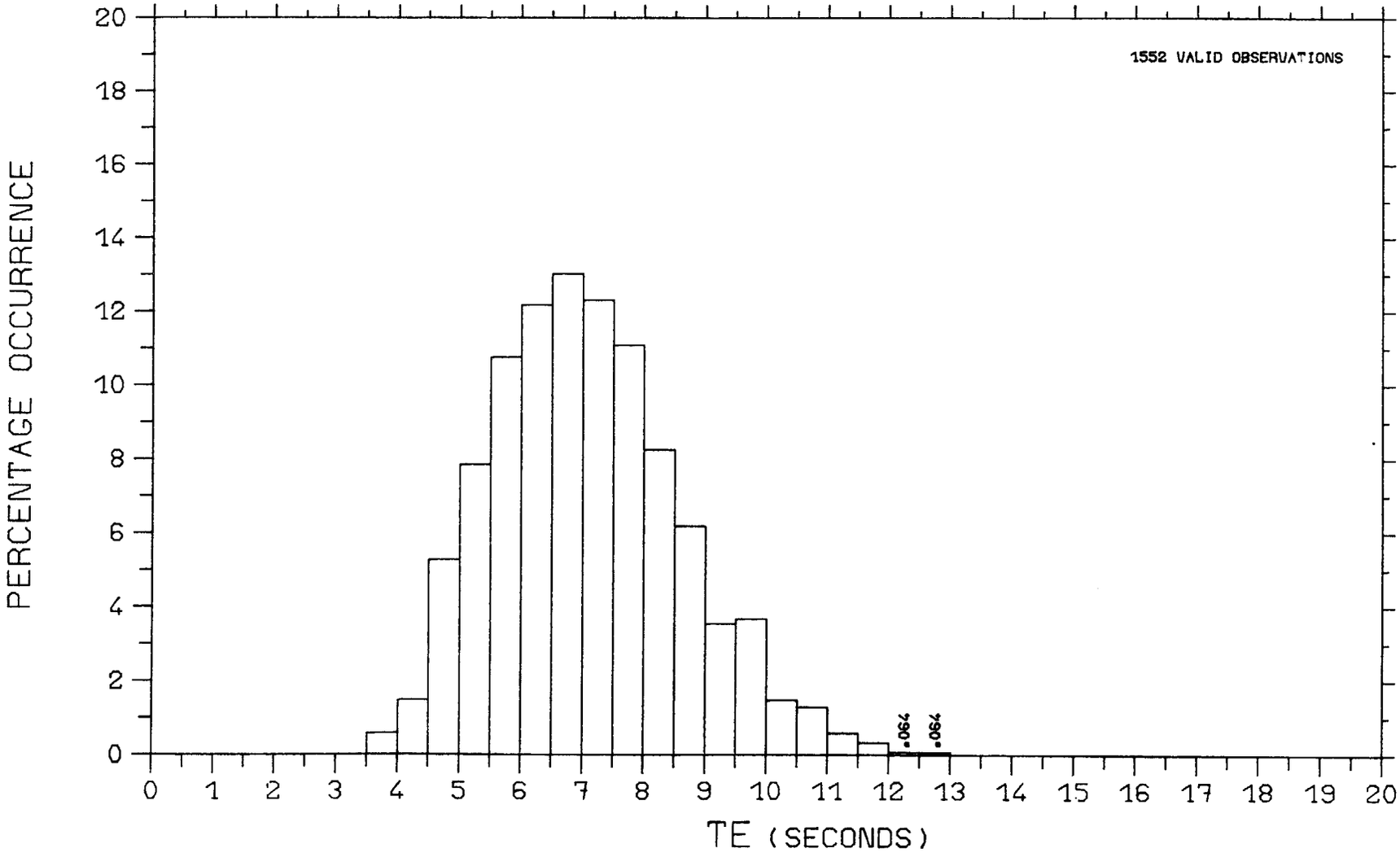


PERCENTAGE OCCURRENCE HISTOGRAM

EDDYSTONE SEPT 1978 - AUG 1981 WINTERS

3.4.3.4

CA7881

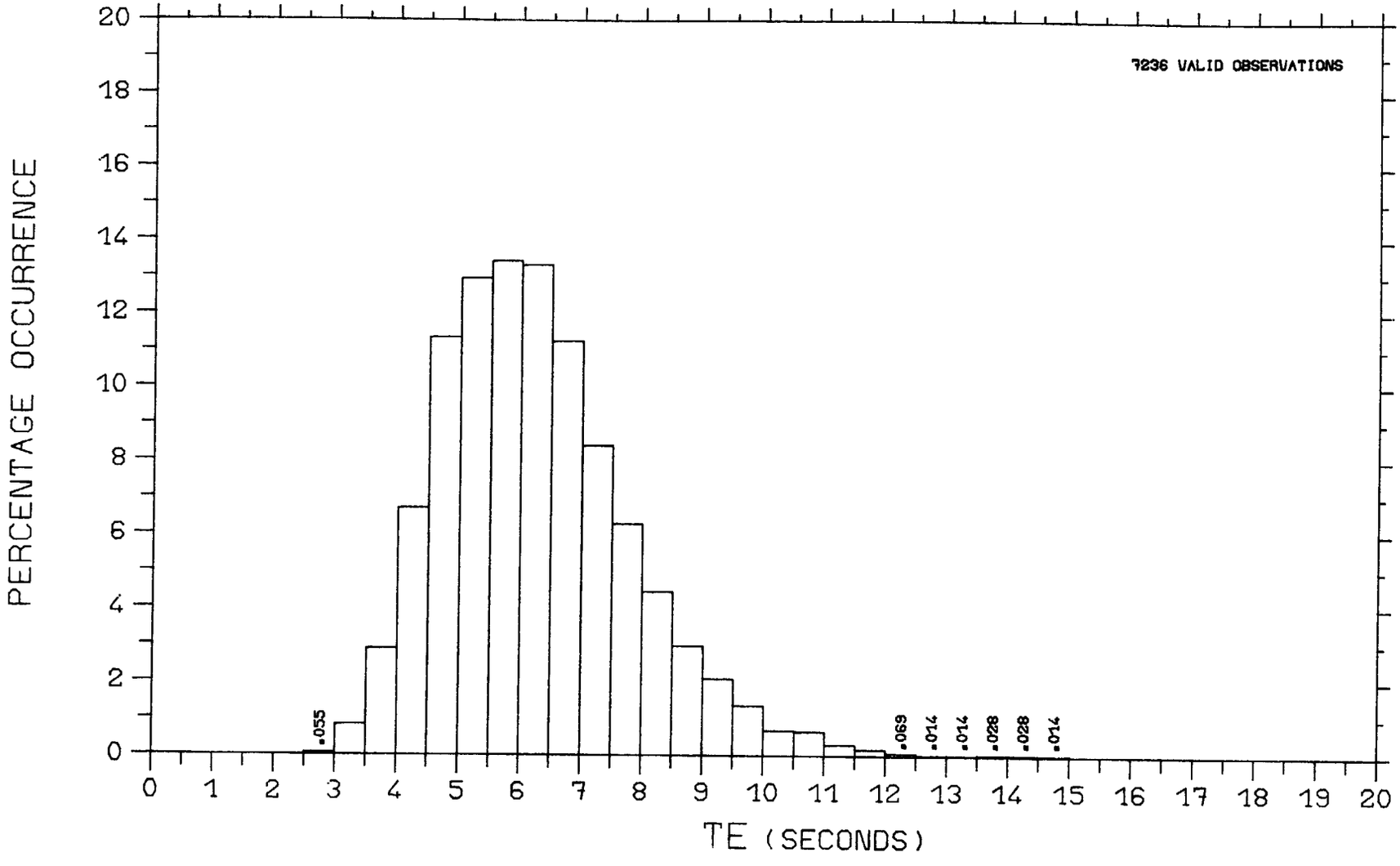


PERCENTAGE OCCURRENCE HISTOGRAM

EDDYSTONE SEPT 1978 - AUG 1981

3.4.3.5

CA7881

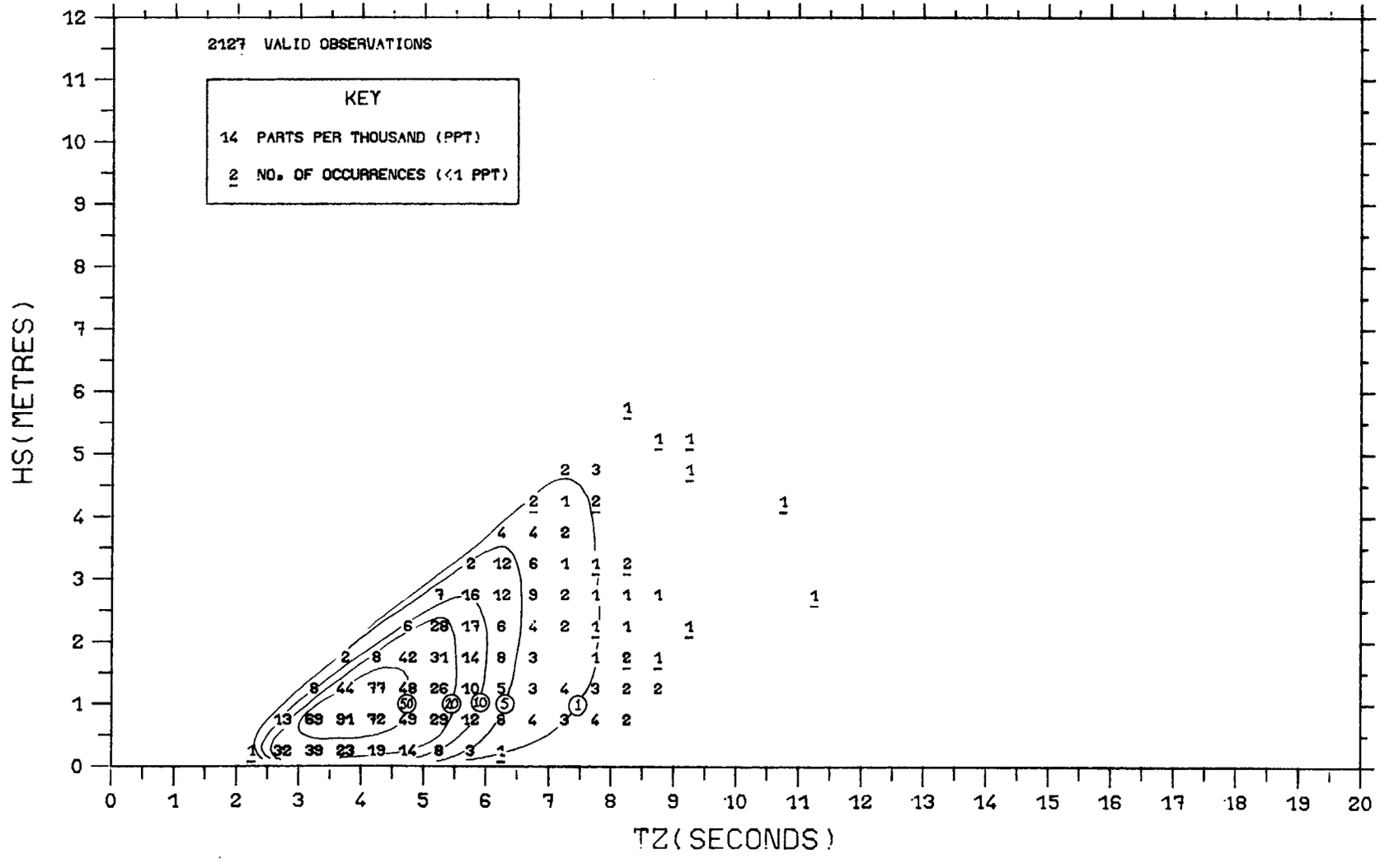


SCATTER PLOT OF HS AND TZ

EDDYSTONE SEPT 1978 - AUG 1981 SPRINGS

FIGURE 3.5.1.1

CA7881

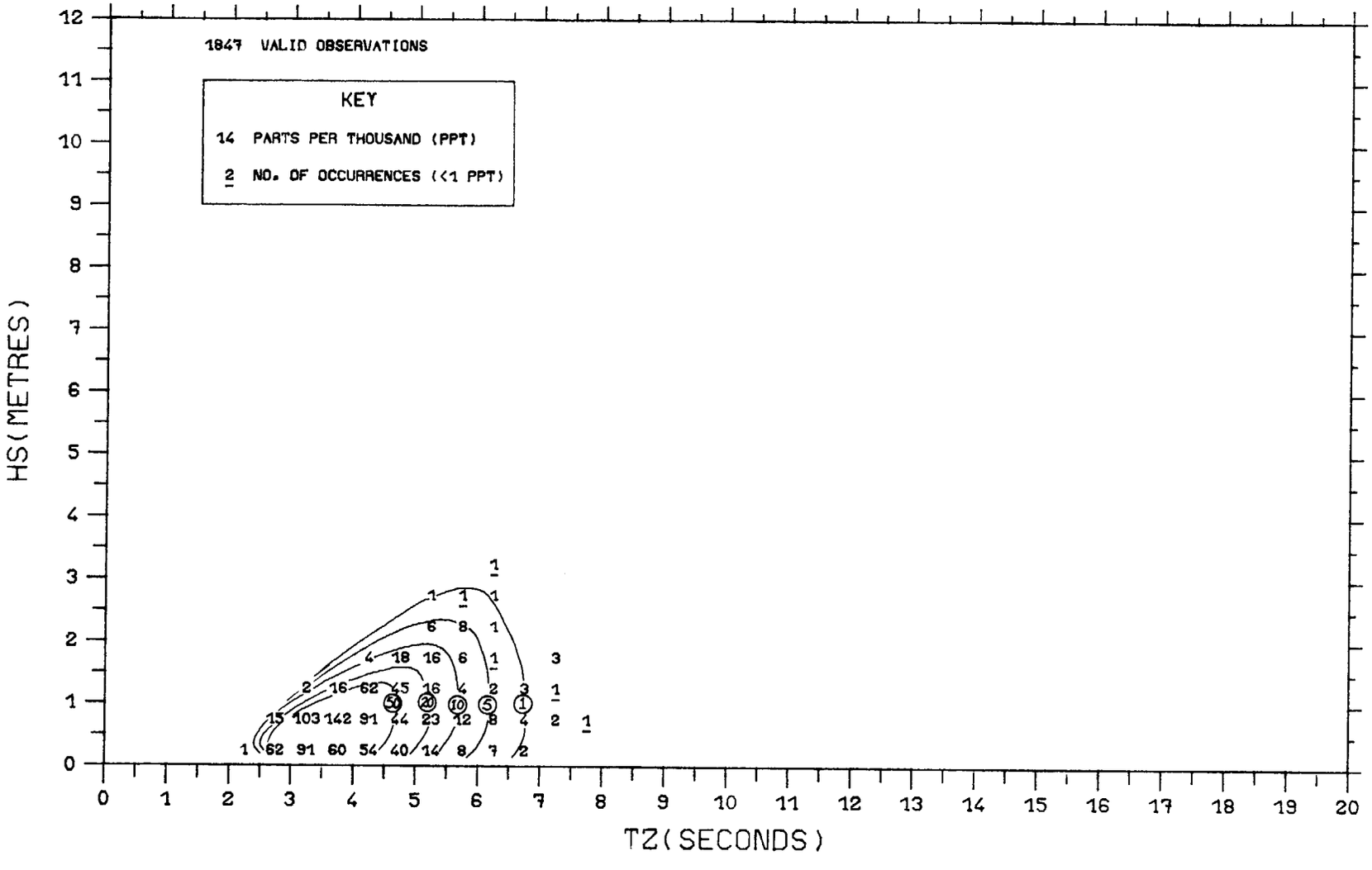


SCATTER PLOT OF HS AND TZ

EDDYSTONE SEPT 1978 - AUG 1981 SUMMERS

FIGURE 3.5.1.2

CA7881

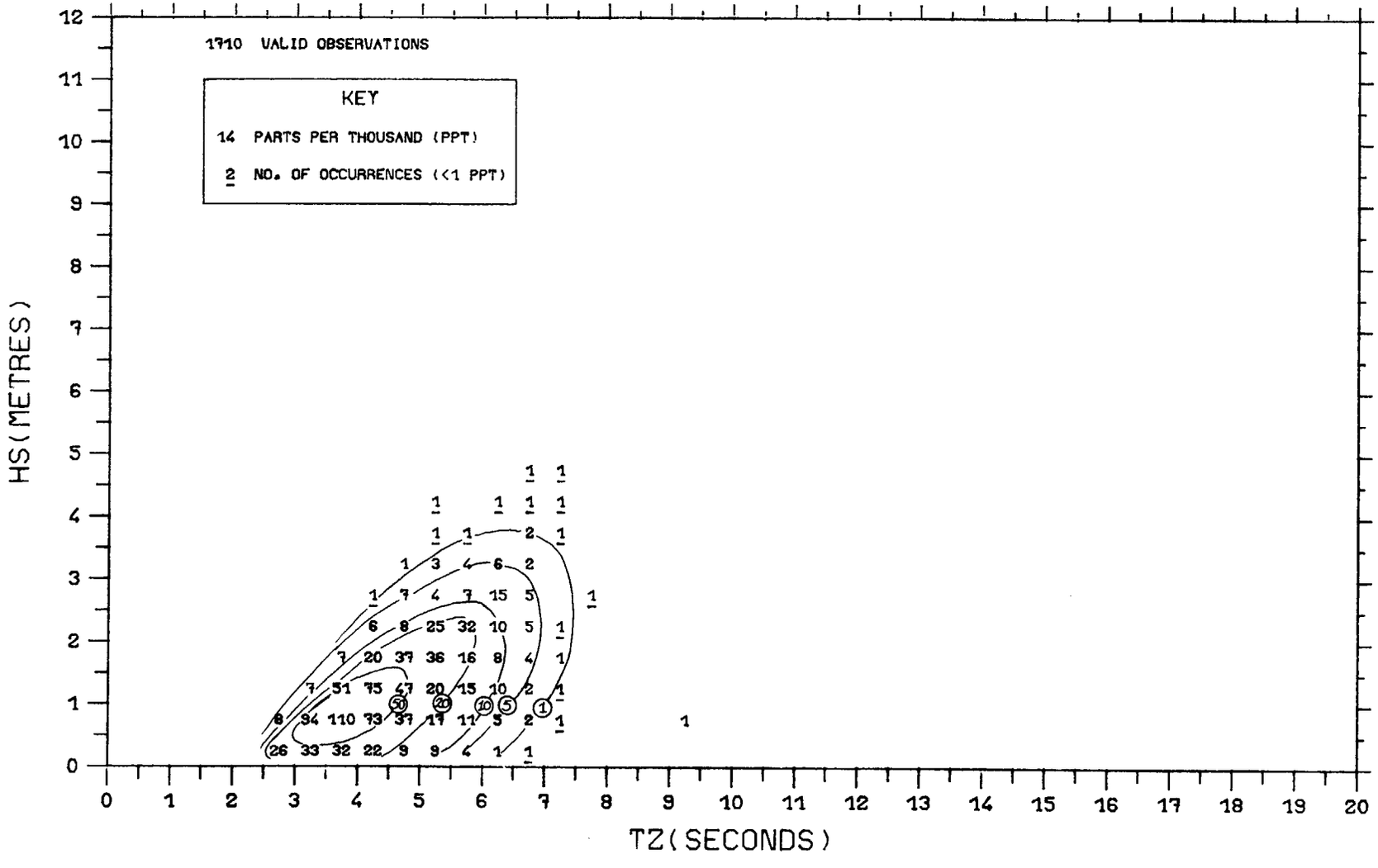


SCATTER PLOT OF HS AND TZ

EDDYSTONE SEPT 1978 - AUG 1981 AUTUMNS

FIGURE 3.5.1.3

CA7881

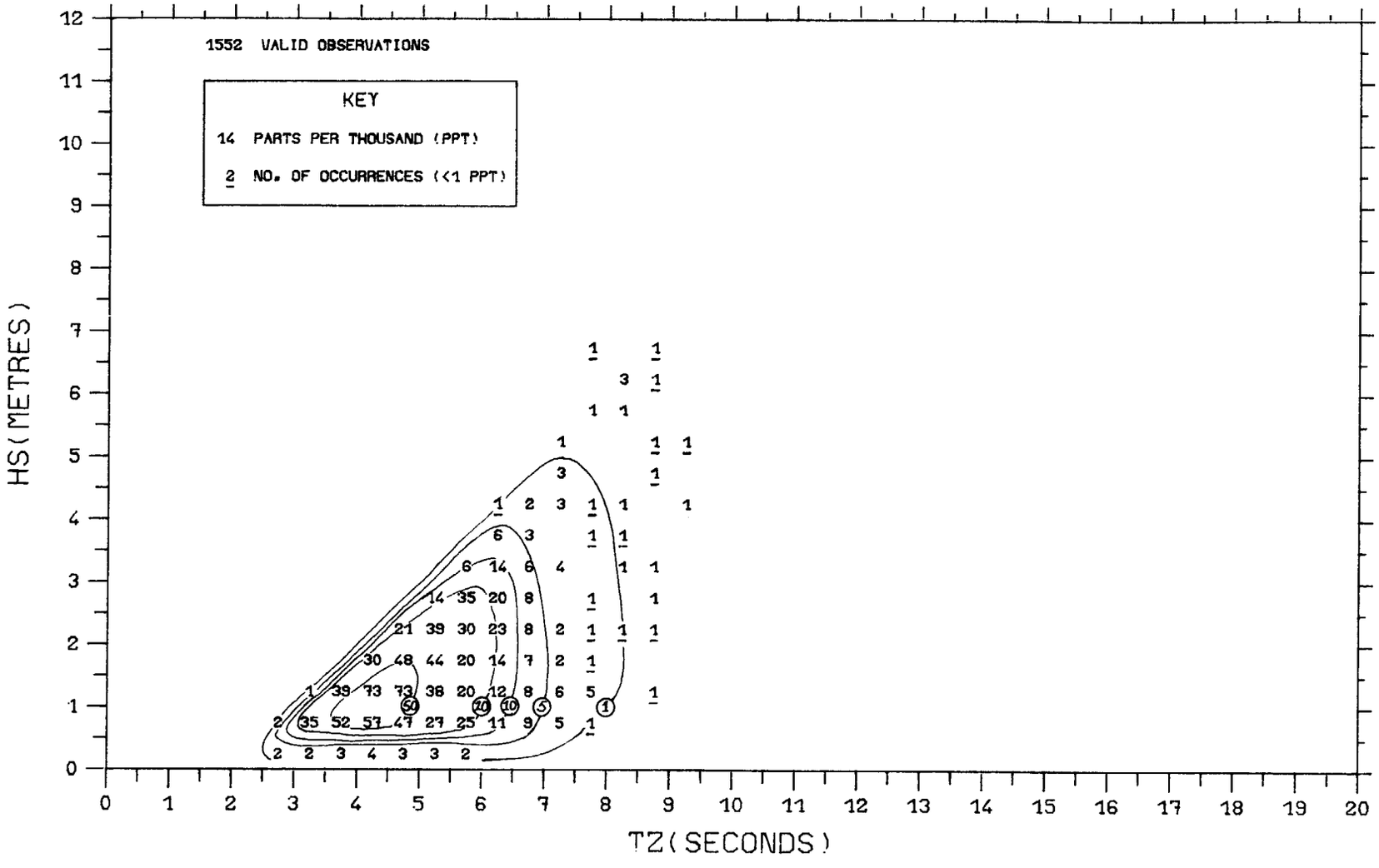


SCATTER PLOT OF HS AND TZ

EDDYSTONE SEPT 1978 - AUG 1981 WINTERS

FIGURE 3.5.1.4

CA7881

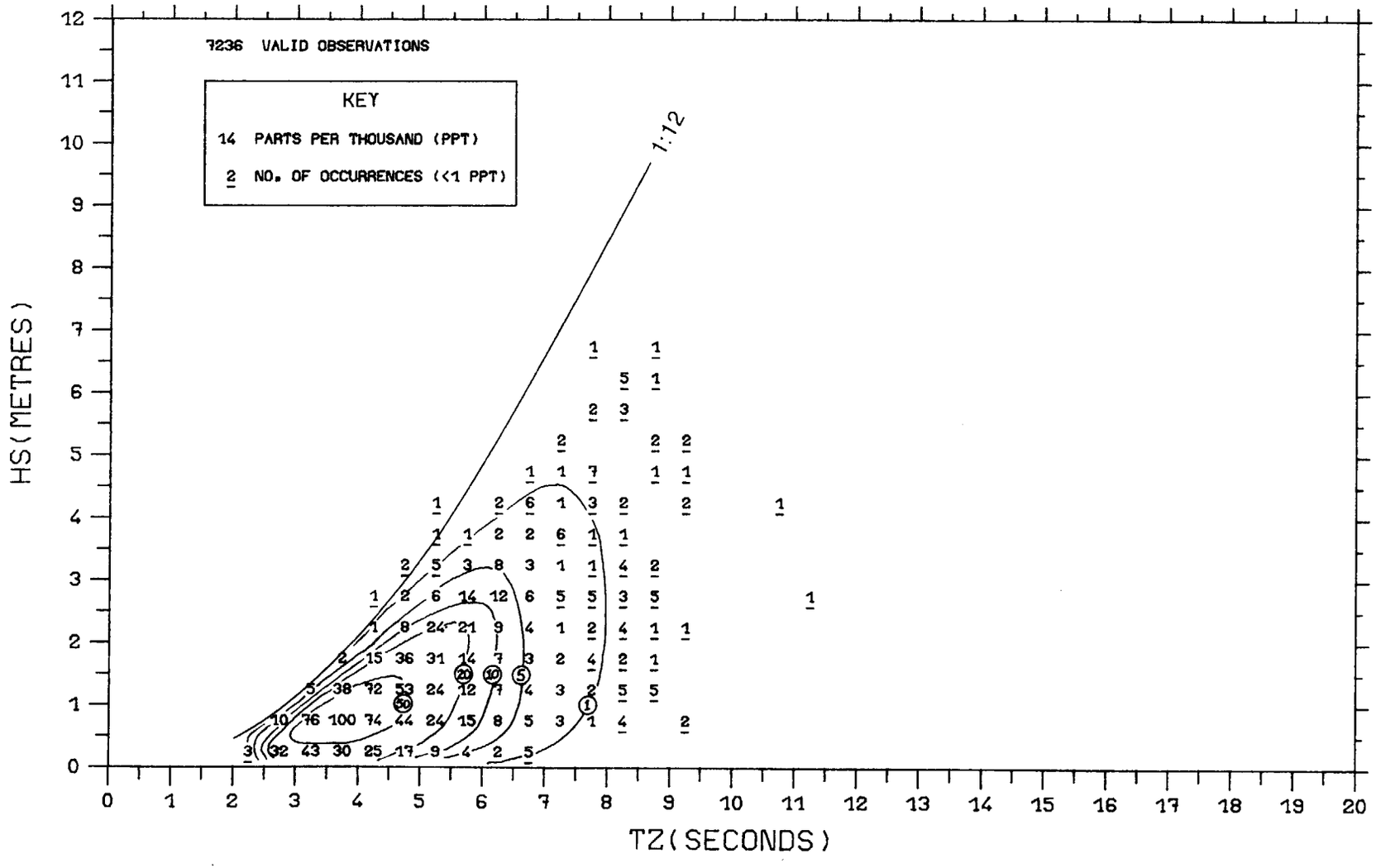


SCATTER PLOT OF HS AND TZ

EDDYSTONE SEPT 1978 - AUG 1981

FIGURE 3.5.1.5

CA7881

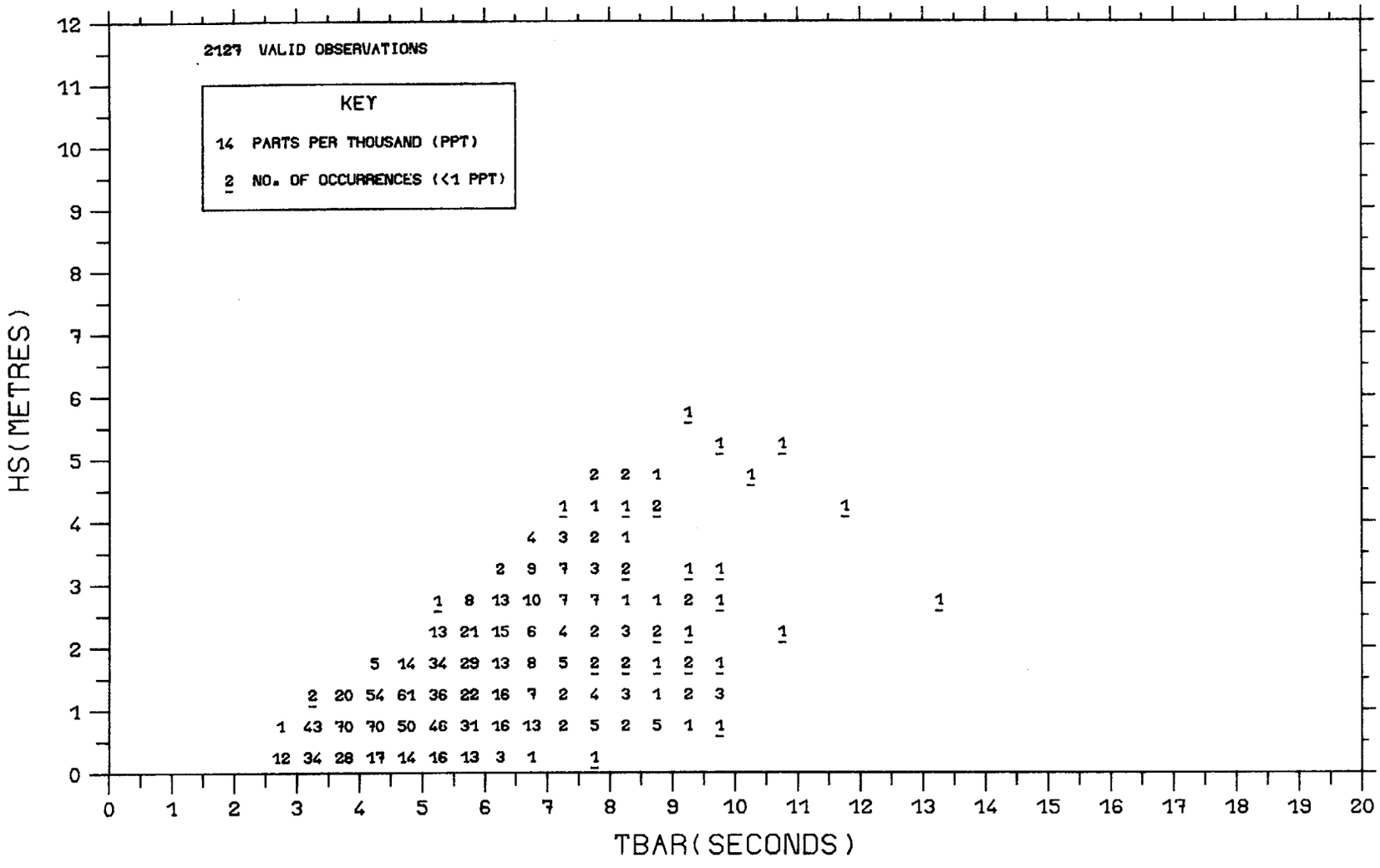


SCATTER PLOT OF HS AND TBAR

EDDYSTONE SEPT 1978 - AUG 1981 SPRINGS

FIGURE 3.5.2.1

CA7881

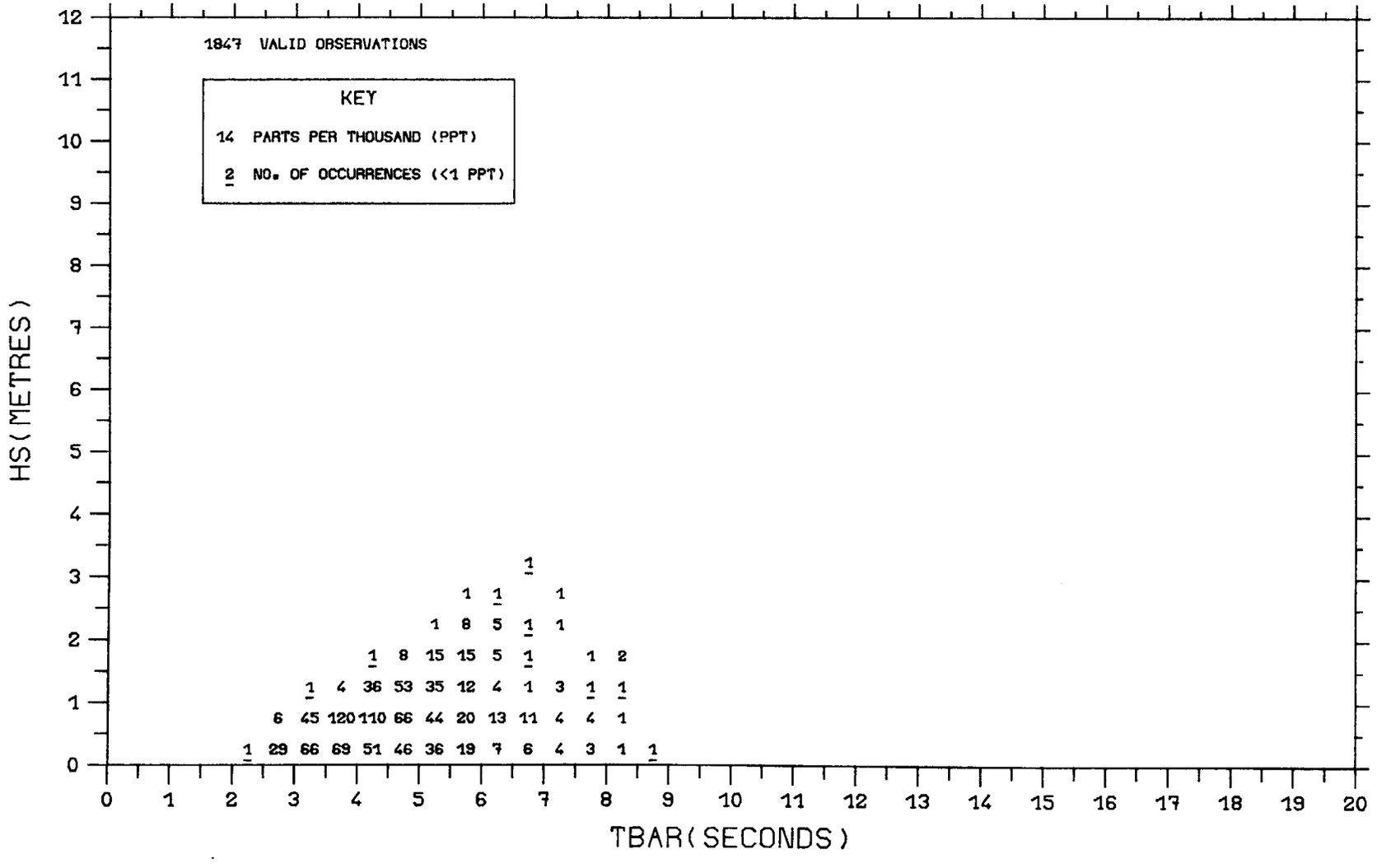


SCATTER PLOT OF HS AND TBAR

EDDYSTONE SEPT 1978 - AUG 1981 SUMMERS

FIGURE 3.5.2.2

CA7881

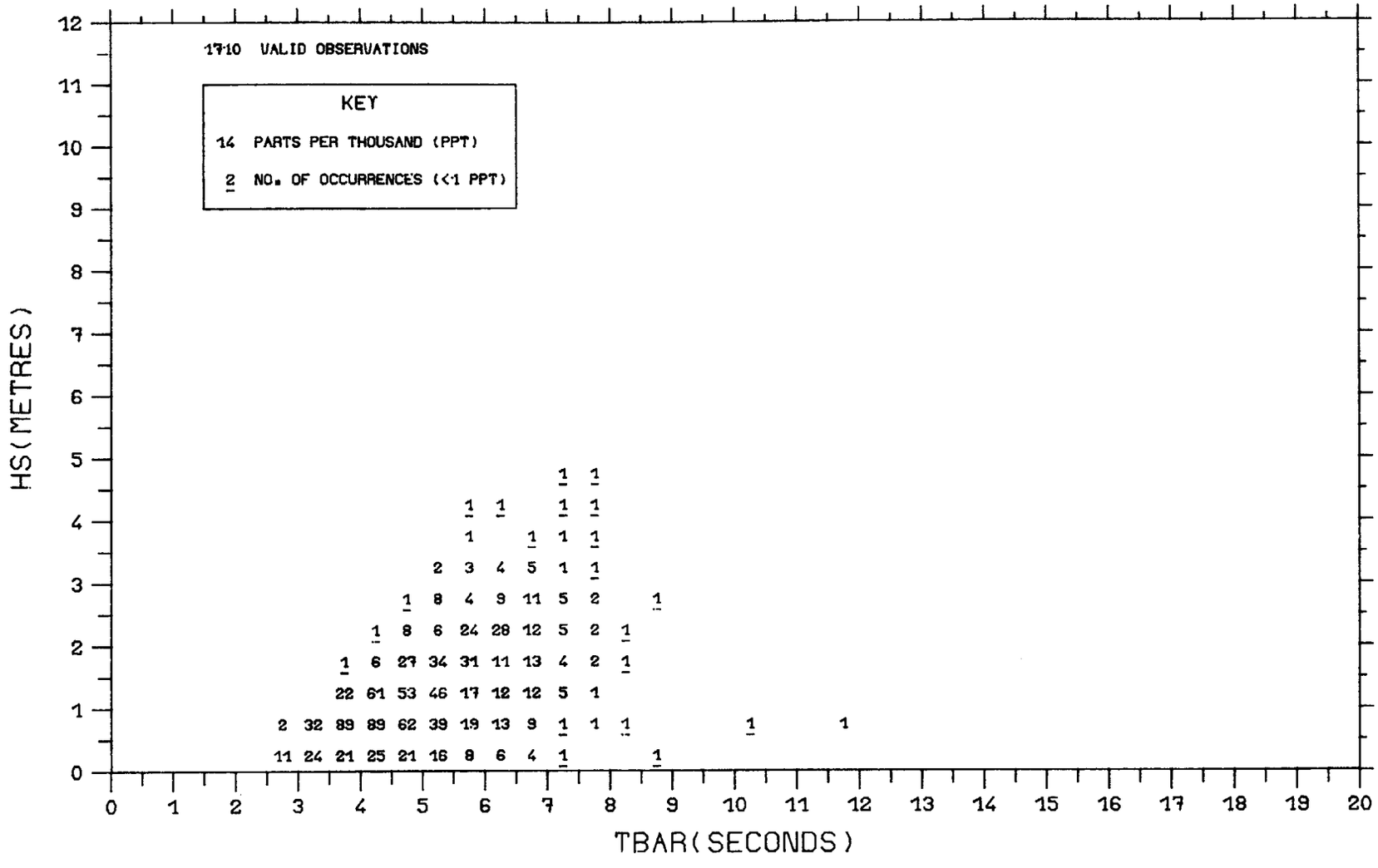


SCATTER PLOT OF HS AND TBAR

EDDYSTONE SEPT 1978 - AUG 1981 AUTUMNS

FIGURE 3.5.2.3

CA7881

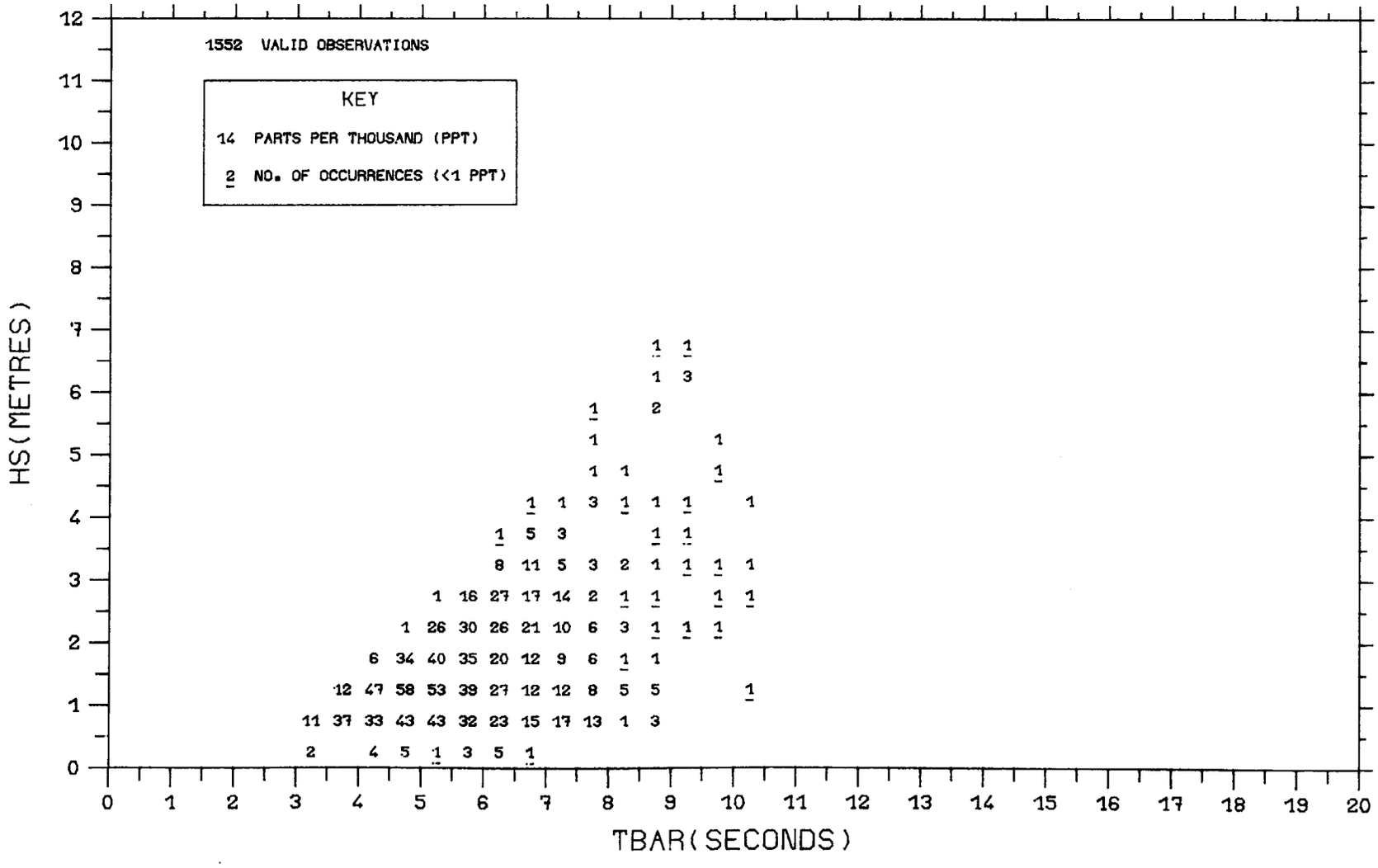


SCATTER PLOT OF HS AND TBAR

EDDYSTONE SEPT 1978 - AUG 1981 WINTERS

FIGURE 3.5.2.4

CA7881

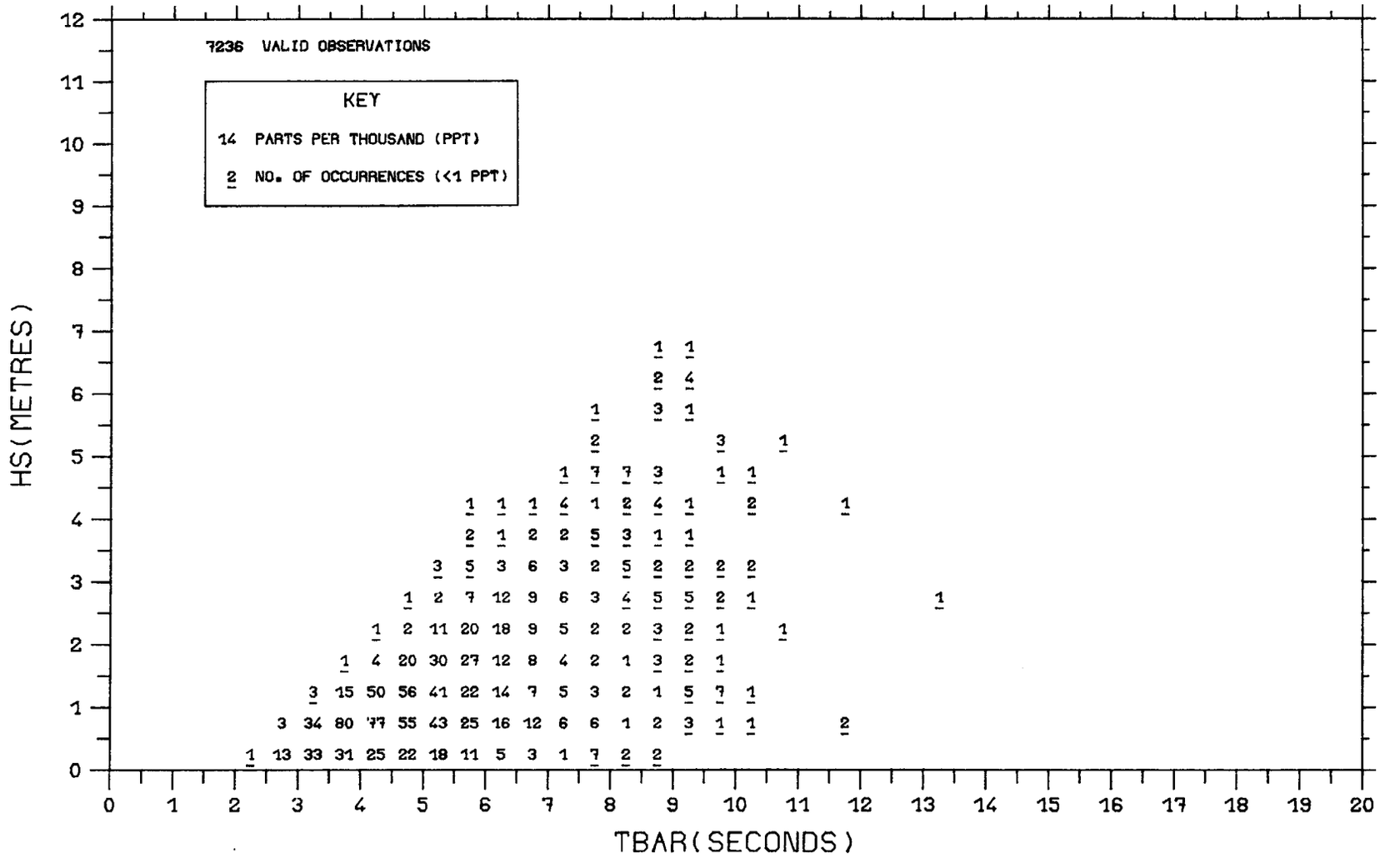


SCATTER PLOT OF HS AND TBAR

EDDYSTONE SEPT 1978 - AUG 1981

FIGURE 3.5.2.5

CA7881

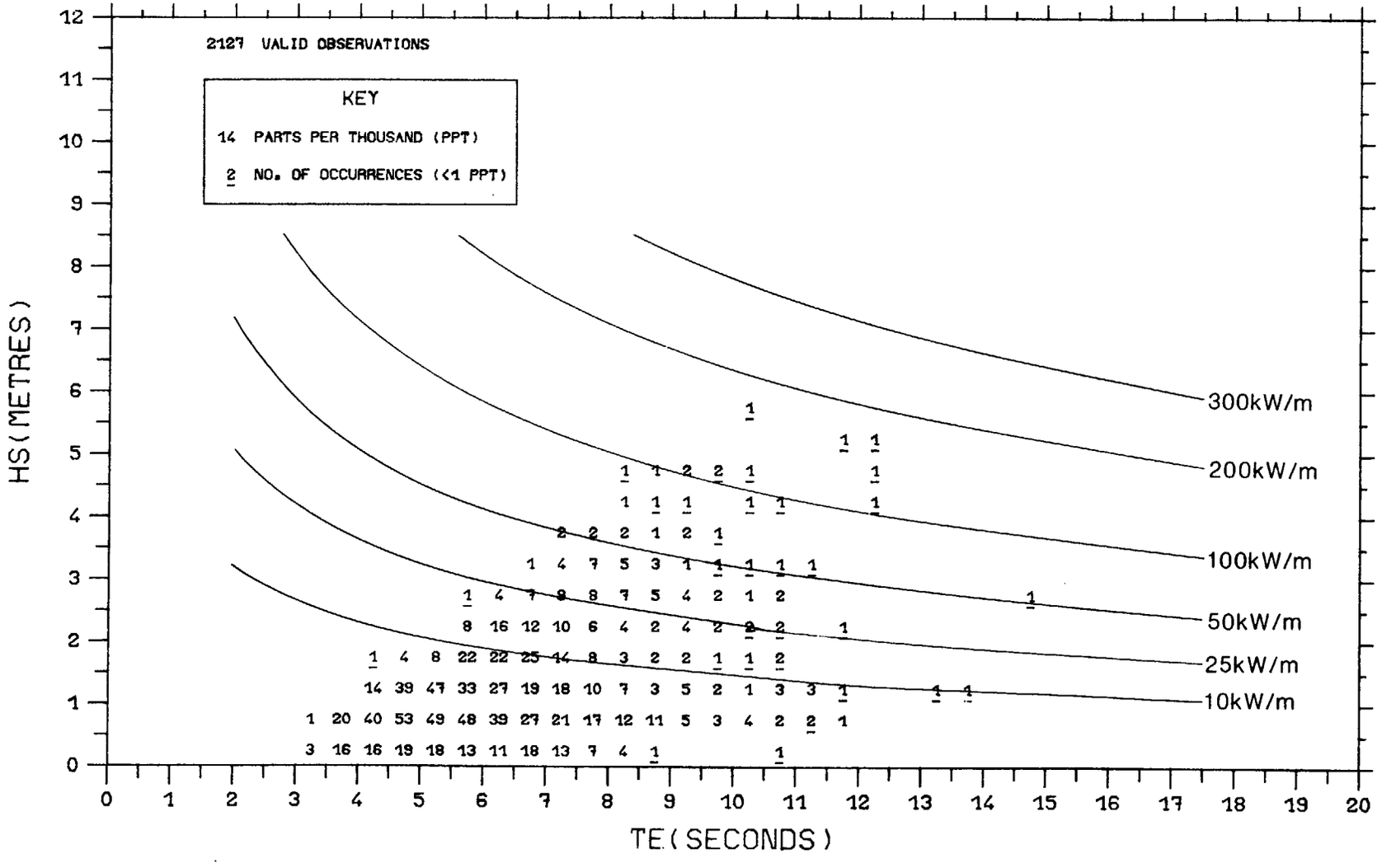


SCATTER PLOT OF HS AND TE

EDDYSTONE SEPT 1978 - AUG 1981 SPRINGS

FIGURE 3.5.3.1

CA7881

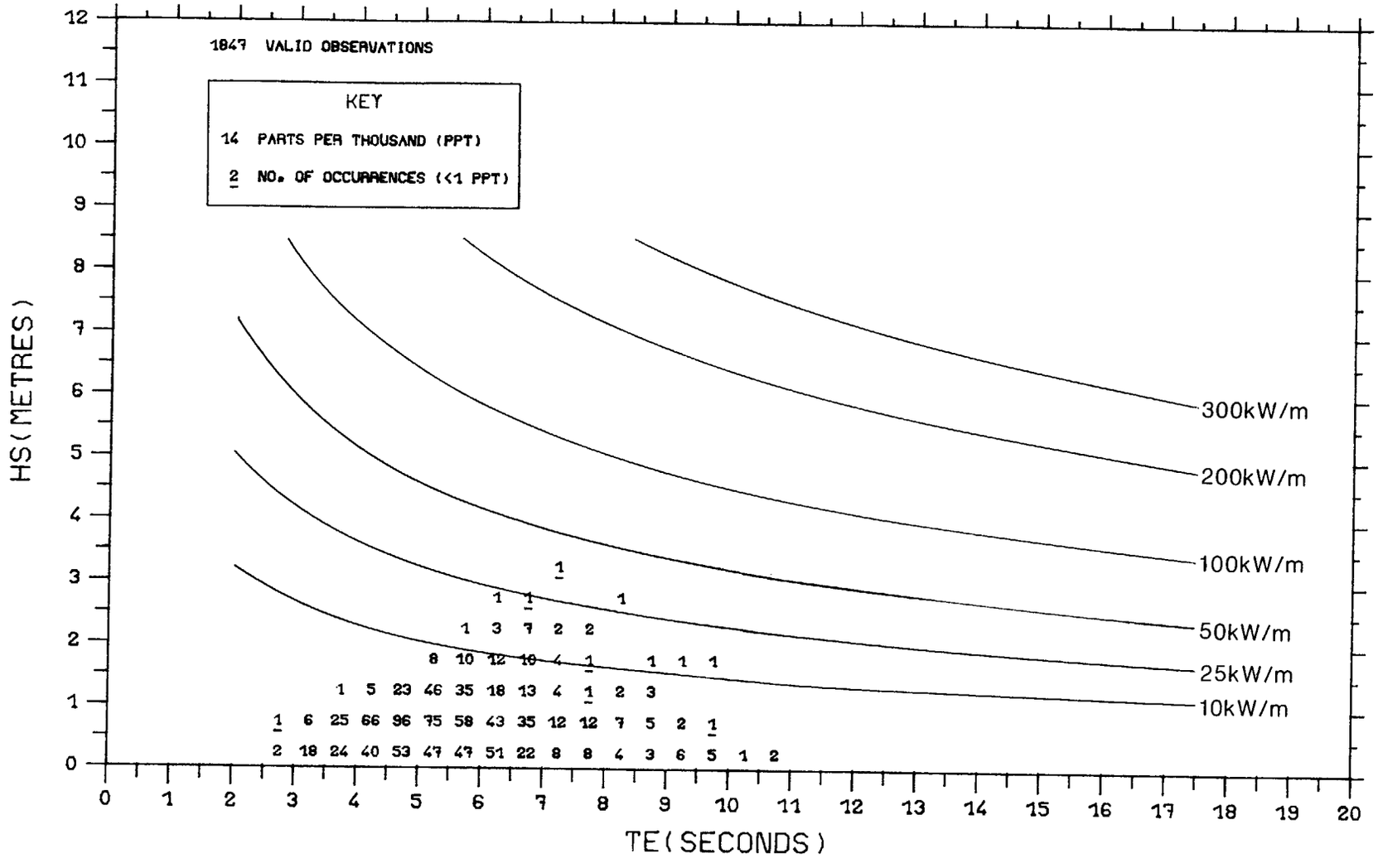


SCATTER PLOT OF HS AND TE

EDDYSTONE SEPT 1978 - AUG 1981 SUMMERS

FIGURE 3.5.3.2

CA7881

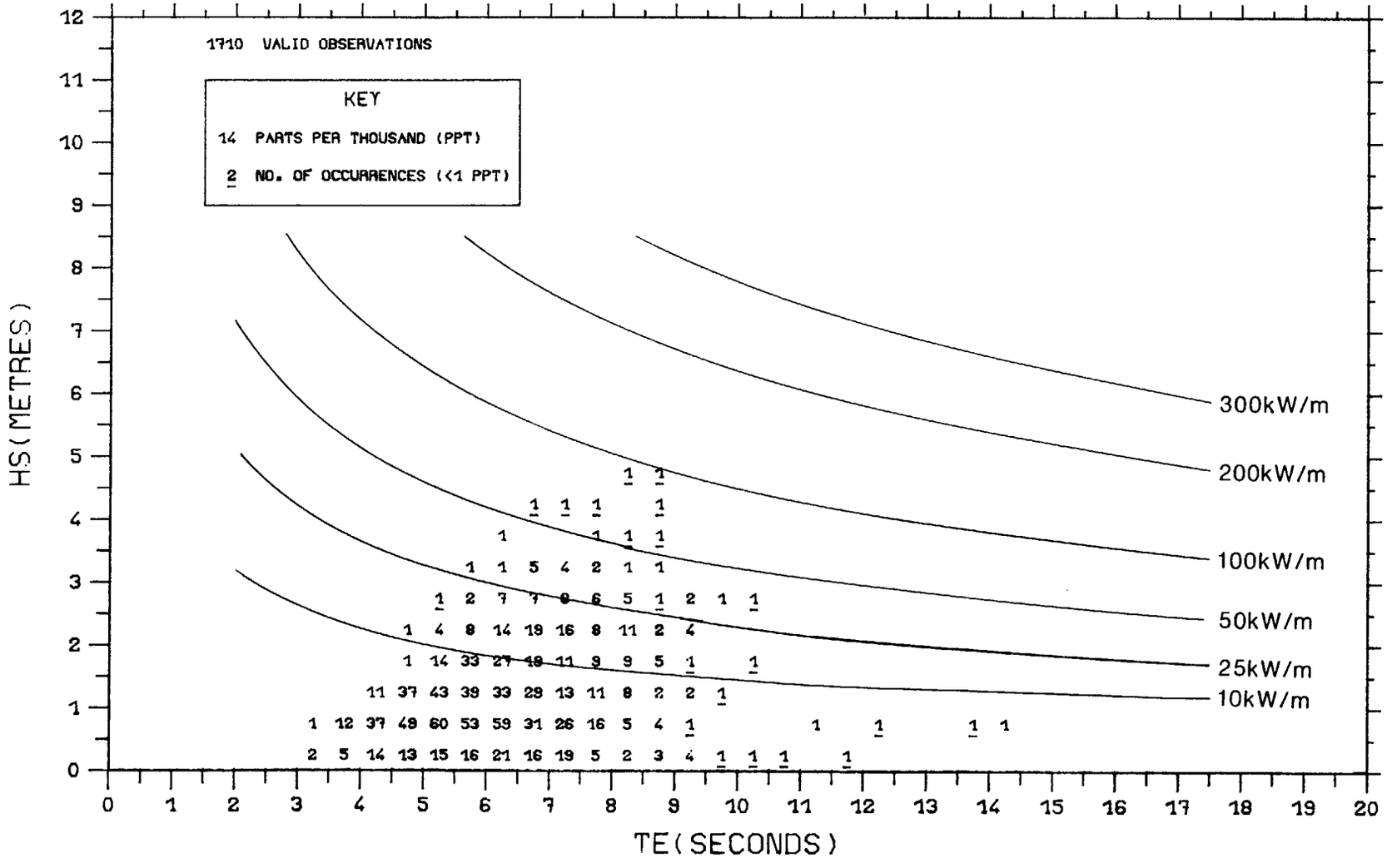


SCATTER PLOT OF HS AND TE

EDDYSTONE SEPT 1978 - AUG 1981 AUTUMNS

FIGURE 3.5.3.3

CA7881

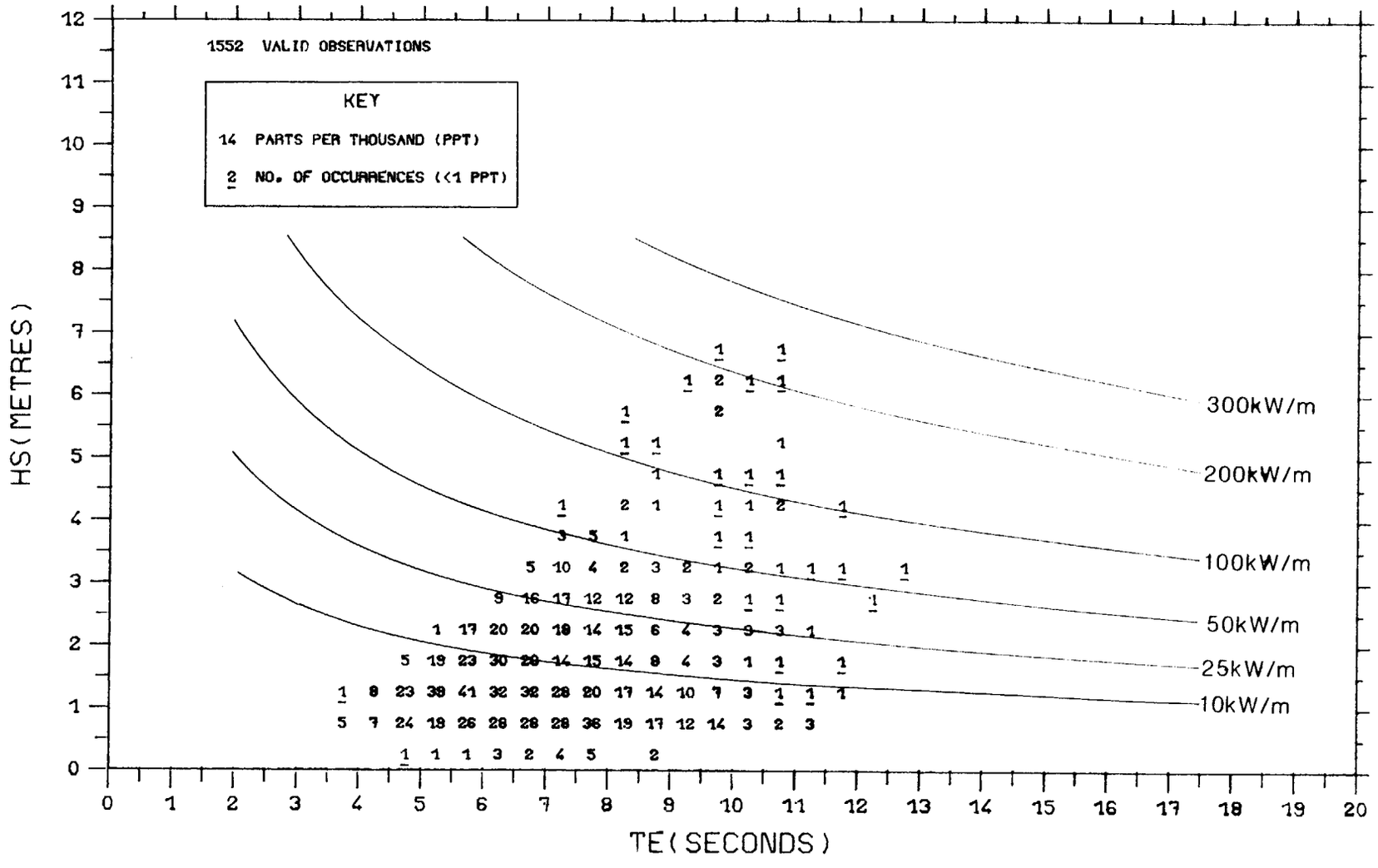


SCATTER PLOT OF HS AND TE

EDDYSTONE SEPT 1978 - AUG 1981 WINTERS

FIGURE 3.5.3.4

CA7881

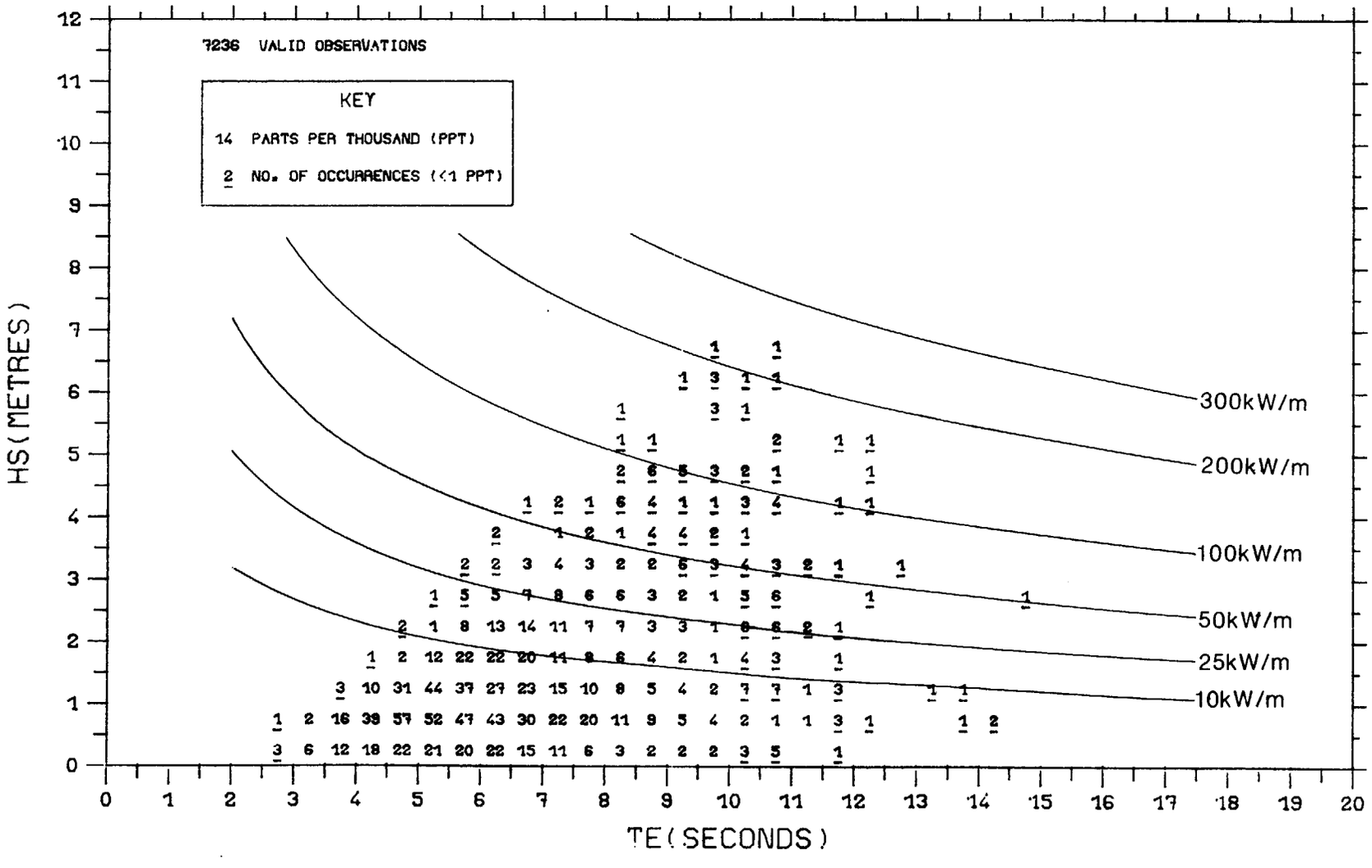


SCATTER PLOT OF HS AND TE

EDDYSTONE SEPT 1978 - AUG 1981

FIGURE 3.5.3.5

CA7881

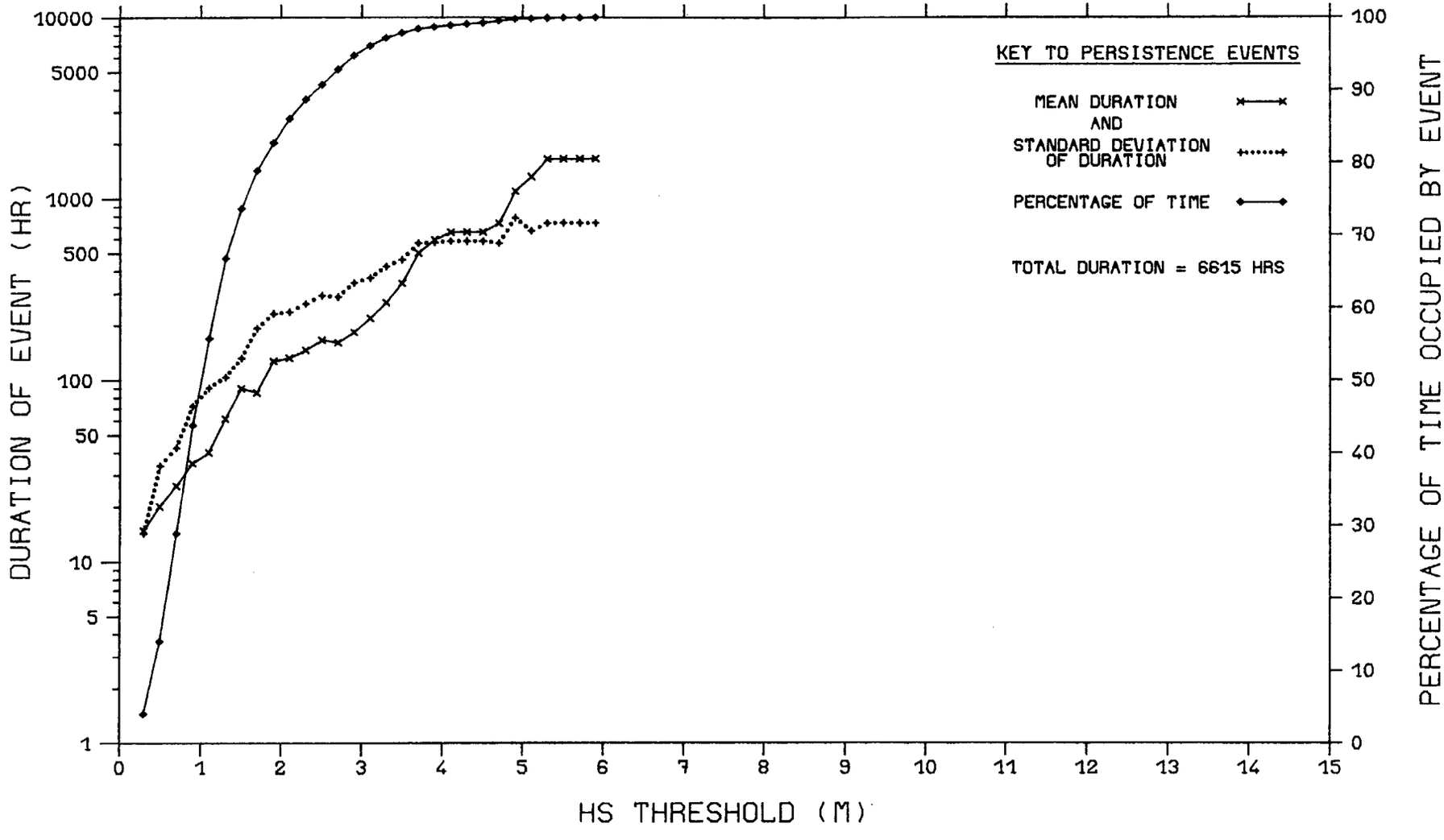


EDDYSTONE SEPT 1978 - AUG 1981 SPRINGS

CALMS

FIG 3.6.1.1

CA7881

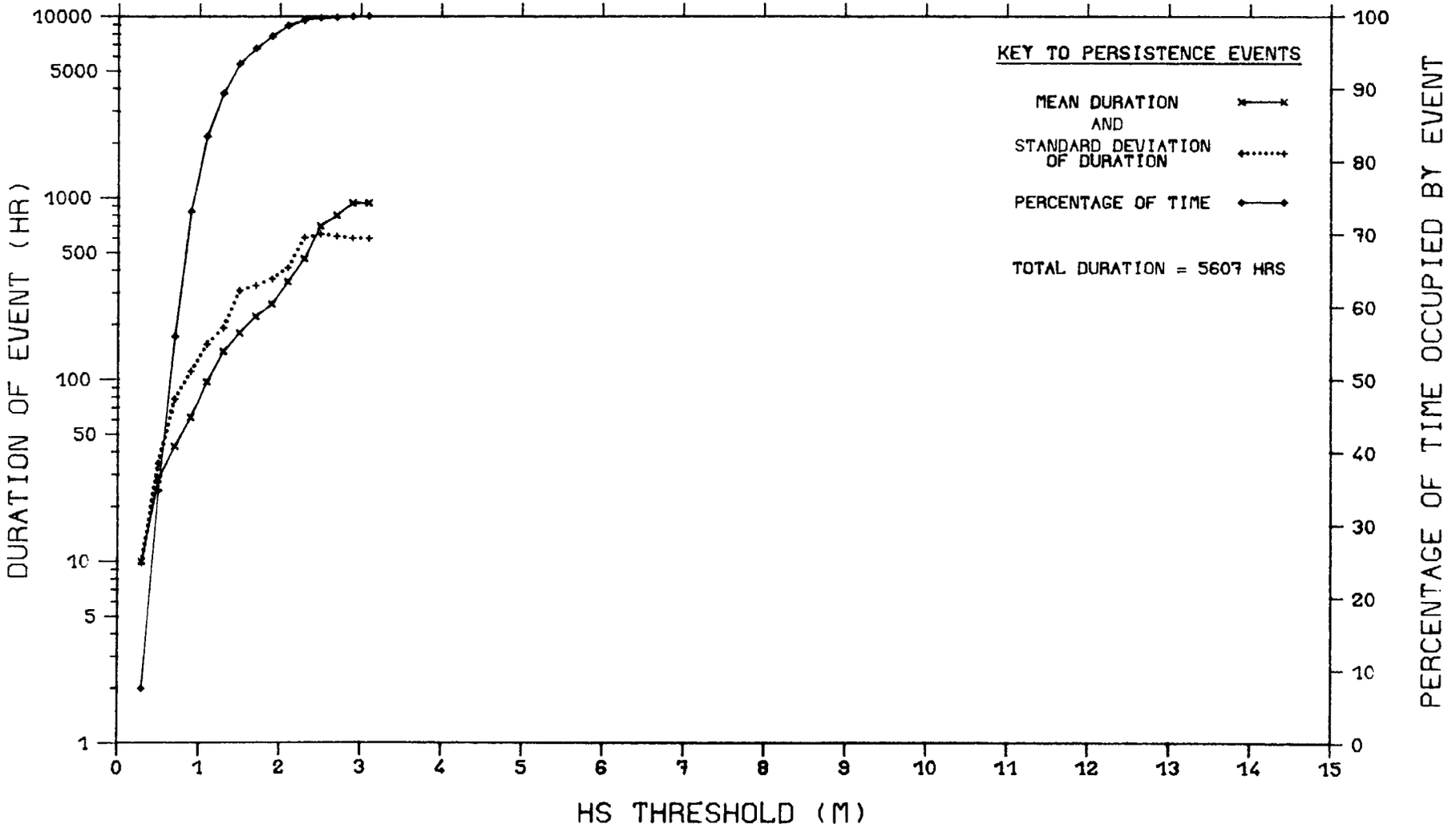


EDDYSTONE SEPT 1978 - AUG 1981 SUMMERS

CALMS

FIG 3.6.1.2

CA7881

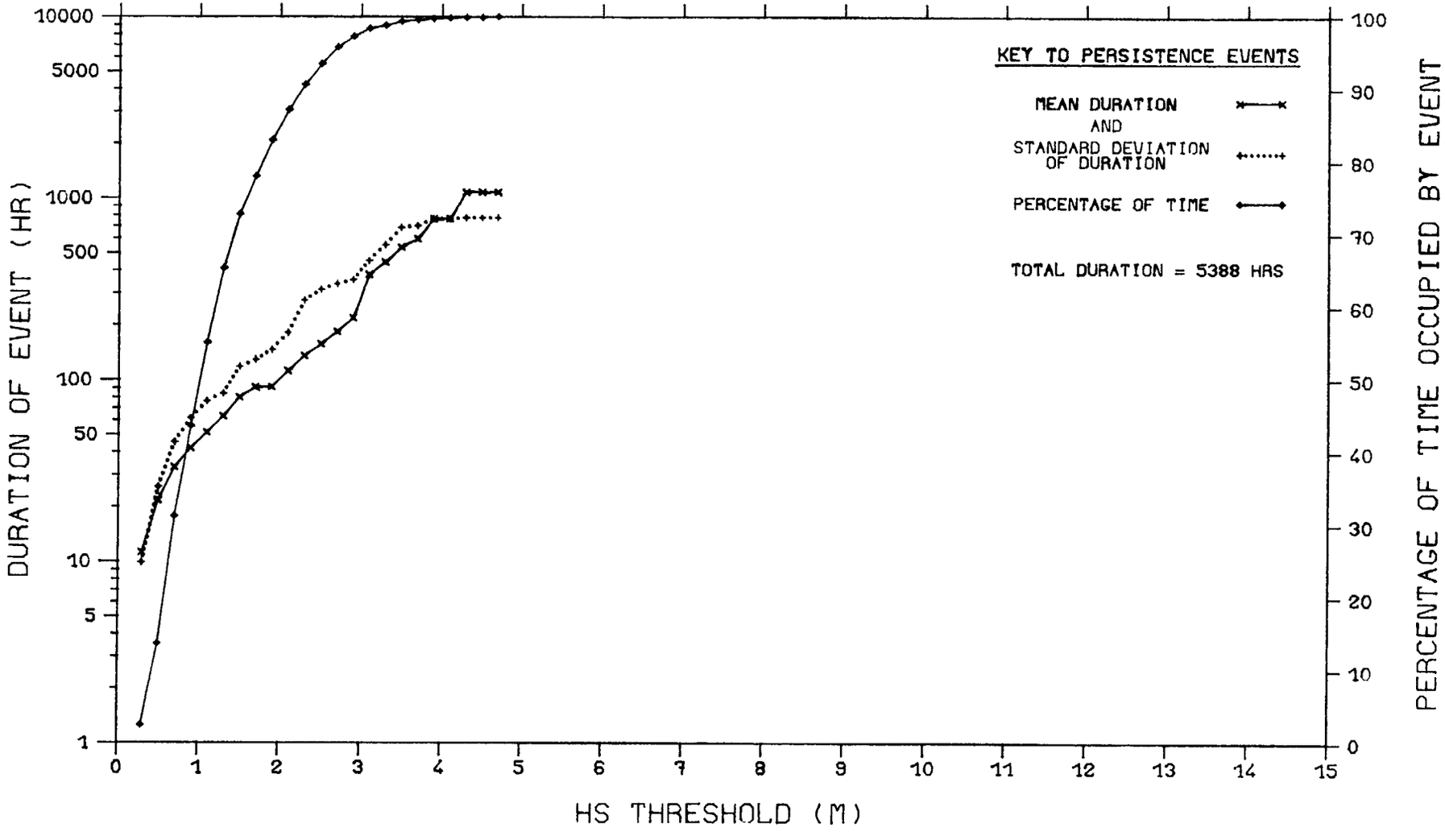


EDDYSTONE SEPT 1978 - AUG 1981 AUTUMNS

CALMS

FIG 3.6.1.3

CA7881

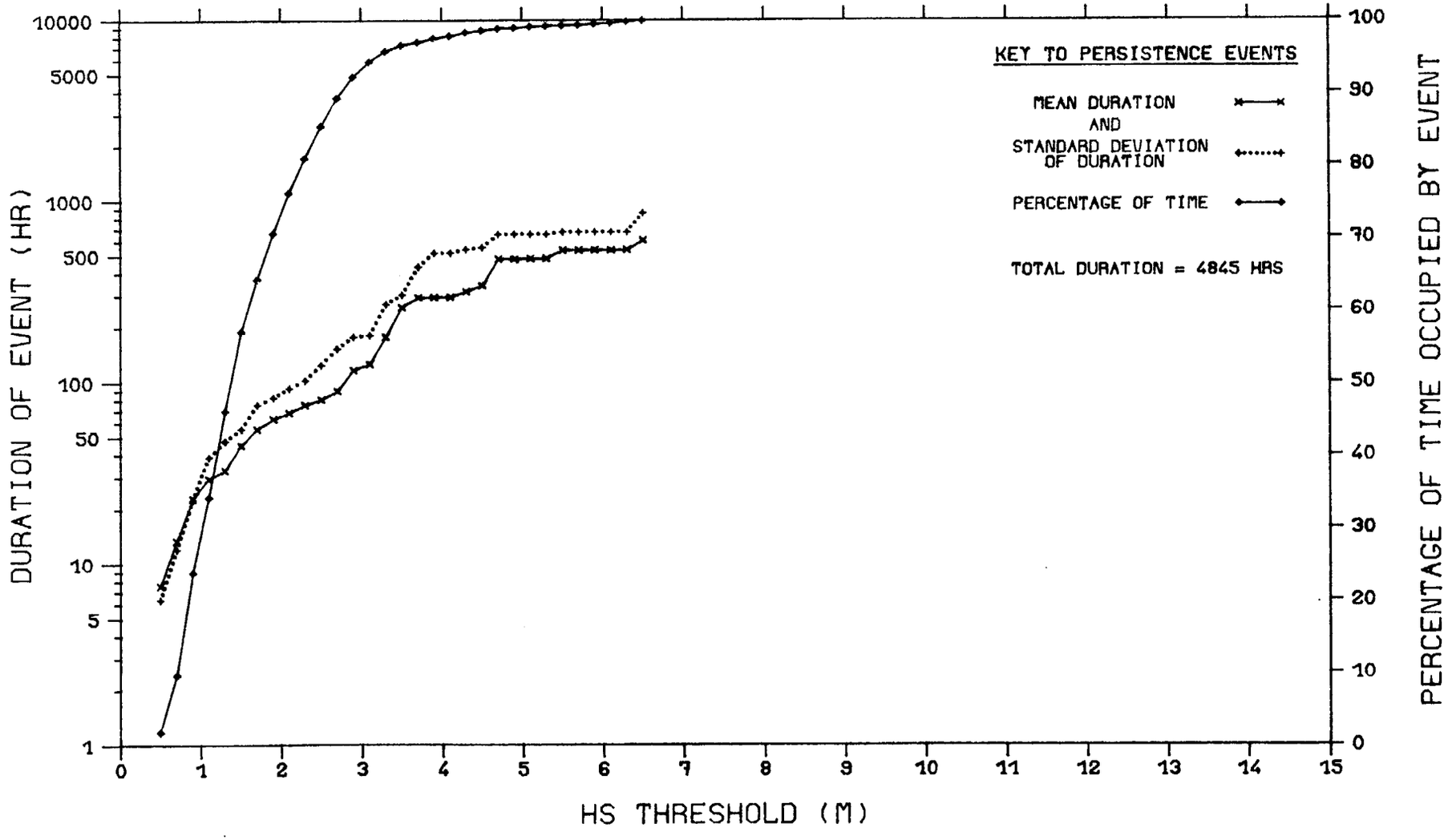


EDDYSTONE SEPT 1978 - AUG 1981 WINTERS

CALMS

FIG 3.6.1.4

CA7881

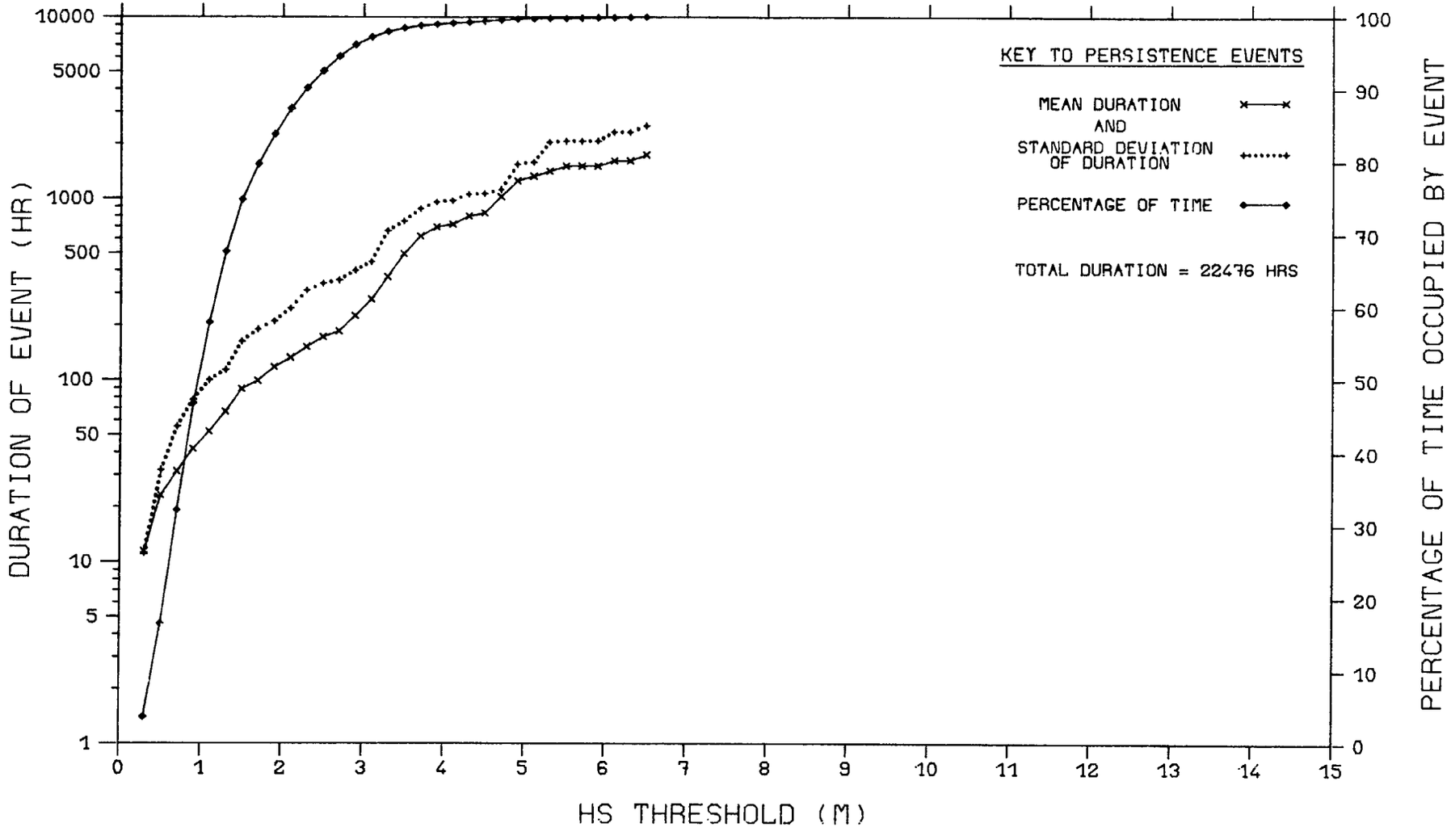


EDDYSTONE SEPT 1978 - AUG 1981

CALMS

FIG 3.6.1.5

CA7881

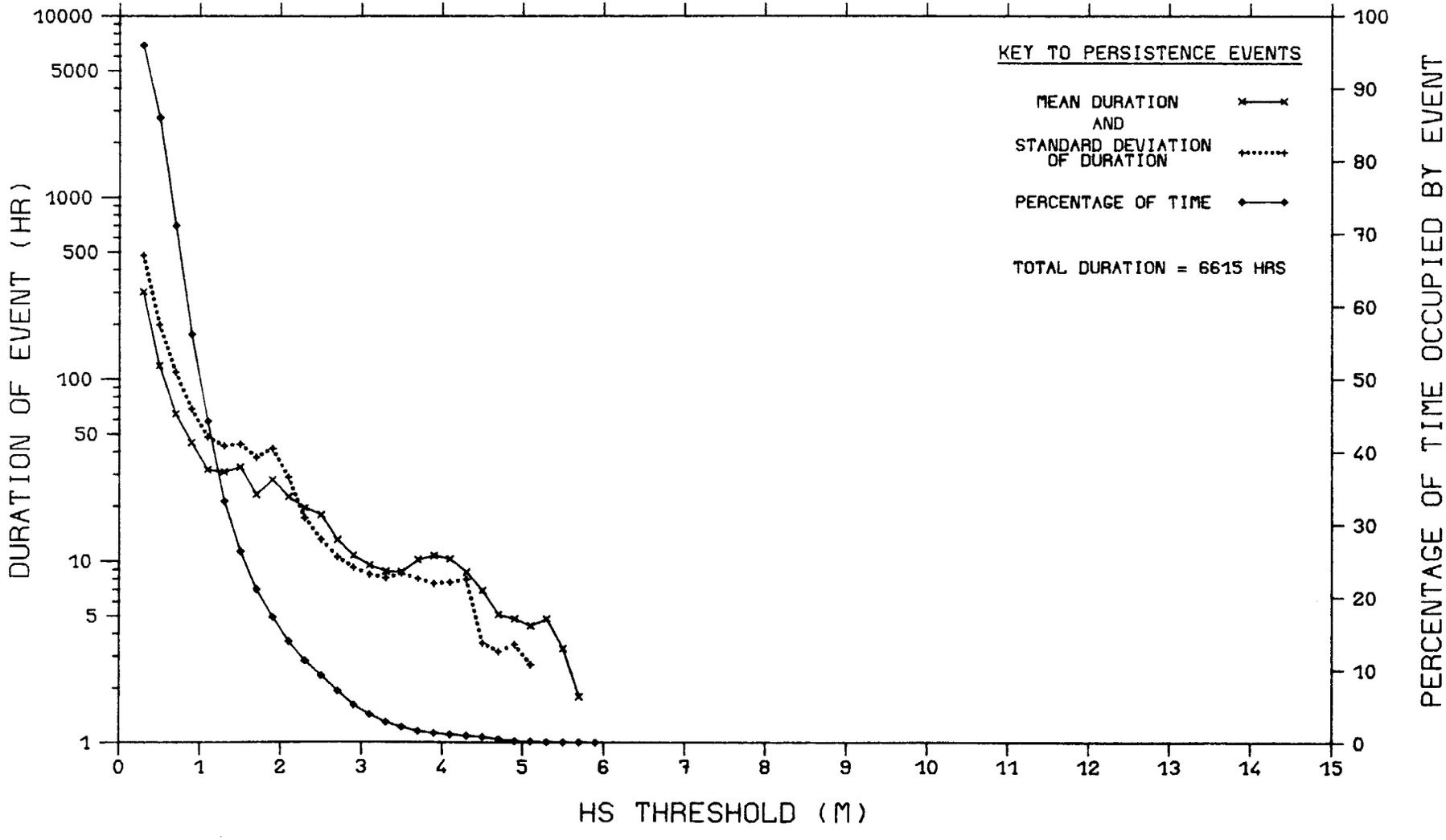


EDDYSTONE SEPT 1978 - AUG 1981 SPRINGS

STORMS

FIG 3.6.2.1

CA7881

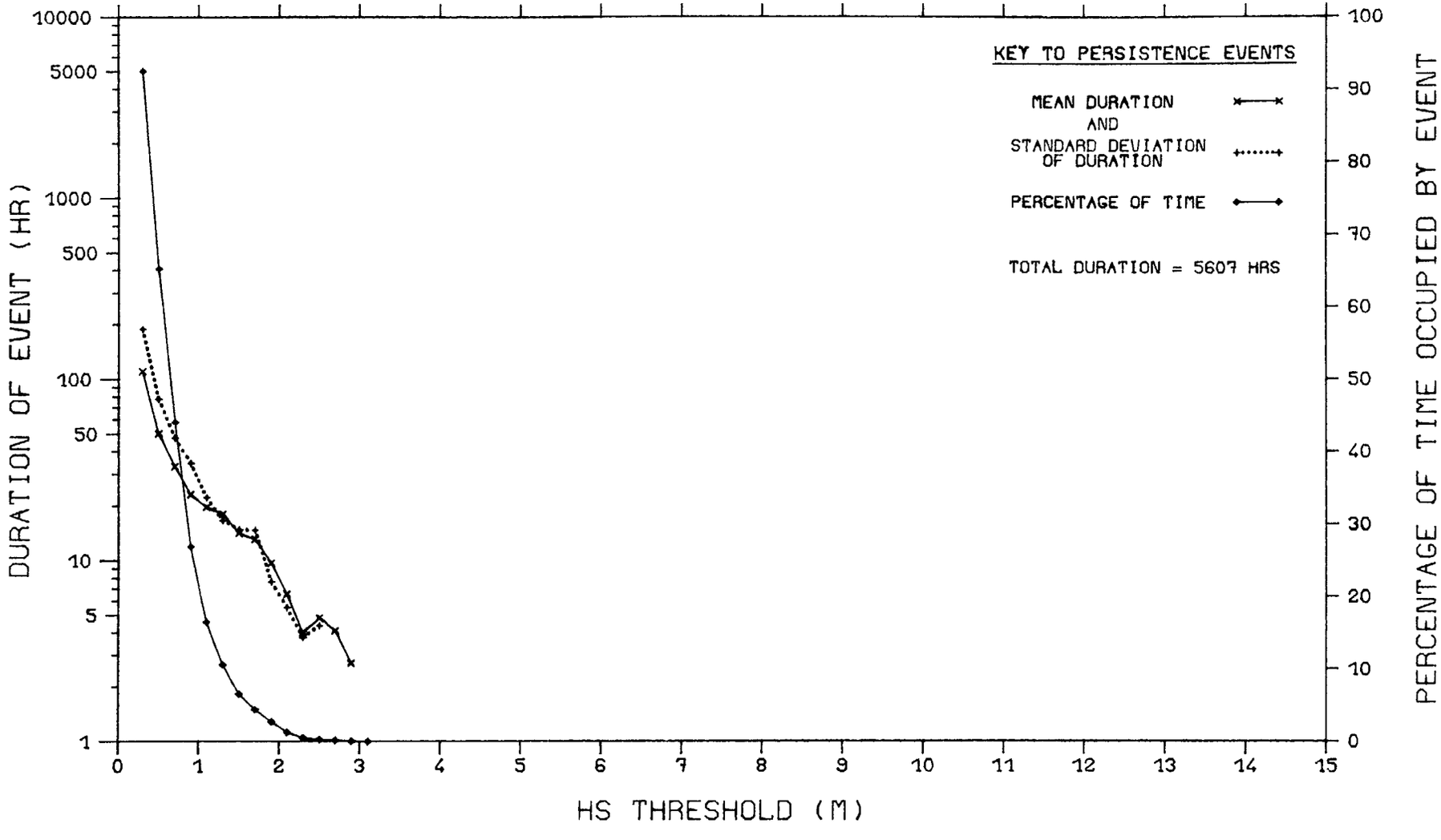


EDDYSTONE SEPT 1978 - AUG 1981 SUMMERS STORMS

FIG 3.6.2.2

CA7881

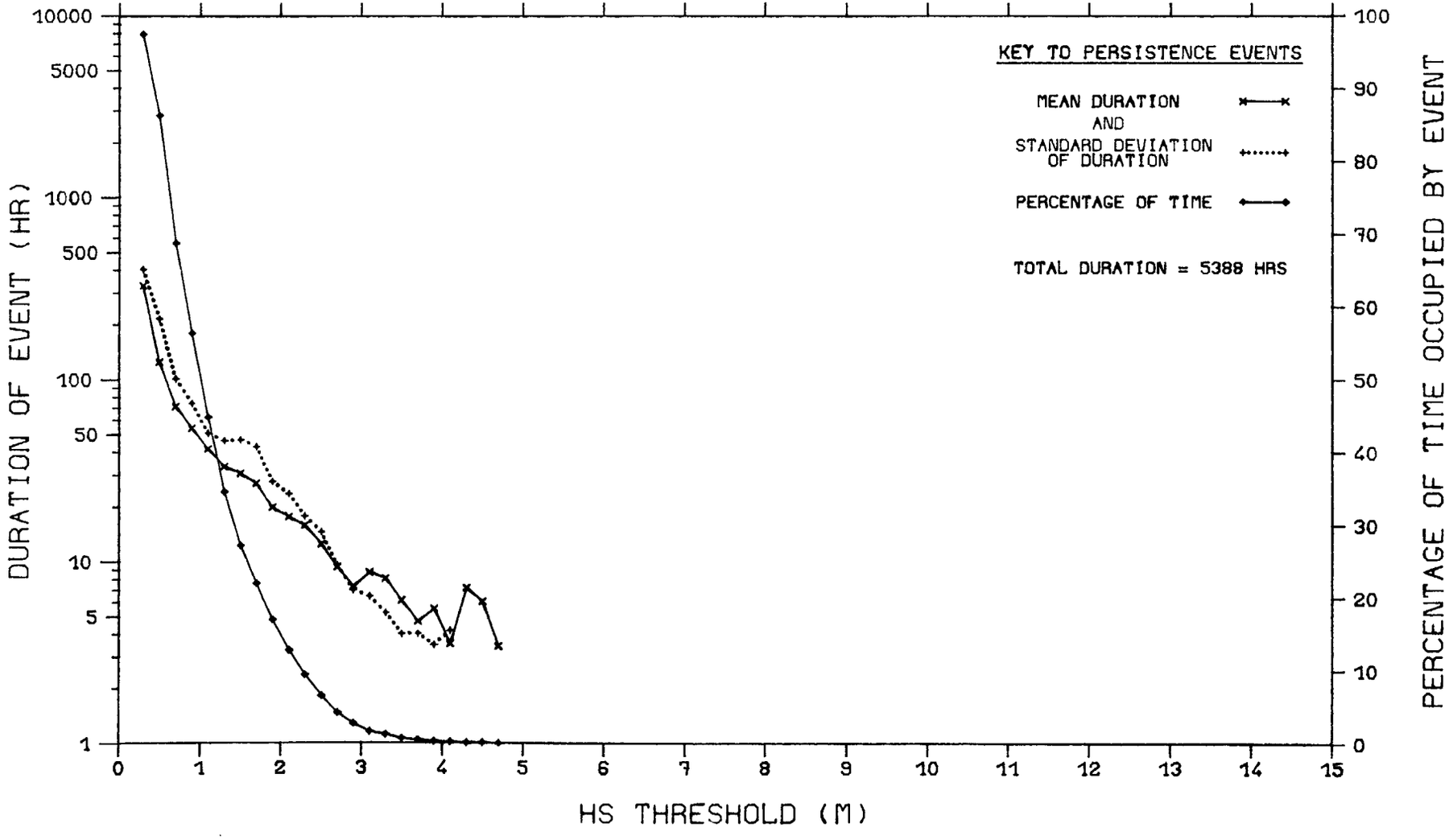


EDDYSTONE SEPT 1978 - AUG 1981 AUTUMNS

STORMS

FIG 3.6.2.3

CA7881

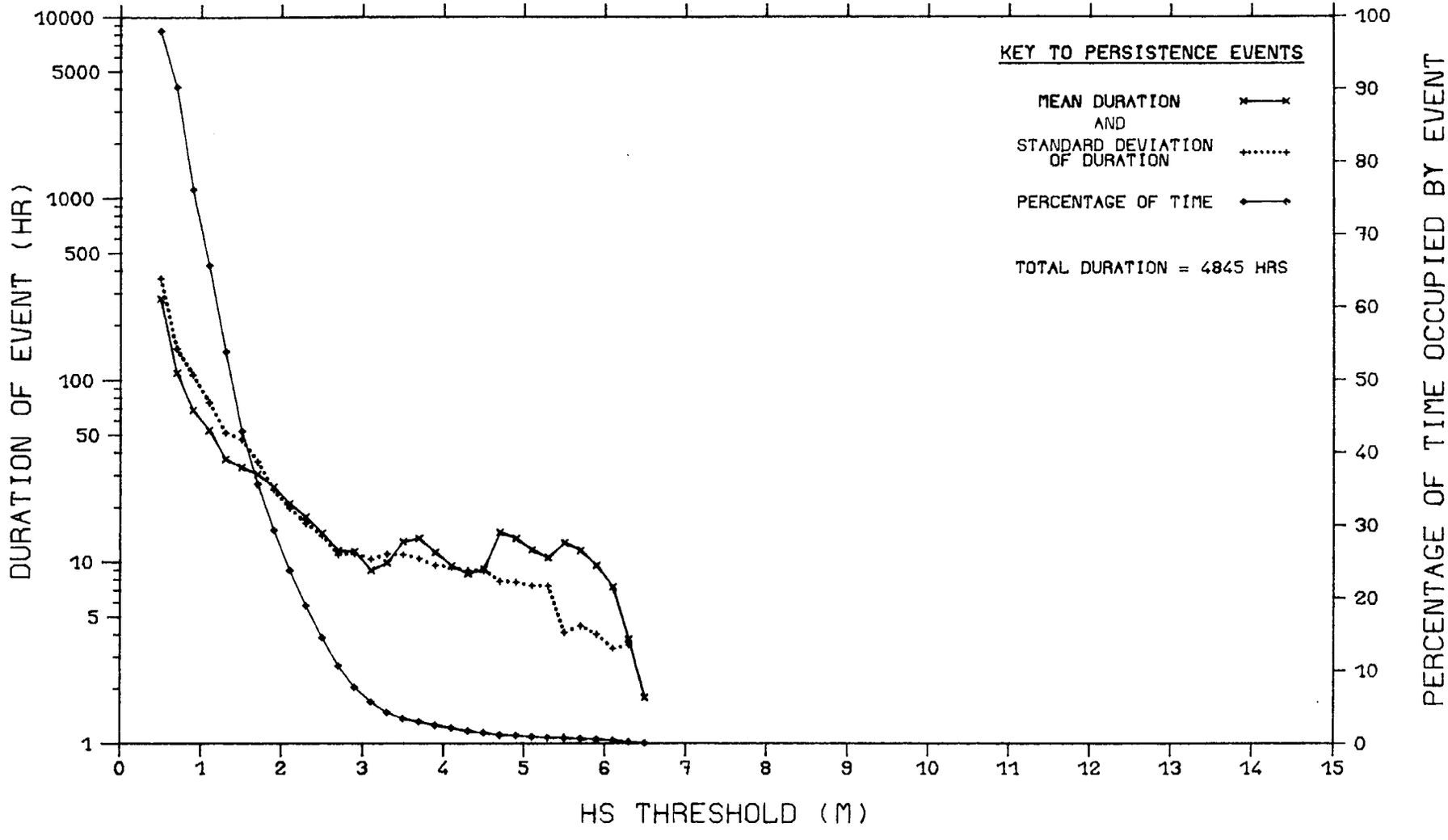


EDDYSTONE SEPT 1978 - AUG 1981 WINTERS

STORMS

FIG 3.6.2.4

CA7881

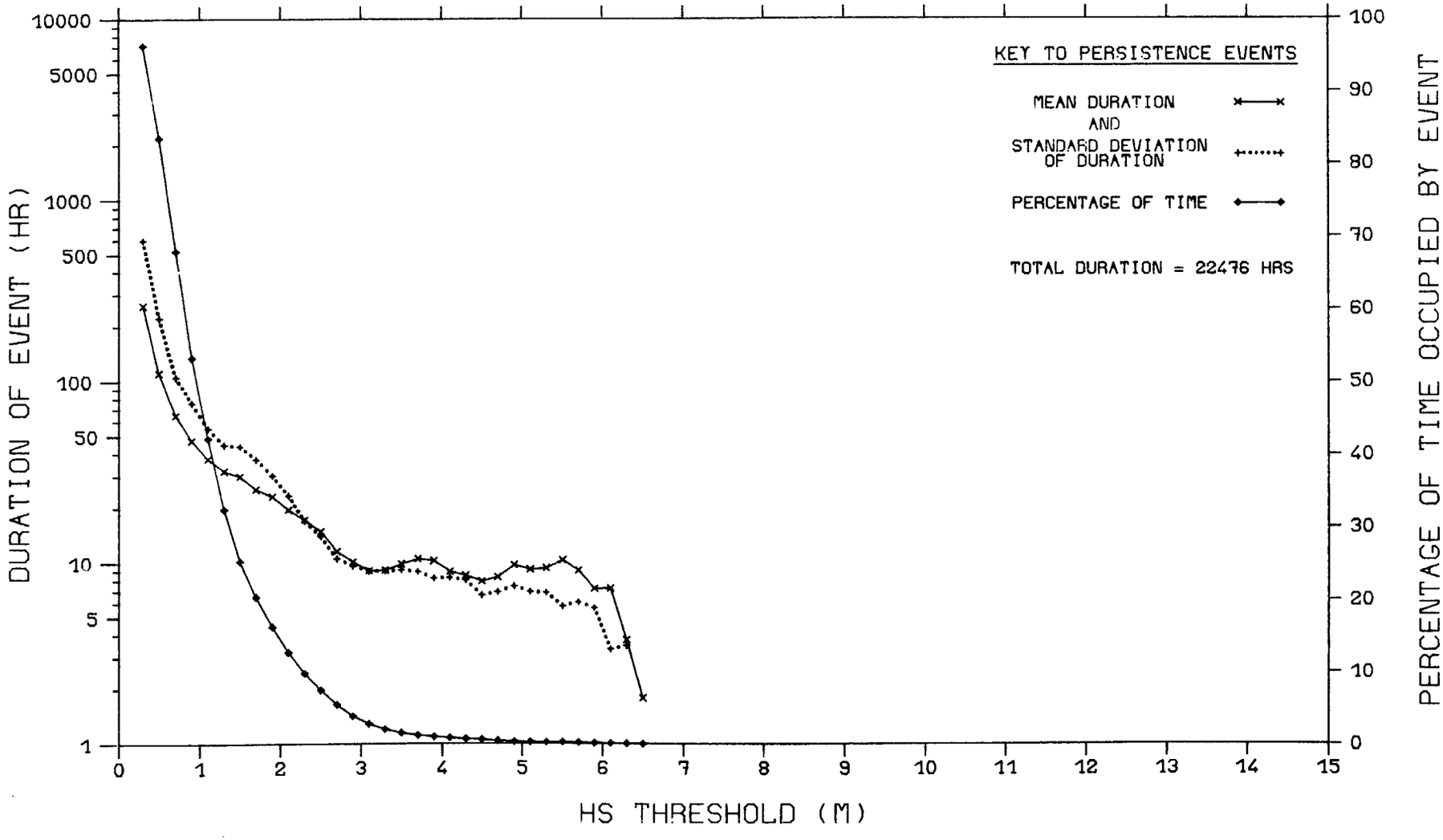


EDDYSTONE SEPT 1978 - AUG 1981

STORMS

FIG 3.6.2.5

CA7881

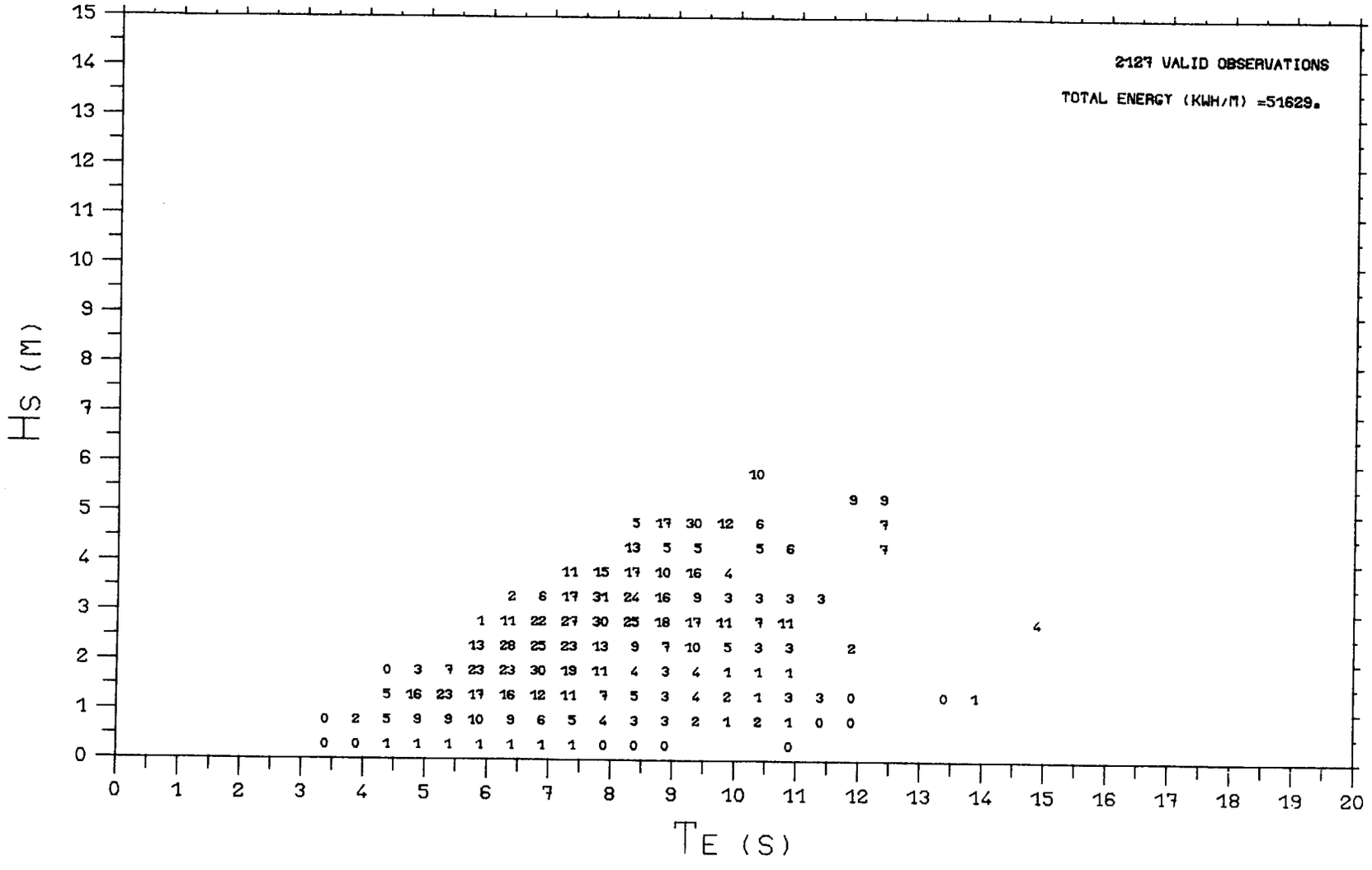


DISTRIBUTION OF TOTAL MEASURED WAVE ENERGY
WITH Hs AND TE (PPT)

EDDYSTONE SEPT 1978 - AUG 1981 SPRINGS

CA7881

FIG 3.7.1

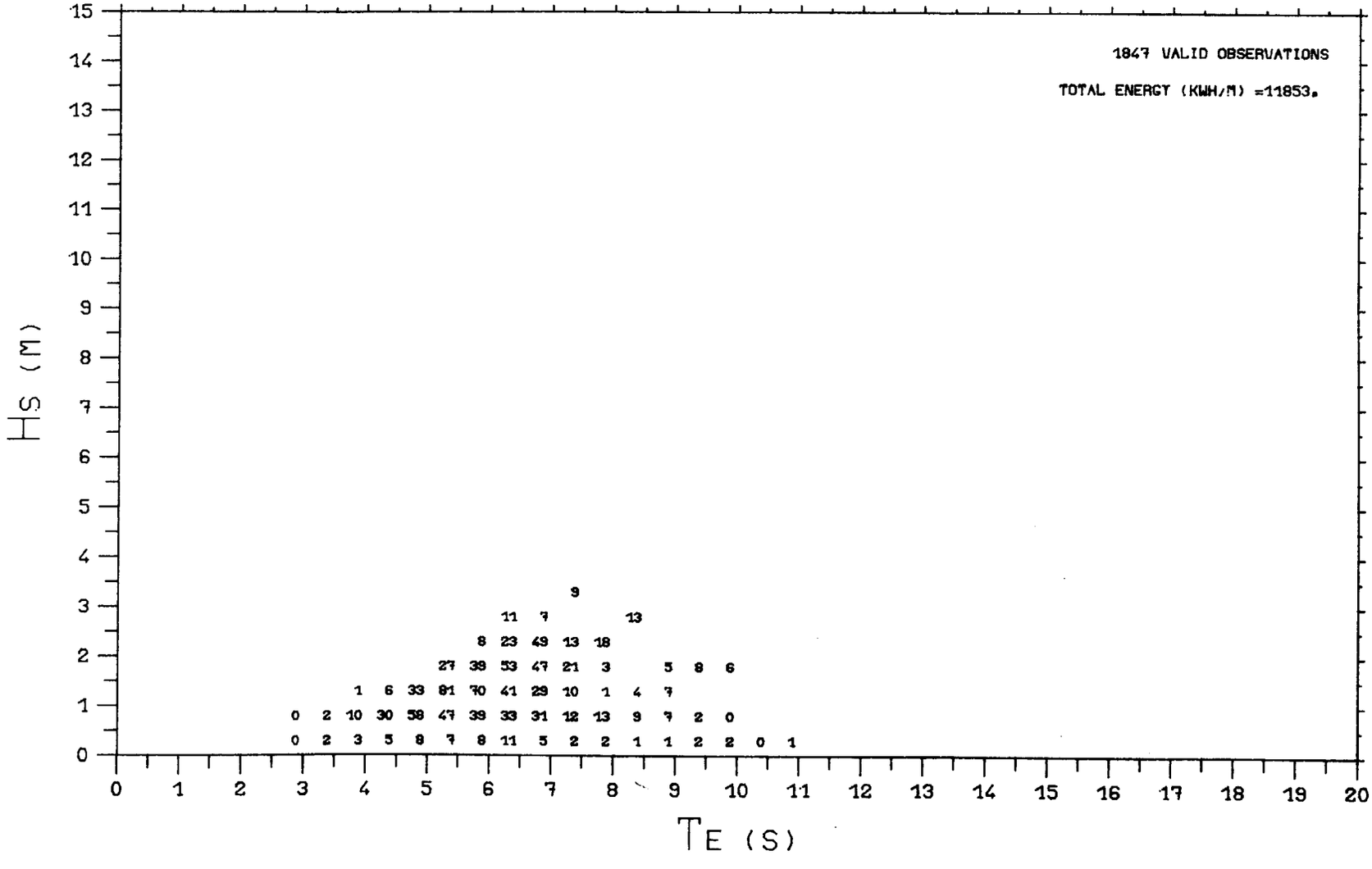


DISTRIBUTION OF TOTAL MEASURED WAVE ENERGY
WITH Hs AND TE (PPT)

EDDYSTONE SEPT 1978 - AUG 1981 SUMMERS

CA7881

FIG 3.7.2

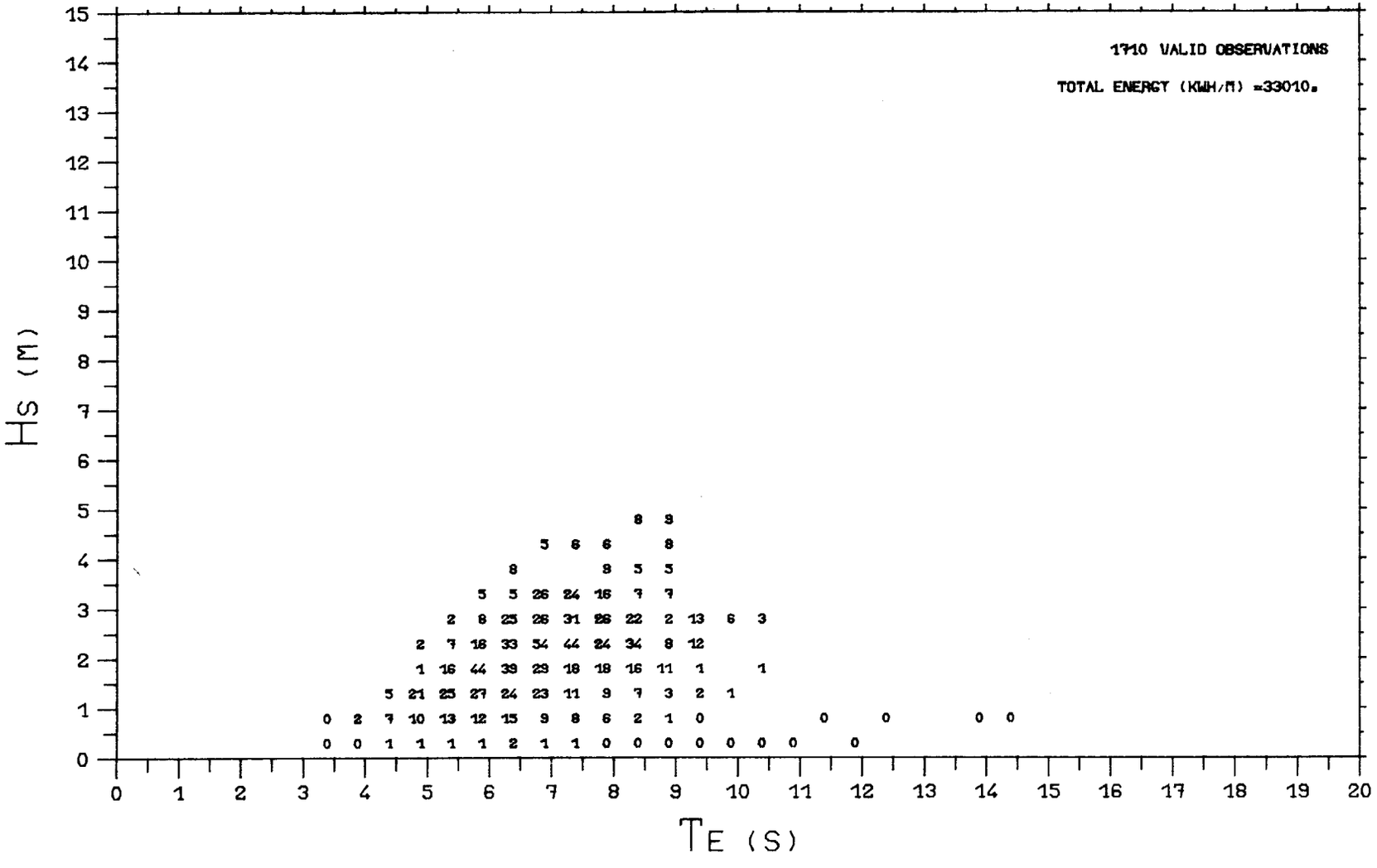


DISTRIBUTION OF TOTAL MEASURED WAVE ENERGY
WITH Hs AND TE (PPT)

EDDYSTONE SEPT 1978 - AUG 1981 AUTUMNS

FIG 3.7.3

CA7881

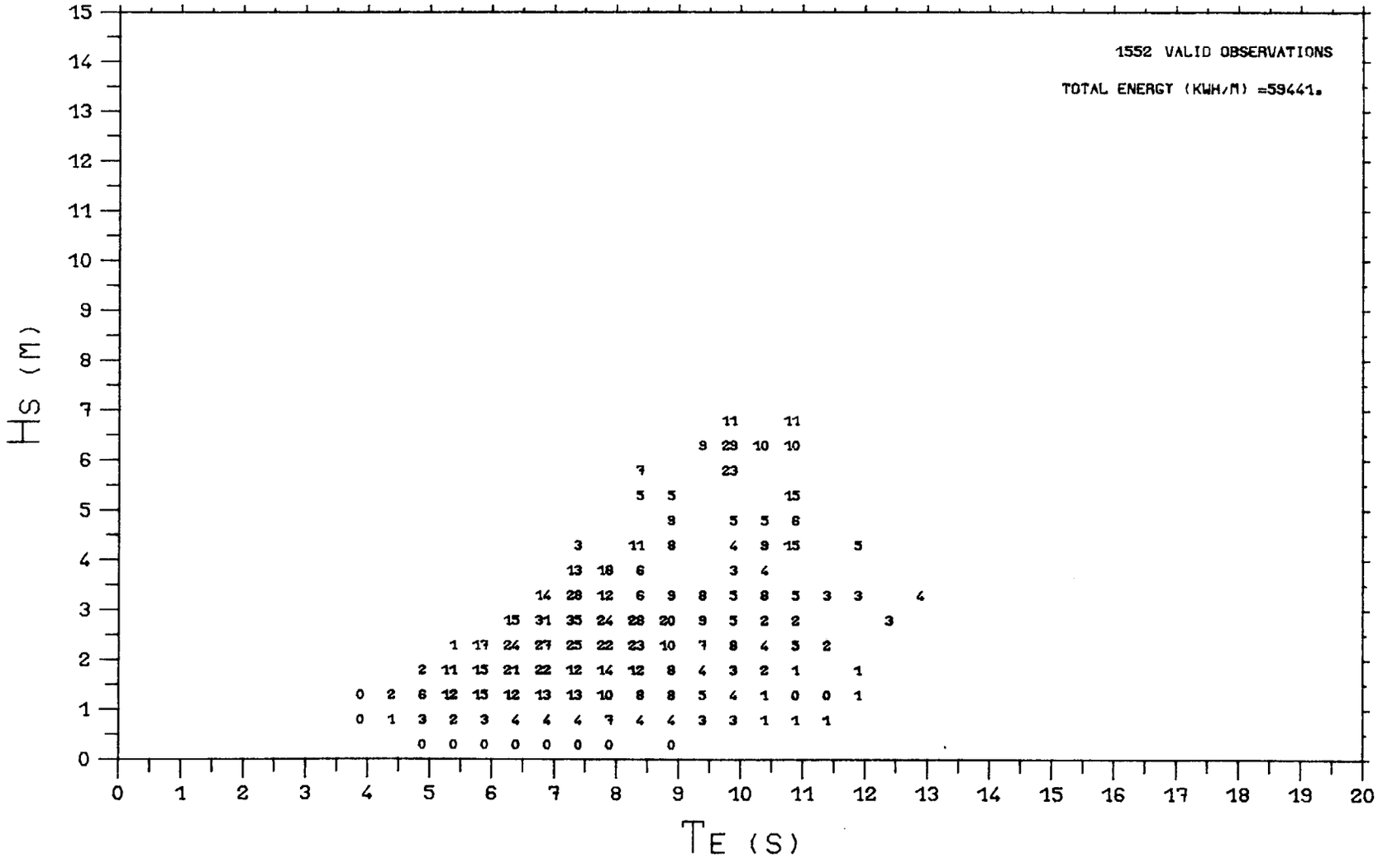


DISTRIBUTION OF TOTAL MEASURED WAVE ENERGY
WITH Hs AND Te (PPT)

EDDYSTONE SEPT 1978 - AUG 1981 WINTERS

CA7881

FIG 3.7.4

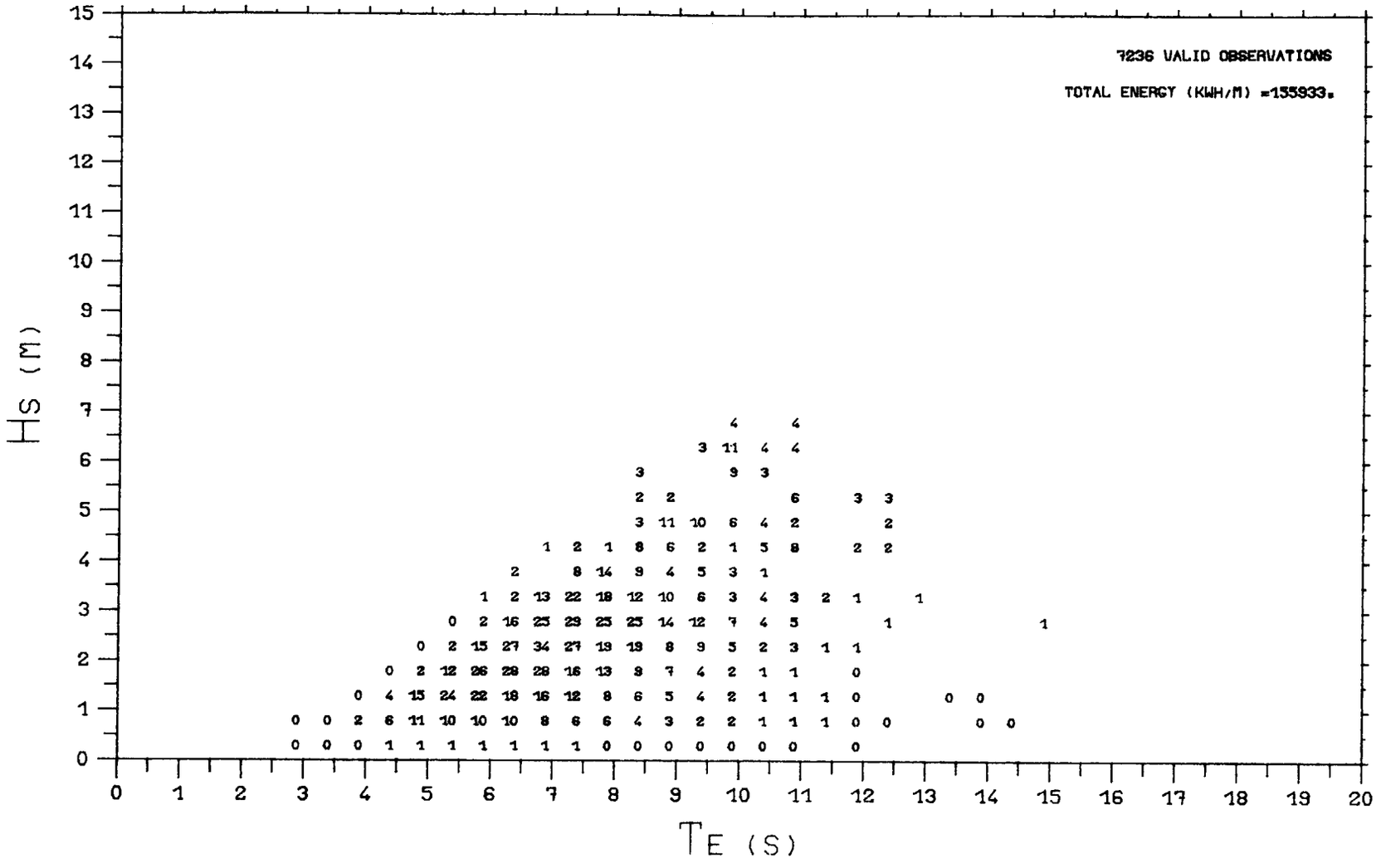


DISTRIBUTION OF TOTAL MEASURED WAVE ENERGY
WITH Hs AND Te (PPT)

EDDYSTONE SEPT 1978 - AUG 1981

CA7881

FIG 3.7.5

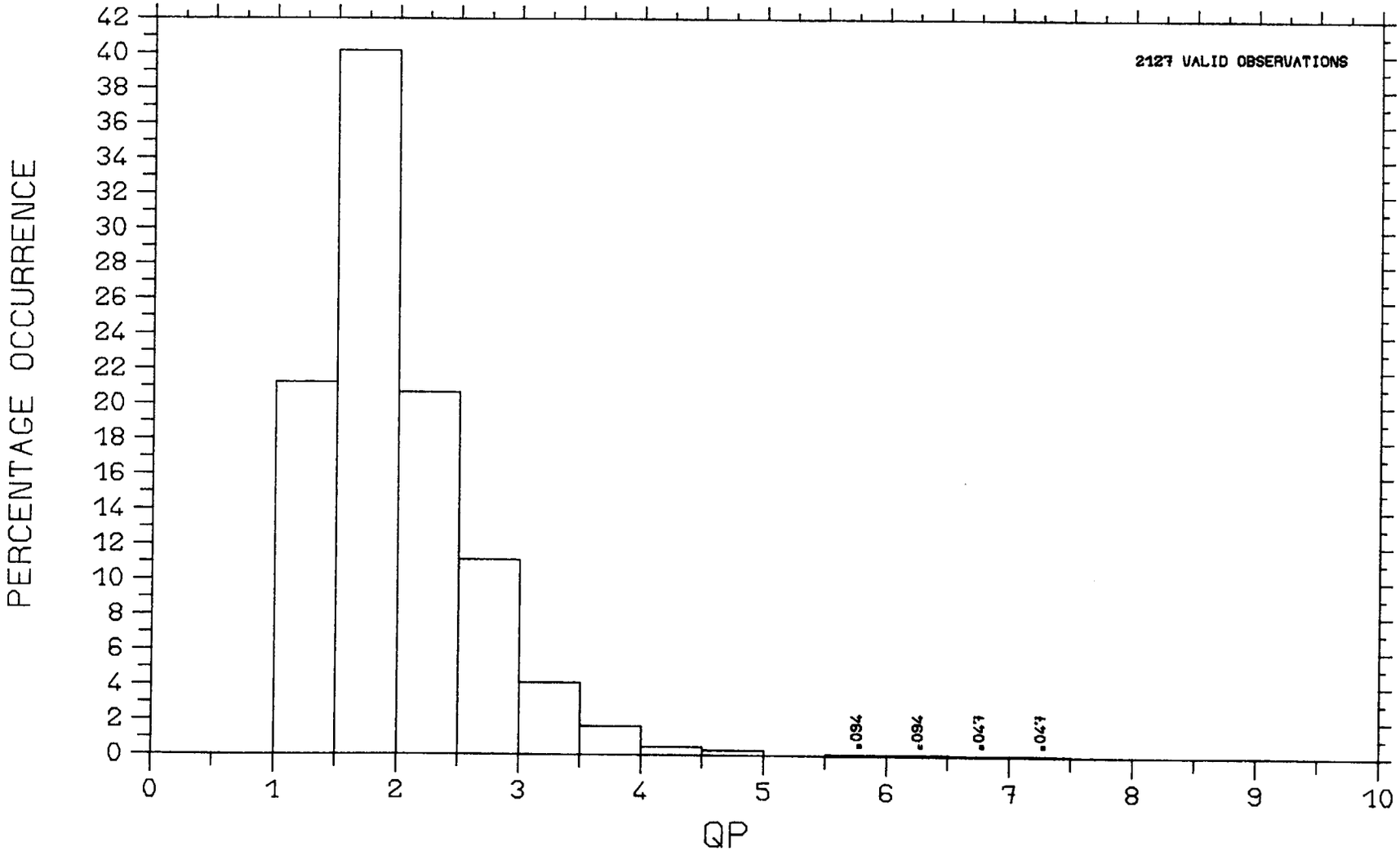


PERCENTAGE OCCURRENCE HISTOGRAM

EDDYSTONE SEPT 1978 - AUG 1981 SPRINGS

3.8.1

CA7881

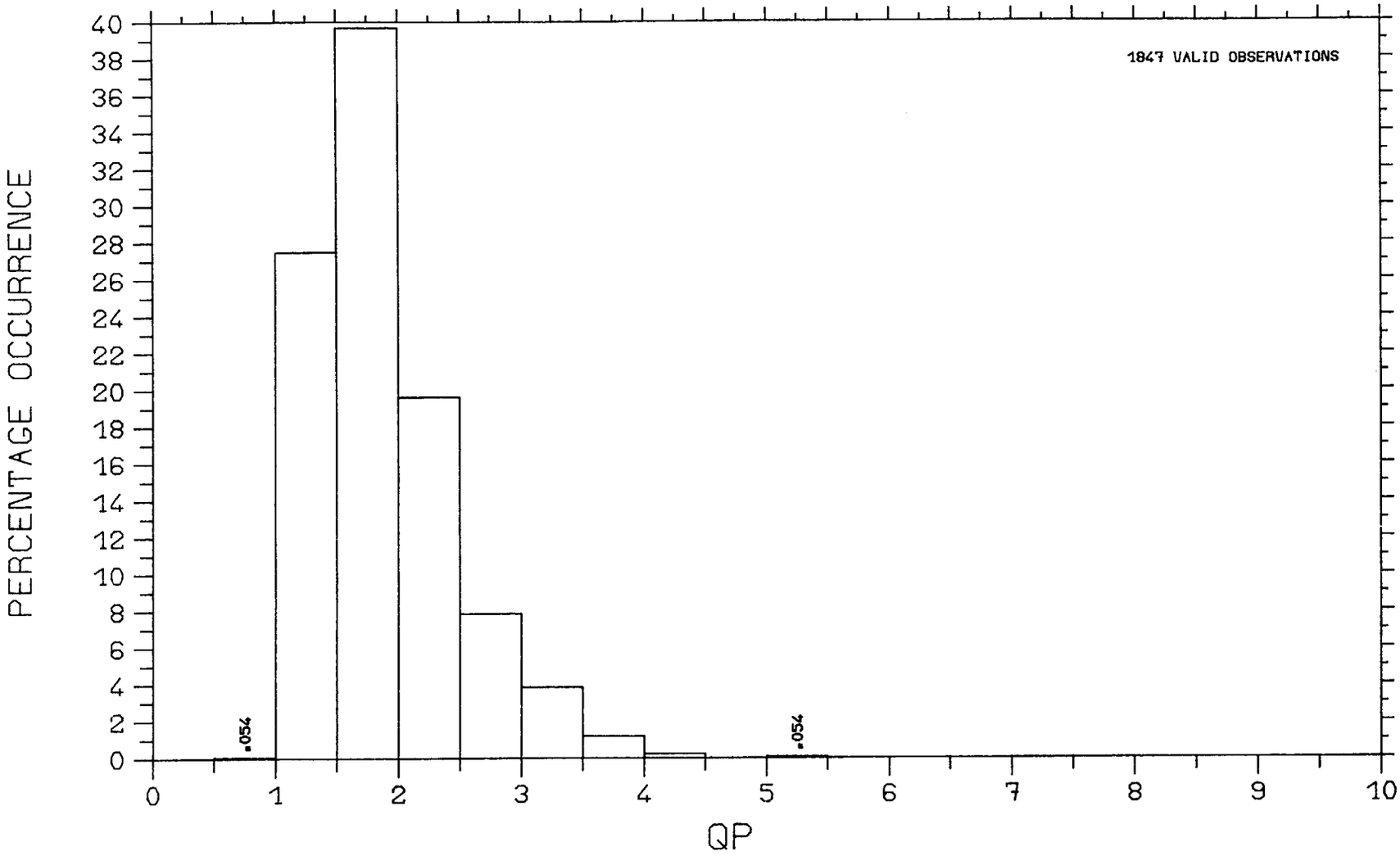


PERCENTAGE OCCURRENCE HISTOGRAM

EDDYSTONE SEPT 1978 - AUG 1981 SUMMERS

3.8.2

CA7881

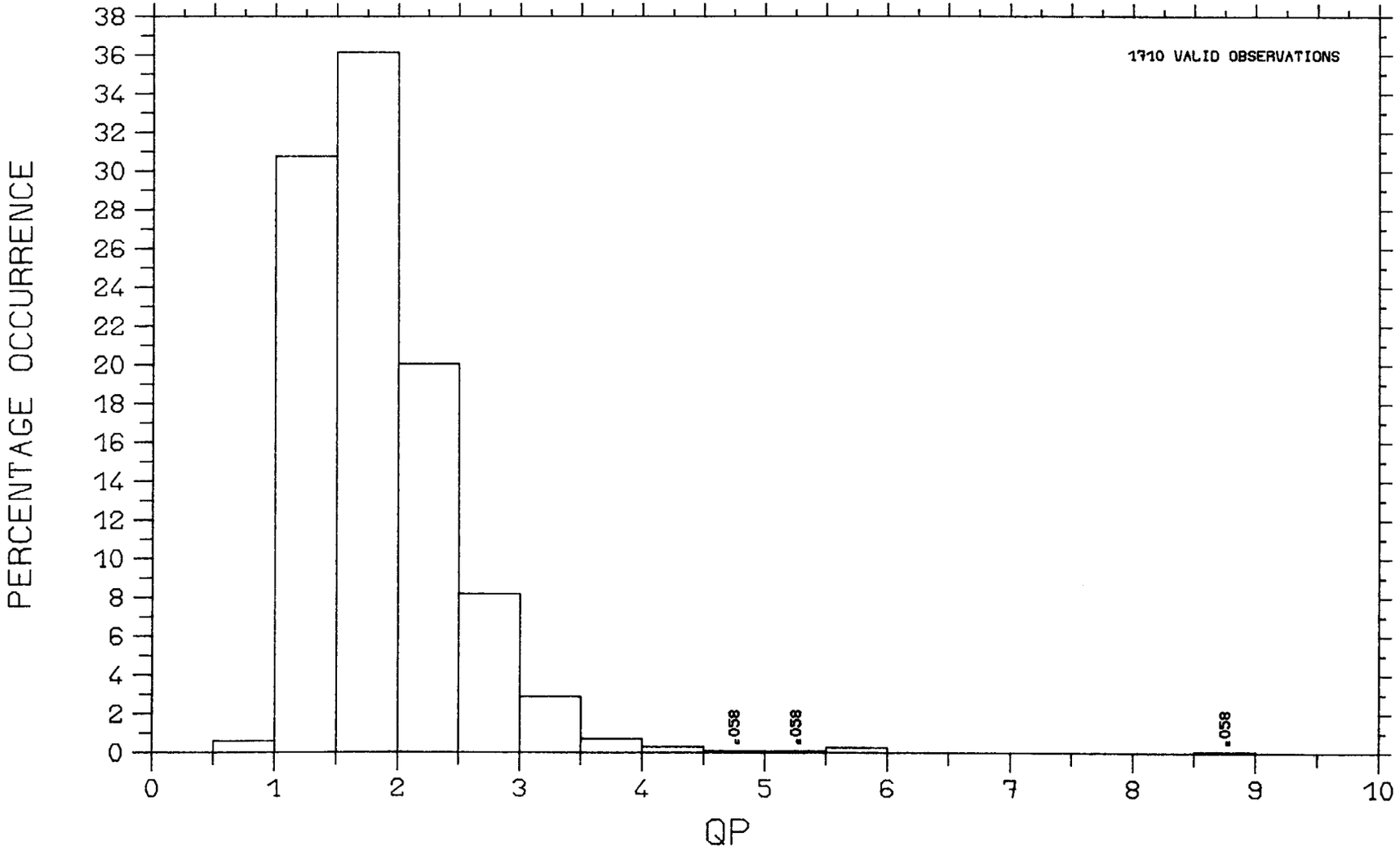


PERCENTAGE OCCURRENCE HISTOGRAM

EDDYSTONE SEPT 1978 - AUG 1981 AUTUMNS

3.8.3

CA7881

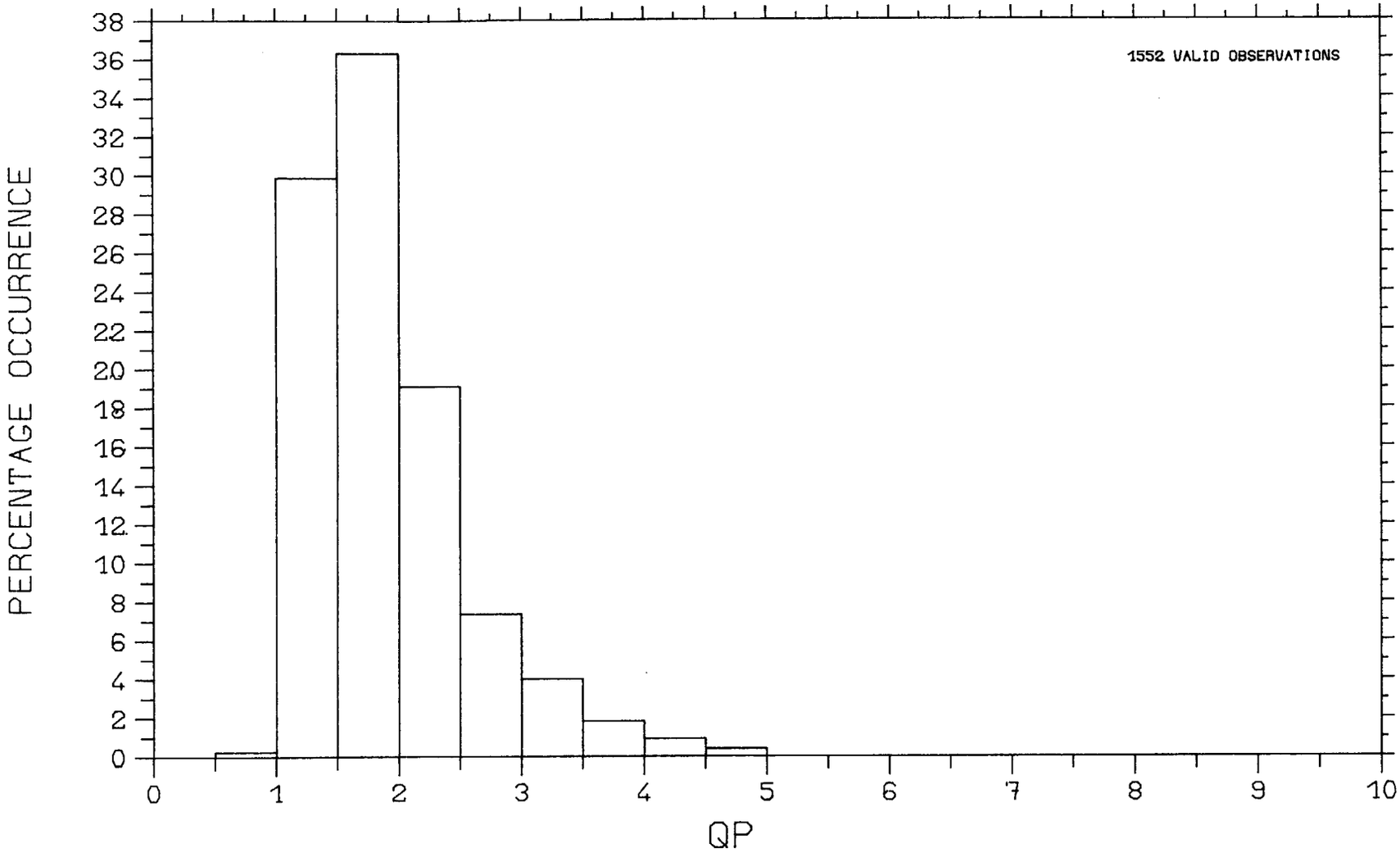


PERCENTAGE OCCURRENCE HISTOGRAM

EDDYSTONE SEPT 1978 - AUG 1981 WINTERS

3.8.4

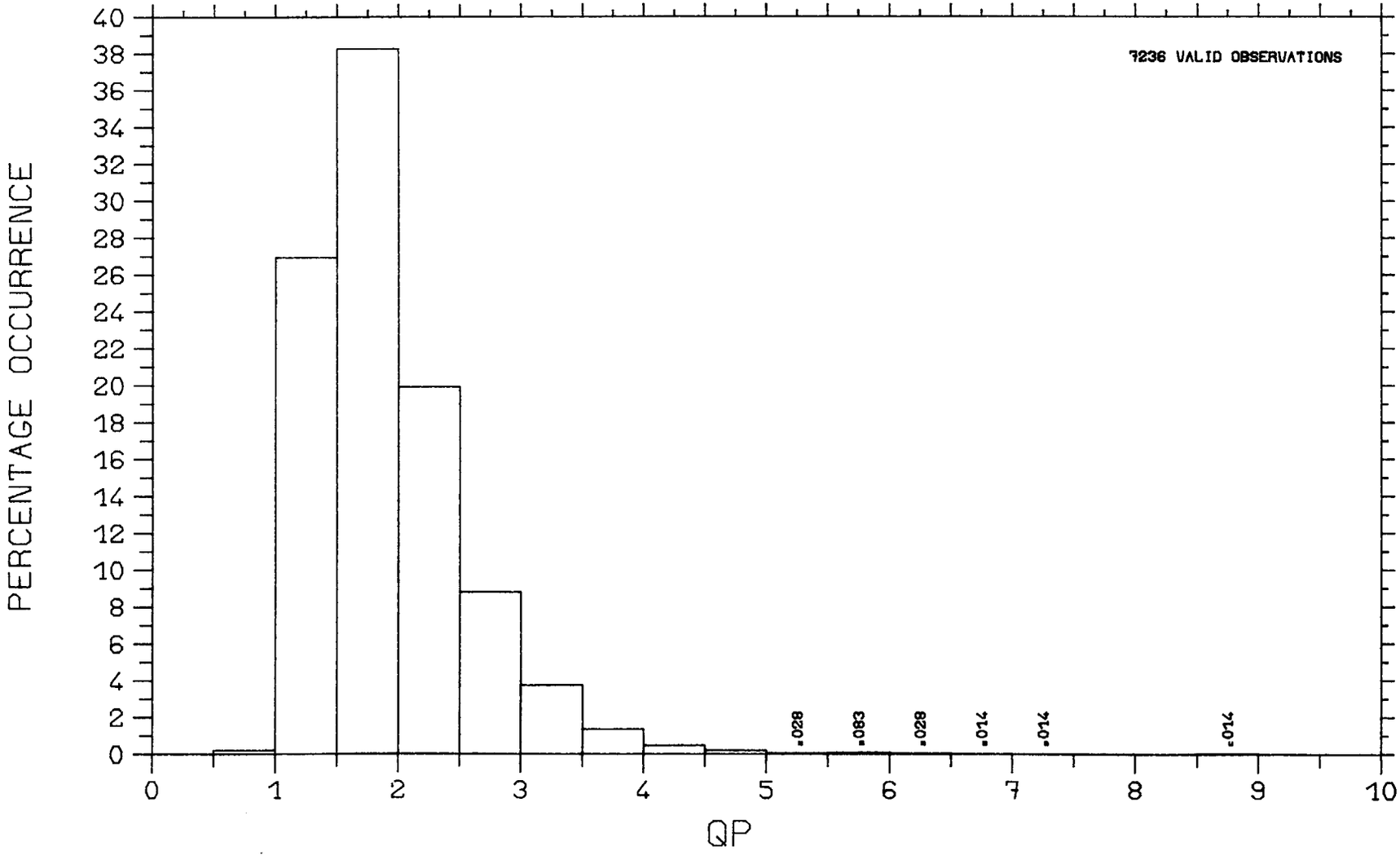


PERCENTAGE OCCURRENCE HISTOGRAM

EDDYSTONE SEPT 1978 - AUG 1981

3.8.5

CA7881

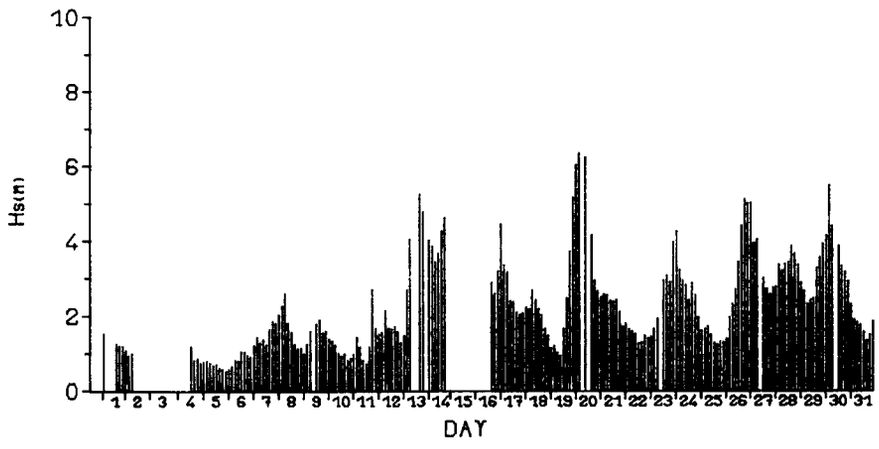


DEC 1981

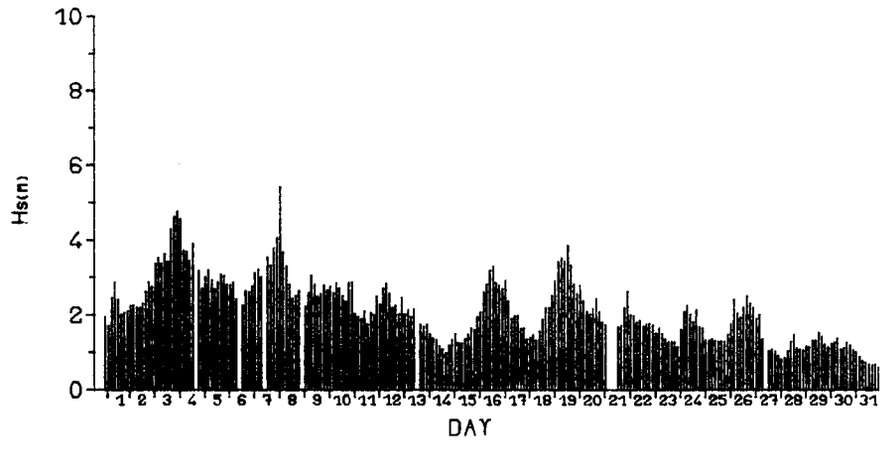


JAN 1982

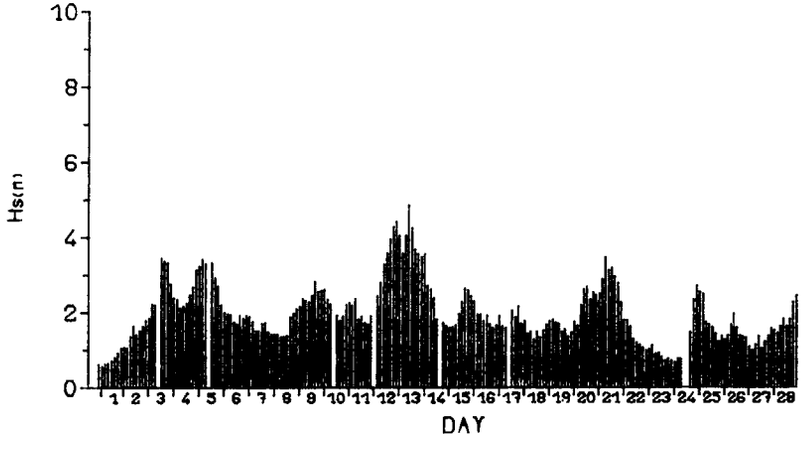


FEB 1982

# TIME SERIES OF Hs

# EDDYSTONE WAVERIDER

Fig 4 1 1

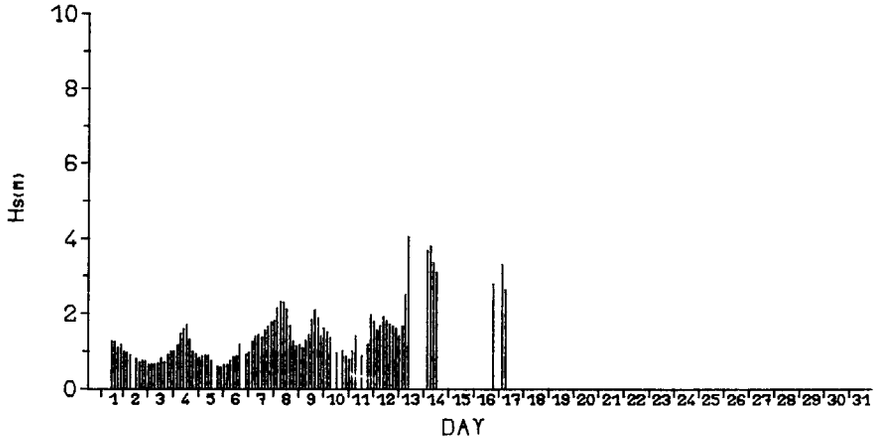


DEC 1981

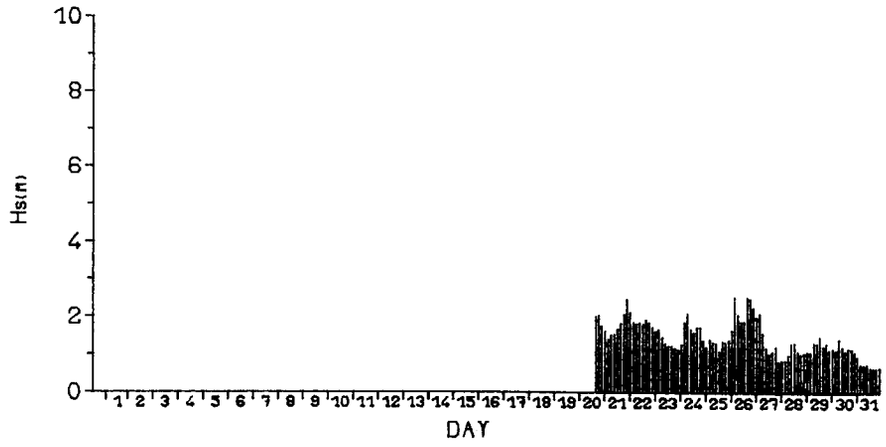


JAN 1982

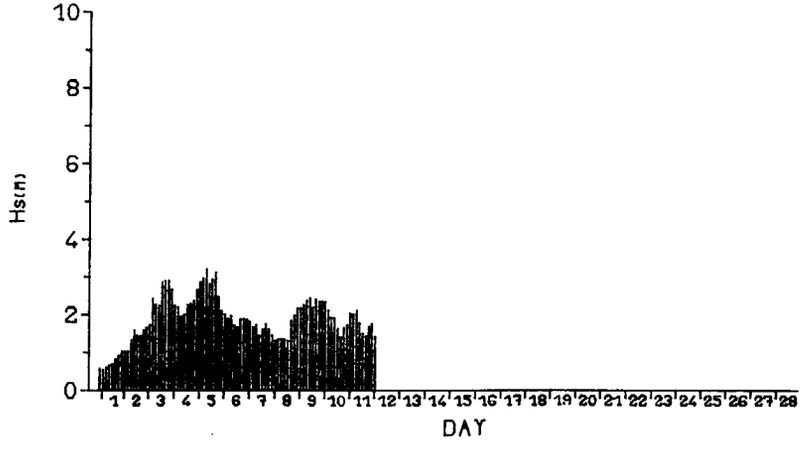


FEB 1982

# TIME SERIES OF Hs

# EDDYSTONE DEEPWATER WAVERIDER

Fig 4.1.2

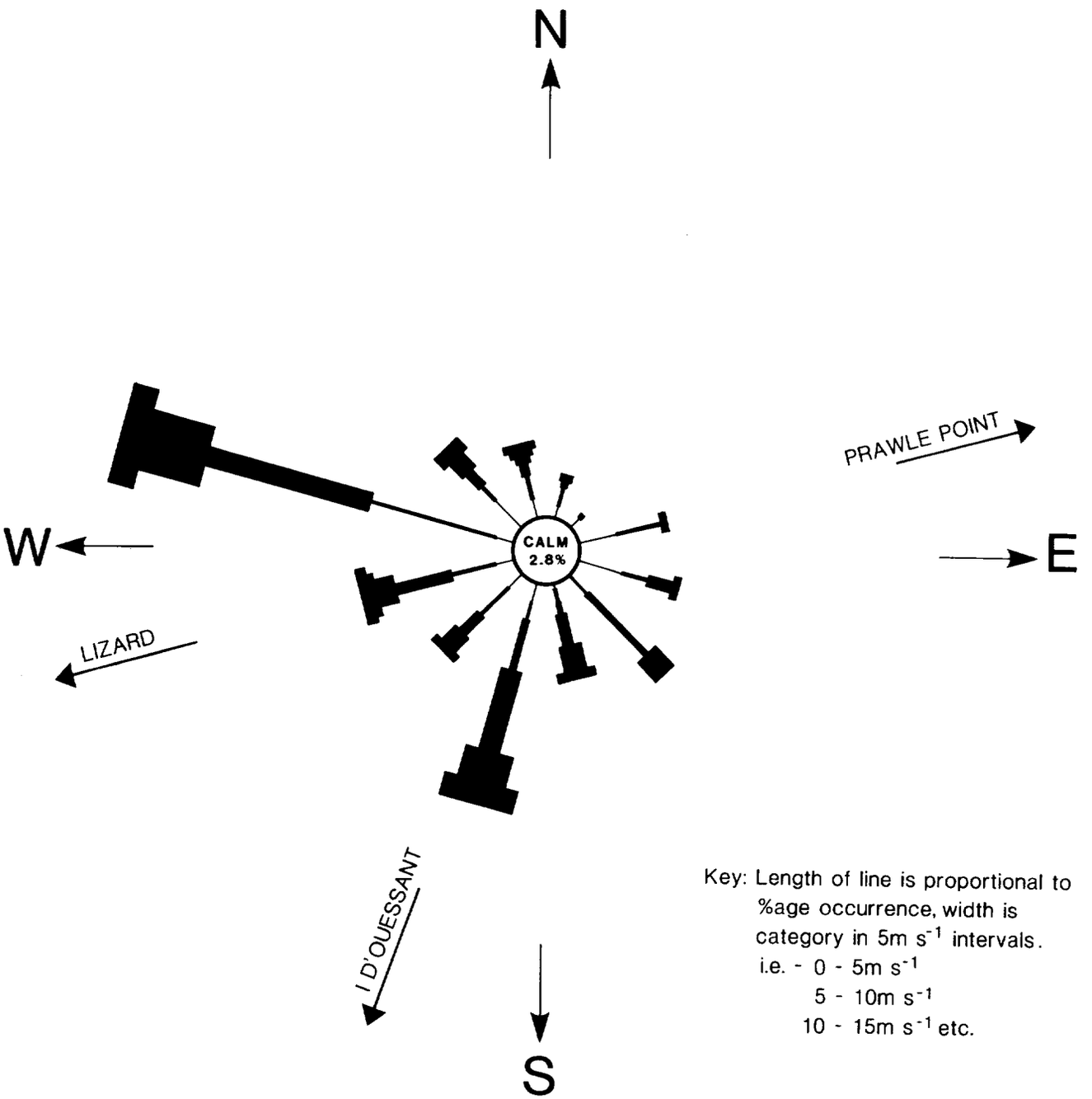


Fig 4.2 Wind rose for times of data comparison.

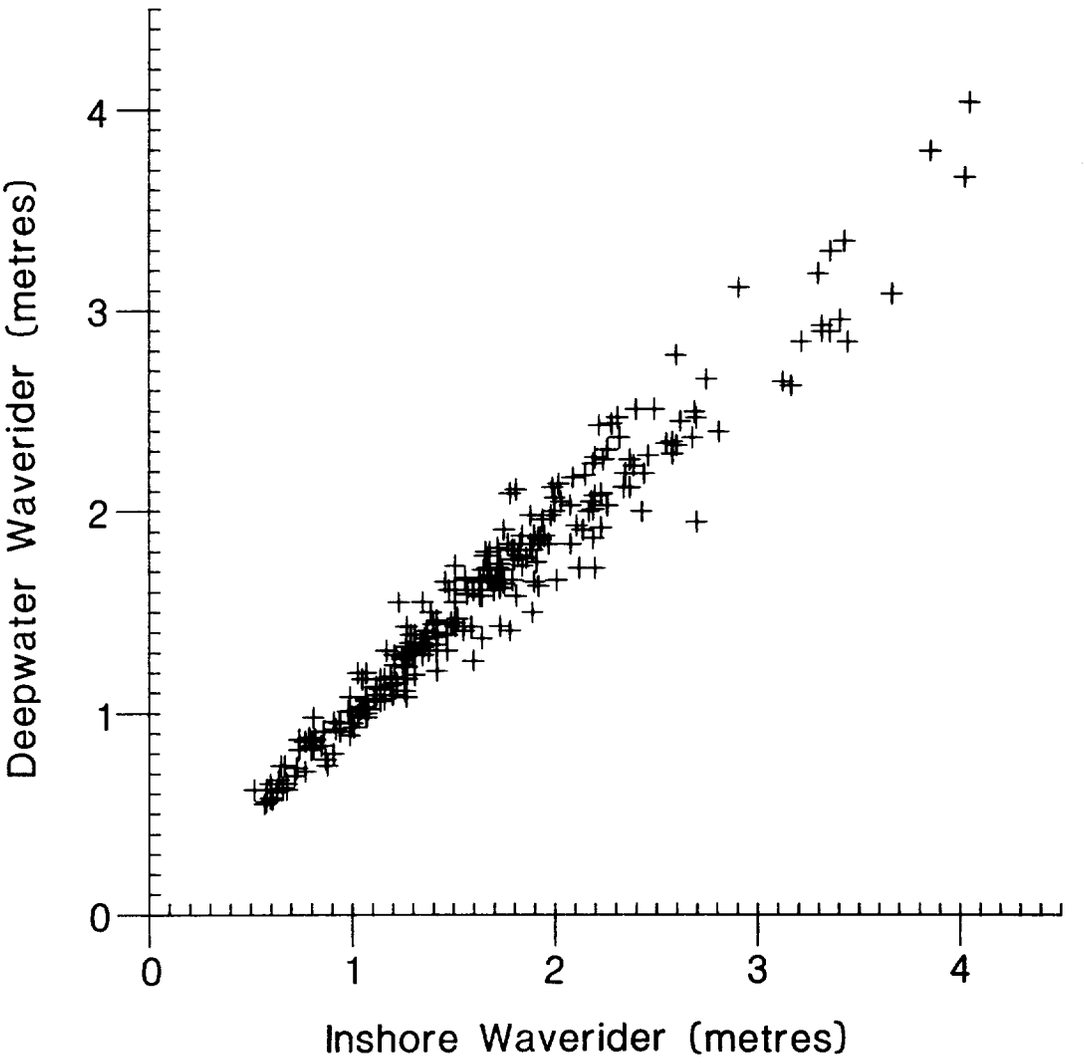


Fig 4.3.1 Comparison of Hs derived from the two buoy positions ($r = 0.976$; $p < 0.001$)

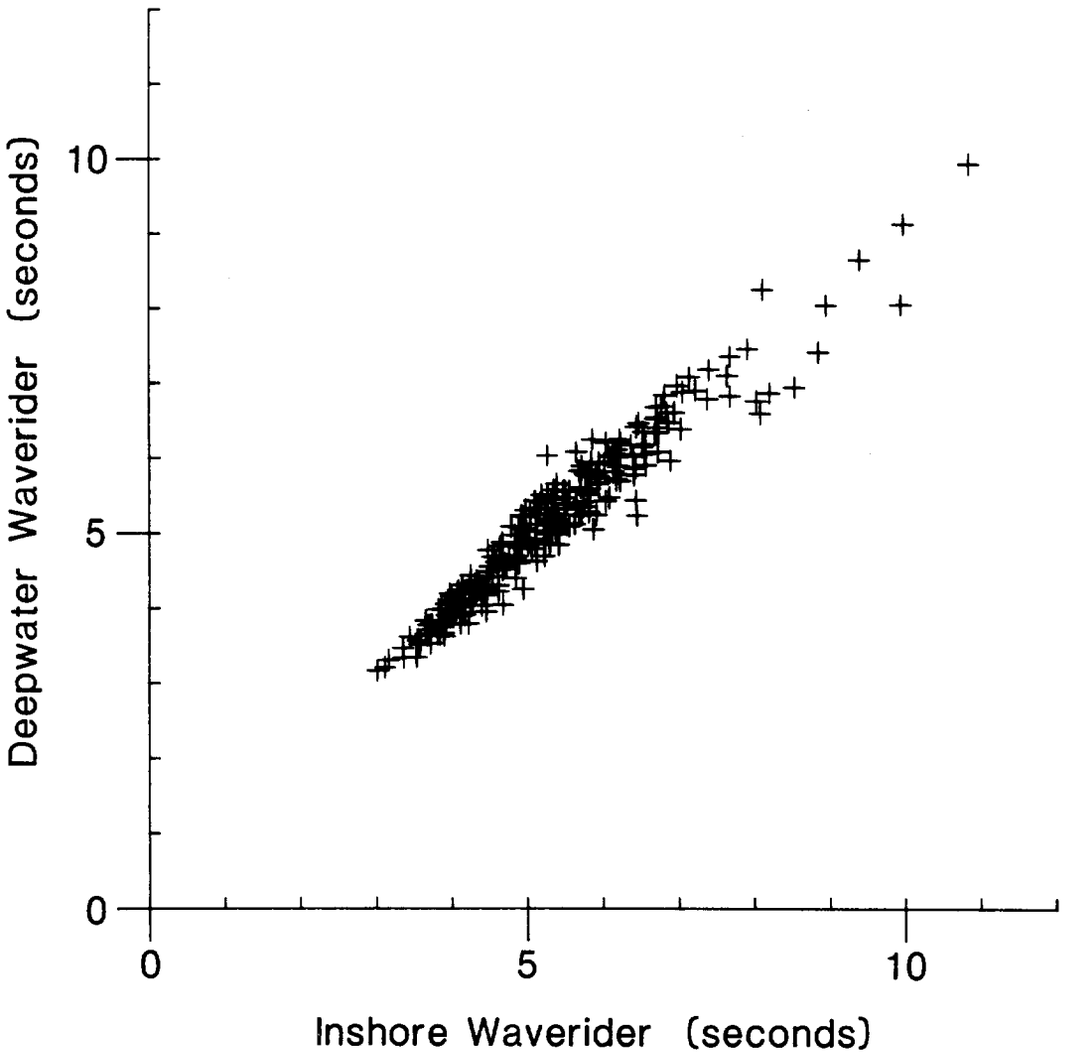


Fig 4.3.2 Comparison of Tz derived from the two buoy positions ($r = 0.968$; $p < 0.001$)

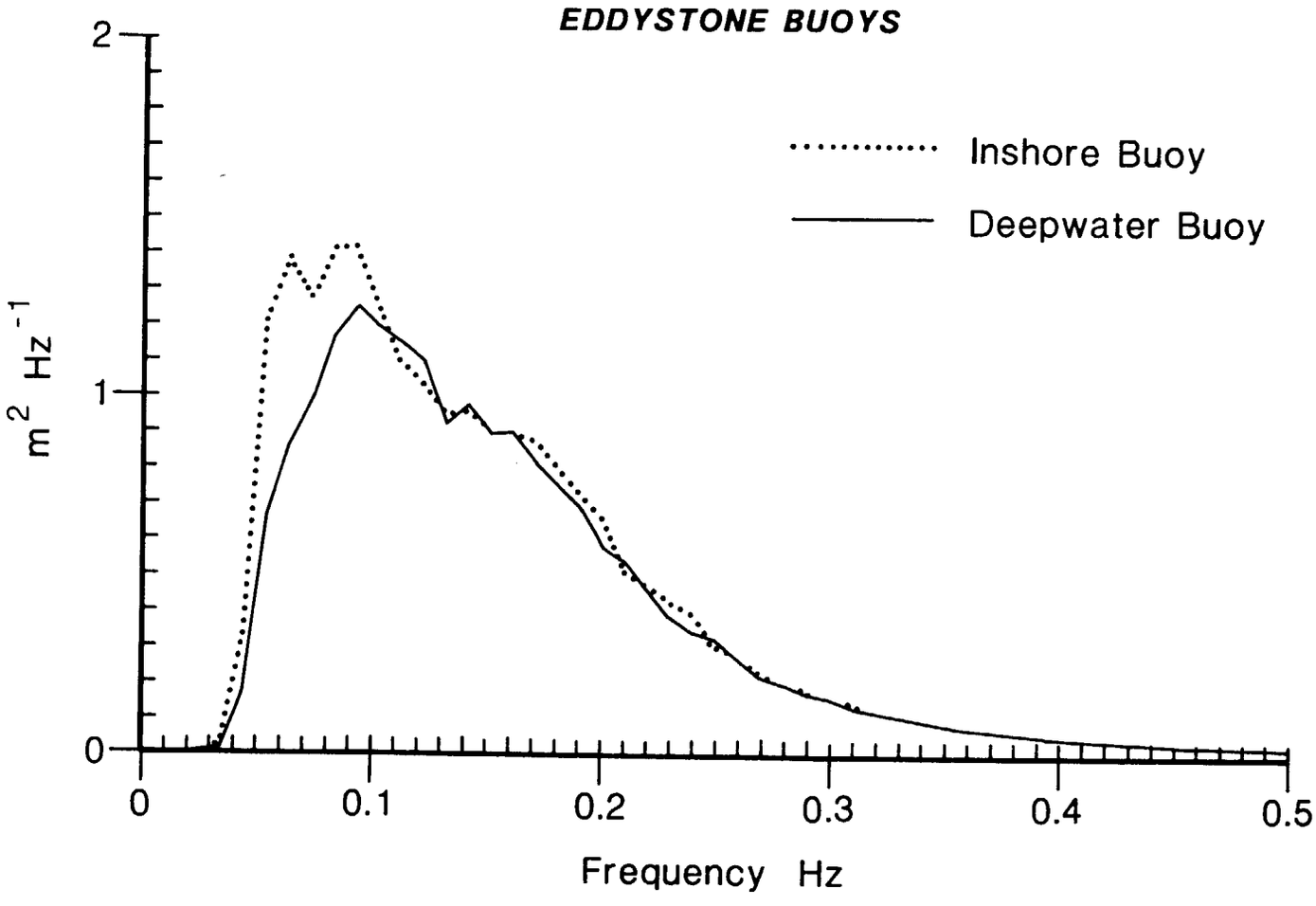


Fig 4.4 Comparison of average spectra from the two buoy positions.

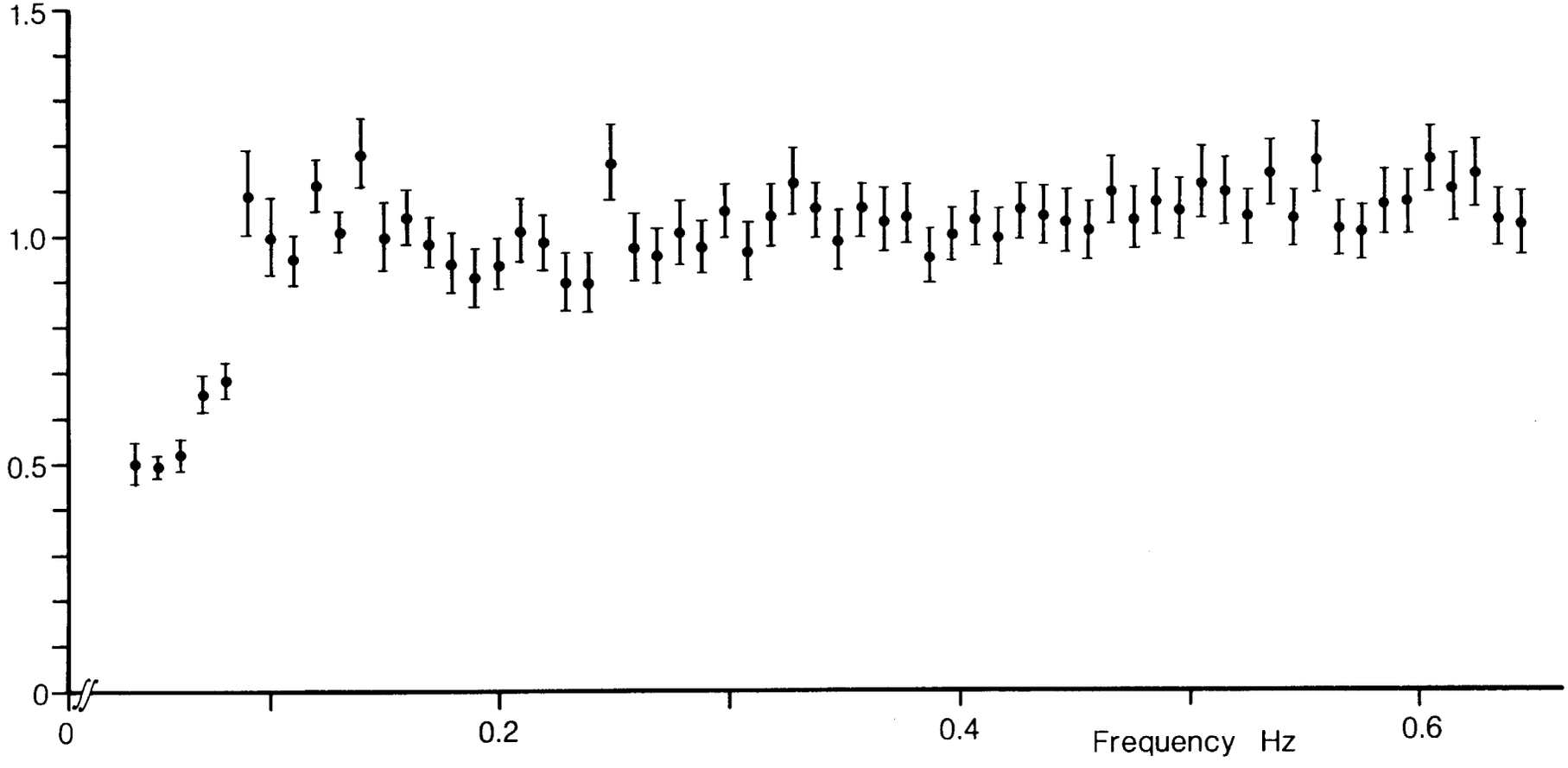


Fig 4.5 Deepwater v Inshore Waverider. Slope, ● , and 95% confidence interval on slope, I , of reduced major axis regression line (constrained through 0,0) fitted to the population of simultaneous spectral densities at each frequency.